FREEZE-DRYING BLACKCURRANT JUICE FOAM – MEASUREMENT AND MODELLING OF DRYING RATE AND ANTHOCYANIN RETENTION

By

DIANA EDITH SALGADO GARCIA

Submitted in accordance with the requirements for the degree of Doctor of Philosophy

The University of Leeds
Food Science and Nutrition

May, 2019

The candidate confirms that the work submitted is her own and that appropriate credit has been given where reference has been made to the work of others.

Acknowledgements

I would like to thank my family and friends for their unconditional support, in particular Dr Richard Gunton.

I would like to express my gratitude to Dr J. Antonio Torres, with whom I co-authored two research publications, for believing in me and for his interest in supporting my career since so long, he is a true inspiration.

I want to thank my supervisor Prof. Brent Murray and Dr Rammile Ettelaie for their support. I would like to thank Dr Peter Rhodes for his technical assistance in the use of the colour spectrophotometer and the analysis of the data obtained. I would like to thank Mr Ian Hardy, Dr Mel Holmes, Dr Caroline Orfila and Dr Christine Bosch for their assistance during this thesis.

Finally I acknowledge the financial support from CONACyT (Consejo Nacional de Ciencia y Tecnologia) throughout my PhD.

Outputs

Conferences

Innovation Match 2015-2016, Guadalajara, Mexico. Oral presentation "Obtainment of stable red high-anthocyanin powder from blackcurrant juice by an optimized freeze-drying process."

Food Colloids 2016, Wageningen, The Netherlands. Poster presentation "Foam-mat Freeze-drying of blackcurrant juice: anthocyanin survival and drying analysis."

MSc thesis contributions

1) Yan, Jingyu. 2016. *Quantification of anthocyanins after submitting a dried anthocyanin-protein based additive to different food process conditions using an enzymatic digestion, and HPLC*. School of food science and nutrition, University of Leeds.

2) Acosta, L. F. 2016. *Anthocyanin influence on the drying rate of freeze-dried foams*. School of food science and nutrition, University of Leeds.

3) Xu, Menghan. 2016. *Effect of different oxidation treatment on both blueberry anthocyanins and anthocyanin-egg albumin complexes*. School of food science and nutrition, University of Leeds.

Abstract

Blackcurrants (*Ribes nigrum* L.*)* are widely found in the market as juice or processed into spreads, infusions, purees and others. They contain high concentrations of anthocyanins which have been shown to have human health benefits. Anthocyanins are also used as food colorants. However, blackcurrants are highly perishable with a short shelf life, and thus drying is used to reduce harvest losses. A relatively new drying technology has been developed to reduce drying times of juices and other preparations. This technology consists in freeze-drying a frozen foam (foam-mat freeze-drying).

This study compared foam-mat freeze-drying and conventional freeze-drying to establish the extent to which the former reduces the drying time of blackcurrant juice, retains its anthocyanin content, and preserves its colour intensity after processing. It also analysed the changes of the characteristics of the foams due to anthocyanin and sugar contents and their effects on the drying rate. To address these questions, foams with different anthocyanin concentrations (made with egg albumin as foaming agent and xanthan gum as stabiliser) and non-foamed blackcurrant juice controls, were prepared and compared during the sublimation freeze-drying stage. A mathematical model was developed to describe differences between foamed and non–foamed blackcurrant juice. In addition, the resulting dried powders were analysed for their anthocyanin content. To do this, a pepsin treatment was developed to separate the egg albumin from the anthocyanin before using light and fluorescence spectrometry to respectively quantify and identify anthocyanins.

Finally, colour spectrophotometry was used to quantify colour changes in dried samples stored for six months.

A faster drying rate in freeze-dried than in foam-mat freeze-dried juice was observed during the first stage of freeze-drying. This was consistent with the predictions of the mathematical model and was explained by the lower free water content in foams. Foams prepared with different anthocyanin concentrations produced different bubble sizes, densities, air volume fractions and viscosities which influenced the drying rate. The foaming and drying processes aided the formation of egg albumin–anthocyanin complexes. Foam-mat freeze-dried juice with high and low anthocyanin content yielded an anthocyanin recovery of 39 and 70%, respectively, while freeze-dried juice obtained 83 and 93% for the same concentrations. Finally, the egg albumin presence in blackcurrant juice reduced the hue intensity after freeze-drying and during storage.

Table of Contents

List of Tables

List of Figures

Abbreviations

A	area [m^2]
a	CIELAB value for red/green
AD	air drying
A_{520nm}	absorption at 520 nm
A_{700nm}	absorption at 700 nm
B	constant
b	CIELAB value for blue/yellow
C	mass [kg]
D	diffusivity [$m^2\ s^{-1}$]
D_{32}	Sauter mean (SM)
DF	dilution factor
FD	freeze-drying
J	mass flux [$kg\ m^{-2}\ s^{-1}$]
k	thermal conductivity [$W\ m^{-1}\ K^{-1}$]
L	latent heat of water [$J\ kg^{-1}$]
L	CIELAB value for lightness
l	sample thickness [m]
MW	molecular weight [g/mol]
mc	moisture content [%]
m_i	initial weight
n	number of moles
P	pressure [Pa]
P_s	partial vapour pressure at the sublimation interface [Pa]
P_o	partial vapour pressure at the condenser [Pa]
P^*	partial vapour pressure at the triple point of water [Pa]
PT	pepsin treatment
q	heat flow [$W\ m^{-2}$]
R	gas constant [461.5 $J\ kg^{-1}\ K^{-1}$]
r	dried layer thickness [m]
T	temperature [K]

T_s	temperature at the sublimation interface [K]
T_o	temperature of the condenser [K]
T^*	temperature at the triple point of water [K]
TA	total anthocyanin content [mg/l]
t	time
V	volume [m^3]

Symbols

ΔC^*_{ab}	change in chroma (from CIE76)
ΔE^*_{ab}	change in perception (Empfindung) (from CIE76)
ΔH	change in hue
ΔM	change in mass [kg]
$\Delta M(t)_e$	change in mass of experimental values [kg]
ε	molar extinction coefficient
ρ_F	density of the foam [g/ml]
ρ_L	density of the liquid before foaming [g/ml]
ϕ	air volume fraction (AVF)
γ	shear rate (s^{-1})
σ	standard deviation
τ	shear stress (N m^{-2})

Chapter 1 Introduction

At present, all industries are attempting to become more ecological and economical. At the same time, processes in the food industry are widely known for decreasing nutrient content and degrading the appearance of foods. Drying, a unit operation used in the food industry to remove water from vegetables, fruits, meat, and others can affect nutrients like vitamins or antioxidants if the temperature for drying is overly high or the process is excessively long. Drying at very low temperatures, under 0 °C, is also possible and it decreases nutrient losses. However, drying at very low temperatures can be very expensive since reaching less than 0 °C and maintaining this low temperature during the typically long drying times requires much energy. Therefore, a food process called foam-mat freeze-drying (Ratti and Kudra, 2006) has recently received attention of food scientists due to the idea of creating a more rapid and hence economical drying process that could also achieve higher retention of food nutrients.

Foam-mat freeze-drying is the combination of two food dehydration technologies. On the one hand, it is the application of foam-mat drying, i.e., the incorporation of foaming agents into the solution to be dried, whipping and spreading on a tray where hot air dries the foam by evaporation (Wilson et al., 2013, Sangamithra et al., 2015). Foaming increases the air contact area with the material to be dried and thus drying rate increases (Azizpour et al., 2014). Freeze-drying, on the other hand, is a process in which water in the sample is frozen and then converted from ice to vapour by sublimation, generally under vacuum to improve mass transfer from the sample to the condensing plate. This

process retains most of the food nutrients (Hua et al., 2010, Barbosa-Canovas and Vega-Mercado, 1996, Karel and Lund, 2003).

Foam-mat freeze-drying is intended as a freeze-drying improvement by increasing sublimation rate and thus reducing drying time. Moreover, because foam-mat freeze-drying occurs at low temperature, nutrients are retained, final products have an improved solubility and rehydration, and shelf life increases (Raharitsifa and Ratti, 2010a). However, research into why and by how much foam-mat freeze-drying reduces drying time remains incomplete. Research is also needed to show if the incorporation of foaming agents and air into the sample affects nutrient retention and product appearance.

This introduction describes what foams are, how they are prepared, the aforementioned drying techniques and their pros and cons, the importance of blackcurrant and anthocyanins in the food industry, the analytical techniques required to conduct this study, and the development of a mathematical model describing the freeze-drying of foams.

1.1 Foams

A foam is a gas dispersion in a continuous phase (Murray and Ettelaie, 2004). Foaming consists of dispersing and stabilizing a gas in a solid or semi-solid continuous phase (Caetano da Silva-Lannes and Miquelim, 2013) by whipping, bubbling, shaking, and other mechanical means. The addition of foaming agents, typically proteins, is generally required (Belitz et al., 2004).

One of the main difficulties when drying foams is that they are very unstable (Vernon-Carter et al., 2001). Means to stabilise them include improving the functional properties of proteins (Murray, 2007), using nanoparticles at

interphases (Dickinson, 2010), adding polyphenols (see references below), or simply by freezing them. Among these, the use of polyphenols was studied in this thesis since anthocyanins, a type of polyphenol present in fruits, are commonly found in foamed products such as meringues, mousses, cakes, bakery fillings, marshmallows, and ice creams.

Polyphenols from green tea have been shown to stabilize foams by interacting with proteins used as foaming agent (Rodriguez et al., 2015, Wu et al., 2007). Other polyphenols such as catechin and tannin present when foaming proteinaceous solutions have also shown foam stabilization effects (Sarker et al., 1995, Delgado-Sánchez et al., 2017). However, important polyphenols such as anthocyanins have not received much attention regarding the formation and stability of foams. Although anthocyanins are widely present or added to foods, past research has only focused on wine anthocyanin-protein interactions (González-Neves et al., 2014). Moreover, protein–anthocyanin complexes studies have focused on protecting the bioactivity of polyphenols, instead of their functional applications in foods (Schneider et al., 2016). It is also important to consider whether the interaction between foaming agents and food components influences the foam freeze-drying rate. In addition, the interaction between foaming agents and food components may change the anthocyanin retention and modify the colour of the dried powders over time.

Proteins commonly used as foaming agents include egg white, gelatins, casein, other milk proteins, soy proteins and gluten (Zayas, 1997, Sangamithra et al., 2015). These stabilise foams by being adsorbed at the interface of the air bubble forming a flexible and cohesive film. This happens when the energy

applied to the proteinaceous solution by whipping, bubbling, shaking and other mechanical means breaks weak links between amino acids leading to an unfolding of globular proteins. Their partial unfolding can bring more hydrophobic groups to the surface of the proteins, increasing their amphiphilic nature and thus their flexibility (Mleko et al., 2007). Hydrophobic groups of the protein are exposed to the air phase (surface and bubbles) while hydrophilic groups will be in contact with the water-like phase. The water-like phase, also called "continuous phase", contains most of the foam solids. Bubbles in foam are known as the "dispersed phase".

Albumin, the main protein in eggs (Sangamithra et al., 2015) is a complex up to 40 different proteins (Mleko et al., 2007). The major proteins involved in the foaming of whipped egg albumin are ovalbumin, globulins and ovomucoid (Mleko et al., 2007). Ovalbumin is a glycophosphoprotein with a peptide chain of 385 amino acid residues, a molecular weight of 42.699 kDa and an isoelectric point at pH 4.5 (Belitz et al., 2004).

1.1.1 Foam stability characterization

The parameters used for the analysis and characterisation of foam stability are:

- *Sauter mean* (D(3,2) or $d_{3,2}$): Estimate of a mean diameter appropriate for describing the average particle in a distribution, also known as mean of bubble size distribution (BSD), and commonly measured photographically (Filippa et al., 2012, Cheng and Lemlich, 1983).

- *Air volume fraction:* This is the relationship between the liquid density before and after foaming and thus describes the air amount in the sample after foaming (Raharitsifa et al., 2006).
- *Density:* Defined as the mass per unit volume.
- *Viscosity:* Defined as the fluid internal friction or its tendency to resist flow (Bourne, 2002)
- *Drainage:* Defined as the movement of liquid through the foam. Figure 1.1 shows three adjacent films intersecting in a channel called the Plateau border (Raharitsifa et al., 2006). The two mechanisms contributing to film drainage are gravity viscous flow through the film interior, and marginal regeneration, the largest contributor to drainage, caused by the exchange of film parts of different thickness with the Plateau border (Prins, 1988).

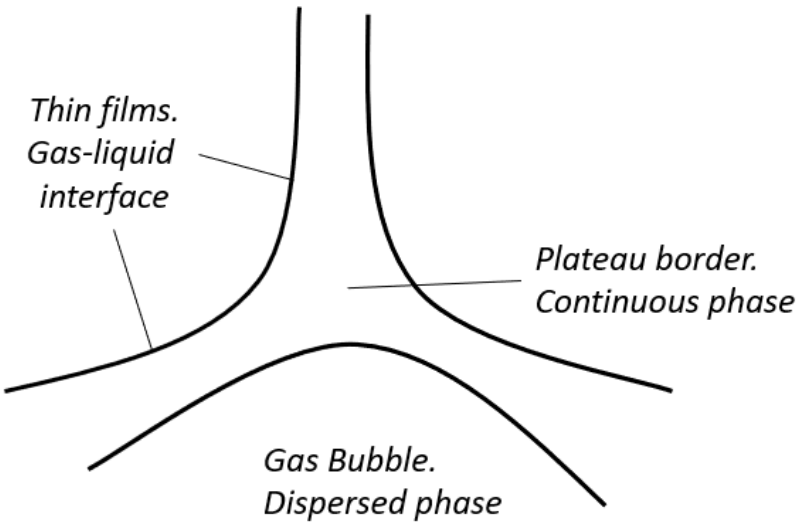

Figure 1.1 Parts of the foam where drainage occurs.

It is important to note that some of these foam properties depend on each other. The air volume fraction and the bubble size affect bubble coalescence and thus, drainage. Moreover, in semi-solid foams, the bubble size distribution influences product appearance and textural properties such as smoothness and lightness (Zayas, 1997).

Strategies for foam stabilization include specialized processing units (e.g., Hyperjets™ (Hettiarachchi et al., 2018)), surfactants that crystalize around bubbles (Ettelaie and Murray, 2015), and synthetic stabilisers (e.g., Tween 20 (Huang et al., 2018)). However, the development of simpler means to stabilize foams, e.g., by adjusting the concentration of product ingredients, is a valuable alternative attractive to consumers interested in healthier foods and environmental sustainability and thus a preference for clean labels and minimum processing (Bruhn, 2007). The foaming properties of proteins can be changed by simply adjusting their concentration (Zayas, 1997), and by adding water–soluble polymer to the solution to be foamed. Water-soluble polymers such as polysaccharides prevent coalescence by assisting the formation of films around bubbles (Caetano da Silva-Lannes and Miquelim, 2013). Although water–soluble polymers may interact with proteins and sugars, they have not been studied as potential foam stabilisers.

1.1.2 Foam viscosity

The viscosity of the continuous phase of foams defines and differentiates them from gaseous liquids such as soda drink. Typically, foam viscosity increases for smaller bubble diameters and lower density (Kroezen et al., 1988). Foams are also described as a semisolid mixture containing bubbles in suspension. As seen

in Figure 1.1, the way in which bubbles are held in the semisolid mixture has a complex structure conferring on foams a particular mechanical behaviour, presenting at the same time, elastic, plastic and viscous properties (Dollet and Raufaste, 2014). Foam viscosity can be measured with rheometers differing in geometry including two plates, cone and plate, and two cylinders in which the foam is sheared at a specific rate (γ) and stress (τ) level. Viscosity (μ) is the ratio between shear stress and shear rate: $\mu = \frac{\tau}{\gamma}$ (Bobert et al., 1997). Figure 1.2 shows the rotation of a cone against a fixed plate containing a sample in a cone-plate geometry.

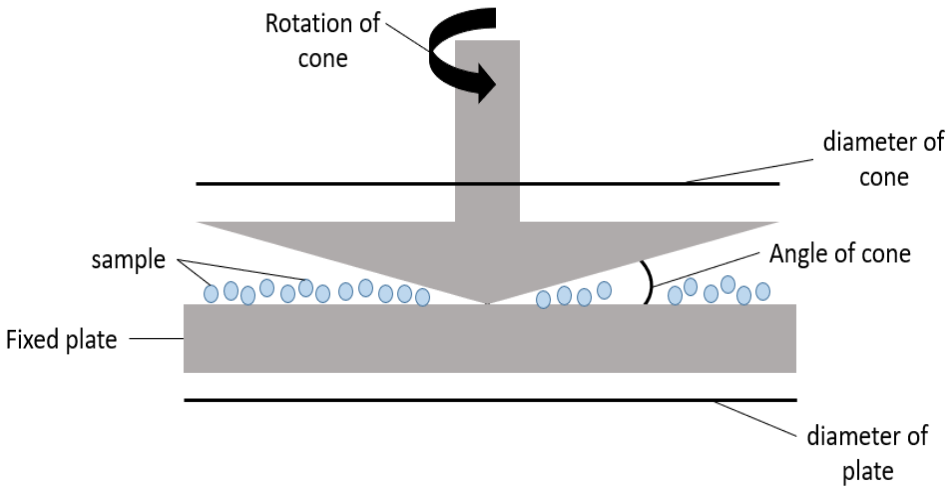

Figure 1.2 Cone-plate geometry of rheometer.

When applying strain slowly, a foam behaves first like an elastic solid (linear increase of shear stress). The continuous application of strain will eventually reach the yield stress where the foam breaks and then, a liquid-like behaviour is observed (Weaire, 2008).

Foam rheology studies describe how foaming agents create macromolecular entanglements modifying the viscosity of the continuous phase (Ptaszek et al., 2014). The same authors concluded that the use of xanthan gum aids the viscoelastic properties of egg white foam. Yang et al. (2009) reported higher foam yield stress in egg white protein (EWP) foams since this protein aided the formation of small and stable bubbles that packed together into structures that are resistant to deformation. In another study, Yang and Foegeding (2010) showed how the addition of sucrose to egg white foams increased the bulk phase viscosity and interfacial rheology which consequently improved the stability of foams. A similar effect was observed when mixing egg white with pectin to produce foams (Sadahira et al., 2016). Finally, air bubbles modify the texture and rheological properties of foam (e.g., smoothness in whipped cream, mousses, ice creams) (Campbell and Mougeot, 1999)

1.2 Foam-mat Freeze-drying

Foam freeze-drying has been investigated to produce packaging materials, insulation for refrigerators, capsules for time-release drugs (Lee et al., 1997), and tissue engineering (Lv and Feng, 2006), among other uses. In food science, milk was among the first materials to be foamed and freeze-dried materials (Sochanski et al., 1990). However, the study of freeze-drying foamed milk was focused on proposing a new approach to model drying foams mathematically. More recent food applications were studied by Raharitsifa and Ratti (2010a) who assessed foam-mat freeze-drying of apple juice observing a reduction in process time due to foaming. The conclusion was that foaming juice reduces the freeze-drying time compared to non-foamed juice only if the

thickness of both foamed and non-foamed samples were the same. They also concluded that drying of foamed materials was limited by heat transfer while drying of non-foamed ones was limited by mass transfer (Raharitsifa and Ratti, 2010a). In a subsequent study, the same authors showed that foamed juice was more stable when stored at 20 °C (Raharitsifa and Ratti, 2010b). However, foamed juice retained less vitamin C and was less soluble. Muthukumaran (2007) studied the suitability of foam-mat freeze-drying egg albumin aided by xanthan gum concluding that the latter improved the stability of the foam during drying and thus drying time. A benefit of foam-mat freeze-drying is that the foam stability is improved by the low temperature. However, the addition of foaming agents and stabilisers to the original food limit the use of the final product or they must be removed by an additional processing step after drying.

1.3 Foam-mat drying

Foam-mat drying is a widely used technique requiring the same equipment as conventional hot air drying (AD). Figure 1.3 depicts the essential components of a hot air dryer, namely a drying chamber, a rack (or set of racks for batch drying) or a conveyor* (for continuous drying), a blower or fan, an air heater, and one input device to enter dry cold air (air intake) and one to expel wet hot air (air exhaust) after gaining moisture by contact with the sample.

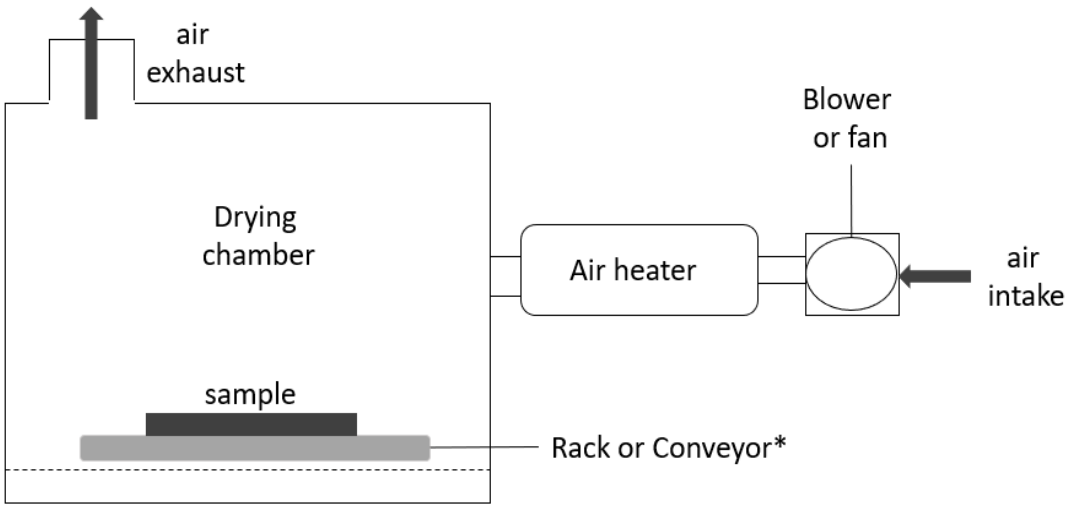

Figure 1.3 Parts of a hot air dryer.

It has been reported that foaming accelerates drying (Brygidyr et al., 1977, Kadam et al., 2012, Raharitsifa et al., 2006, Azizpour et al., 2014, Wilson et al., 2013, Raharitsifa and Ratti, 2010a, Raharitsifa and Ratti, 2010b, Kandasamy et al., 2014, Sangamithra et al., 2015). Additionally, it seems that some foamed materials dry faster at the beginning of the process (soy milk, star fruit) while others at the end (tomato paste, banana) (Kadam et al., 2012). Foam-mat dried products reported in the literature include: ovalbumin or mesquite gum with tamarind (Vernon-Carter et al., 2001), egg albumen with banana (Thuwapanichayanan et al., 2008), glyceryl monostearate or egg albumin with cowpea (Falade et al., 2003), microwave-assisted drying of foams of either glycerine monostearate or soy protein isolate with blackcurrant juice (Zheng et al., 2011), air injected foams of mono and diglyceride stabilizer with tomato paste (Brygidyr et al., 1977), and foams made with Methocel™ and starfruit (Karim and Wai, 1999). In general, the authors of these studies concluded that compared to other drying methods foam-mat drying is a lower-cost technique,

suitable for sticky-viscous materials, and useful to preserve raw food materials, particularly during crop production peaks. However, there is a disagreement in whether air drying (AD) aids the retention of the volatile compounds (Kadam et al., 2012, Ratti and Kudra, 2006) or not (Vernon-Carter et al., 2001, Kandasamy et al., 2014, Falade and Okocha, 2012)

1.4 Freeze-drying

Freeze-drying is the best method to remove water while retaining the characteristics of the original product (colour, flavour and nutrients) when compared to other drying methods (Walters et al., 2014, Ratti, 2001). It was developed to overcome the loss of compounds responsible for the flavour and aroma in foods, which are lost during conventional drying. Food products that are commercially freeze-dried include coffee, tea, vegetables, fruits, meats, and fish. While they do not need refrigeration during storage, they must be protected from moisture uptake (Barbosa-Canovas and Vega-Mercado, 1996). As depicted in Figure 1.4, freeze-drier components include the drying chamber, vacuum pump, refrigeration system, and cold trap or condenser (Hua et al., 2010).

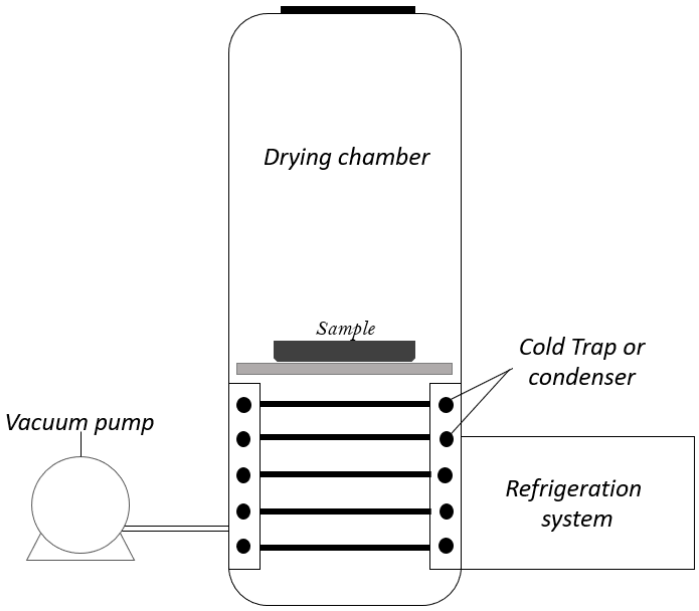

Figure 1.4 Parts of a freeze-dryer.

Freeze-drying is normally divided in two stages according to the kind of water removed from the sample. In the first stage, water is removed by ice sublimation and, in the second stage it is by water desorption. The first stage removes mainly free water, while the second one removes sample-bound water (for which heat plates are needed in the drying chamber). Freeze-driers without heating plates can only be used to study the first stage. Most importantly, a very low vapour pressure inside the drying chamber is required for ice sublimation. Ice sublimation occurs at pressures and temperatures below the triple point for water (Figure 1.5), as described mathematically by the Clausius-Clapeyron equation (Equation 1.1). Equation 1.1 provides the relationship between the saturated vapour pressure P_0 and temperature T_0 of a reference point and the corresponding pressure P_s and temperature T_s of the sample. A is a constant characteristic of the sample (Velasco et al., 2009).

Equation 1.1

$$\ln\left(\frac{P_s}{P_0}\right) = A\left(\frac{1}{T_0} - \frac{1}{T_s}\right)$$

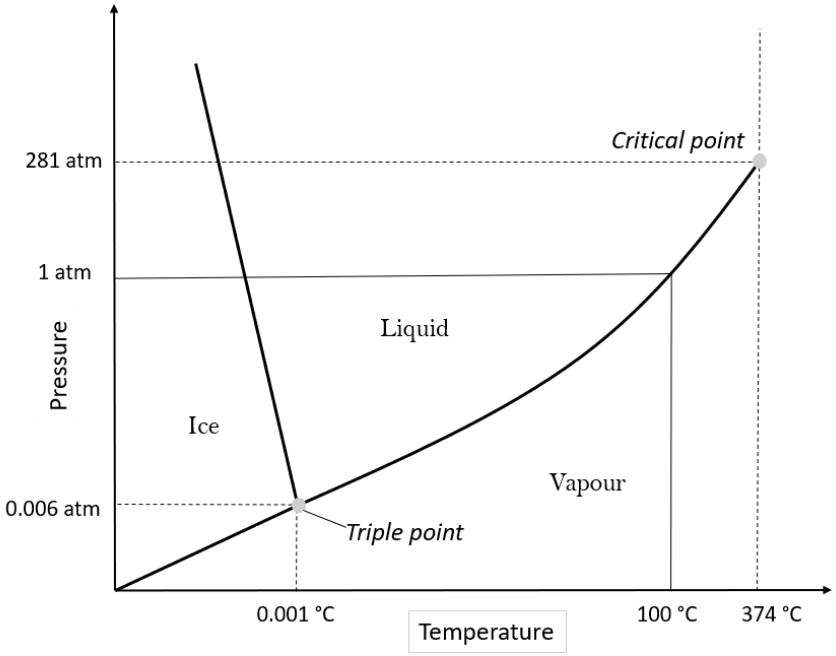

Figure 1.5 Water phase diagram

The freeze-drying process needs the continuous removal of vapour from the surroundings of the sample since sublimation requires a vapour pressure below the triple point. The need of removing vapour from the drying chamber can be described with two equations. The first one is the ideal gas equation (Equations 1.2 and 1.3) which relates the temperature $T$and pressure P of a determined system to the concentration $\frac{n}{V}$ of vapour of a substance (n = number of moles; V = volume). R is the gas constant (461.5 J kg^{-1} K^{-1}).

$$PV = nRT$$ **Equation 1.2**

Or rearranging:

$$C = \frac{n}{V} = \frac{P}{RT}$$ **Equation 1.3**

The second equation is Fick's law (Equation 1.4) which describes the mass flux. Mass flux J occurs in a gradient from a high to low concentration dC of a certain substance through a particular medium over a distance r, the distance between the sublimation interface and the sample surface facing the drying chamber. Since r increases with drying time, it will be referred to as the "dried layer" thickness. D corresponds to the diffusivity of the substance in the media, in this case, the dried layer.

$$J = -D\frac{dC}{dr}$$ **Equation 1.4**

By substituting Equation 1.3 into Equation 1.4 and solving, it can be mathematically described how the mass flux from the sample to the drying chamber occurs when P_s and T_s are larger than P_o and T_o (Equation 1.6). A faster J will occur if the diffusivity (D) is larger. l refers to the thickness of the sample.

$$\int_o^l J\, dr = -\frac{D}{R}\int_o^l d\left(\frac{P}{T}\right)$$ **Equation 1.5**

or

$$J = \frac{D}{Rl}\left(\frac{P_s}{T_s} - \frac{P_o}{T_o}\right)$$ **Equation 1.6**

During freeze-drying, the process stops drying when pressure and temperature reach equilibrium, i.e., when the vapour concentration is the same inside the sample and in the drying chamber and a concentration differential no longer exists. Thus, a constant water removal with condensers or other systems is needed to continue the drying process. A low-temperature condenser inside the drying chamber removes vapour from the surroundings by "trapping" the water molecules as ice. Equation 1.6 also suggests that an increase in D will

increase *J*, and consequently, the drying time will decrease. Samples with air bubbles may have higher mass diffusivity values than samples without air bubbles and thus will dry faster.

One of the main challenges of freeze-drying is the high production costs due to the need for expensive equipment and a long-time process under vacuum and refrigeration (Mascarenhas et al., 1997). Thus to reduce energy costs, it is necessary to cut drying times by improving heat and mass transfer and by finding alternative means to maintain a low water vapor pressure in the chamber (Ratti, 2001). In addition to sample foaming, technical improvement alternatives include microwave assisted freeze-drying (Zheng et al., 2011), use of a desiccant instead of a low-temperature condenser, fluidized atmospheric freeze-drying (Ratti, 2001), and ultrasonic assisted atmospheric freeze-drying (Bantle, 2011). A promising option is "atmospheric freeze-drying" which can be environmentally friendly and economically favourable when combined with heat pumps (Claussen et al., 2007). Freeze drying at atmospheric pressure is possible because the diffusion of water vapour from the drying boundary through the dried layers is driven by the vapour pressure gradient and not by absolute pressure gradients (Claussen et al., 2007). Some products in which atmospheric freeze-drying has been used include fish, strawberries, potatoes, bacteria, and wood pulp (Claussen et al., 2007).

1.5 Foam-mat (hot air) drying versus freeze-drying

Ratti (2001) explained that one of the main advantages of hot air drying (foams or whole or chopped food) compared to freeze-drying was that the cost of the former is 4-8 times lower. However, the use of high temperatures to

evaporate water in hot air-drying affects the nutritional value of the food (Kadam et al., 2012, Kandasamy et al., 2014). Also, the final products obtained by hot air drying and freeze-drying show significant differences in rehydration ratios, storage stability, and sensorial characteristics. The rehydration ratio of freeze-dried foods is generally 4-6 times higher than for hot air-dried foods (Ratti, 2001). This is because the sponge-like structure of the freeze-dried products allows a rapid and more complete rehydration (Barbosa-Canovas and Vega-Mercado, 1996). Michalczyk et al. (2009) compared the storage stability of air- and freeze-dried berries showing that over 10 months at room temperature the latter were less stable. Although Que et al. (2008) observed stronger antioxidant activities in hot air dried pumpkin flour than in the freeze-dried one, Asami et al. (2003) reported higher levels of total phenolic compounds in freeze-dried marionberries, strawberries and corn. Finally, it has been reported that the redness in strawberries (Orak et al., 2012) and pumpkin flour (Que et al., 2008) was better conserved using freeze-drying than by hot air drying. Moreover, Krokida and Philippopoulos (2006) showed that flavour was better retained in freeze-dried apples than in air dried ones.

Because of these hot air drying limitations, foam-mat freeze-drying was proposed as an alternative low-cost food preservation method. Unlike freeze-drying, foam-mat drying is conducted under atmospheric pressure so it can be performed in a continuous process (Sangamithra et al., 2015). Although continuous atmospheric freeze-drying is possible (Meryman, 1959), freeze-drying without vacuum requires pre-treatments such as spray freezing or

foaming (Claussen et al., 2007). The sample pre-treatment before drying increases production costs due to the need for foaming agents and equipment.

1.6 Methodologies to preserve blackcurrants

Blackcurrants (*Ribes nigrum L.*), one of the major berries consumed in processed form, are produced mainly in central and northern Europe and northern Asia (Zheng et al., 2011, Khoo et al., 2012). They are a highly perishable fruit and susceptible to mechanical damage during postharvest handling and transportation (Zheng et al., 2011). Processing could reduce postharvest losses, retain nutritional quality, and yield products with increased shelf life.

Methodologies used to preserve blackcurrants include canning (jams), chilling, freezing, pressing into fruit juices, and dehydration. Fresh and processed blackcurrants are rich in vitamins, sugars, minerals, and polyphenolic compounds (Lefevre et al., 2011) and can be consumed directly or used in product formulations such as puddings, cakes, bakery fillings, fruit dishes, meringue, ice cream, yogurt, fruit bars, and cereal flakes (Zheng et al., 2011). Several studies have identified the nutritional composition changes of blackcurrants after processing in various ways (Boccorh et al., 1998, Zheng et al., 2011, Jaworska et al., 2011, Mattila et al., 2011, Sandell et al., 2009, Hollands et al., 2008, Svensson, 2010). Blackcurrants have also shown high anthocyanin content when compared to other berry fruits and vegetables (Jakobek et al., 2007, Lefevre et al., 2011). Phenolic compounds in blackcurrants are strong antioxidants with a diverse range of biological activities (Khoo et al., 2012).

1.7 Anthocyanins

Anthocyanins are a subclass of polyphenols called flavonoids which represent the largest group of water–soluble pigments in the plant kingdom (Bridle and Timberlake, 1997, Takeoka and Dao, 2002, Yang et al., 2011). Anthocyanins contain three rings (conventionally named A, B and C) with hydroxyls (OH), carbohydrates (e.g., glucose), and other groups attached (Figure 1.6). Anthocyanins also contain an unpaired oxygen (O^+).

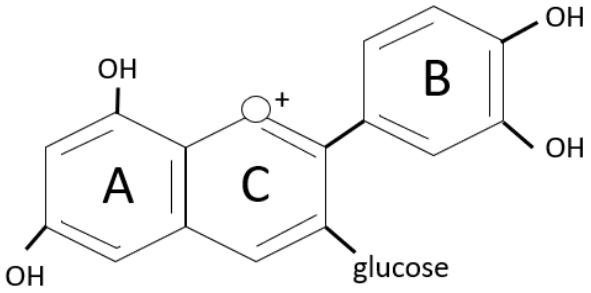

Figure 1.6 Example of an anthocyanin structure.

Dietary anthocyanins are receiving increased attention since they may have a role in the prevention of degenerative diseases (Minihane et al., 2015, Vauzour et al., 2015, Esposito et al., 2015, Lefevre et al., 2011, Nile and Park, 2014, Anttonen and Karjalainen, 2006). Although their antioxidant, anti-carcinogenic, anti-inflammatory, and anti-angiogenic properties have been characterized, the related mechanisms are not yet fully understood (Hellstrom et al., 2013, Lee et al., 2002, Padayachee et al., 2013, Lefevre et al., 2011).

Anthocyanins show great use versatility and have been used in solar cells construction (Narayan, 2012, Hao et al., 2006, Calogero et al., 2012), as pH indicators in nature (Michaelis et al., 1936), in intelligent food packaging (Choi

et al., 2017), as colorants (Chung et al., 2016, Jadwiga, 2006, Hubbermann et al., 2006, Mazza and Brouillard, 1987), and as food supplements (Nile and Park, 2014). Anthocyanins are also used as quality factors in berry juices because their concentration correlates well with the darkness of the berry colour (Hellstrom et al., 2013). Due to their amphoteric structure, the colour of anthocyanins and their stability are pH dependent (Zoecklein et al., 1995).

Isolated anthocyanins are typically unstable and highly susceptible to chemical degradation, which leads to colour fading and loss of bioactivity (Chung et al., 2016). This is primarily caused by oxidation, cleavage of covalent bonds, and oxidation reactions enhanced when an anthocyanin solution is heated (Patras et al., 2010, Ahmed et al., 2004). The stability of anthocyanins depends on several factors including the formation of co-pigments with other phenolic compounds or self-association, their chemical structure and concentration, storage temperature, and the presence of light, oxygen, enzymes (Hellstrom et al., 2013) and various metallic cations (Zoecklein et al., 1995). Anthocyanins are generally more stable in acidic solutions (Tsao, 2010).

Some researchers have analysed the retention of anthocyanins in different matrices subjected to various processing operations including drying. Teixeira-Barcia et al. (2014) analysed anthocyanins in grape skins, observing higher retentions in freeze-dried than oven- or spray-dried samples. Nualkaekul et al. (2012) investigated new non-dairy products containing probiotics, showing that freeze-drying is a gentler technique for anthocyanins because it minimises the thermal degradation of phenolic compounds which is believed to be the main cause of anthocyanin destruction (Teixeira-Barcia et al., 2014,

Mphahlele et al., 2016). However, limited information has been reported on how foam-mat freeze-drying affects anthocyanin retention and recovery. Colour changes after freeze-drying with and without foaming agent have not been reported.

1.8 Food Colour

Most food materials are subjected to some form of processing before reaching consumers. Manufacturers replace colour pigments lost during processing or add them to colourless and unappealing products (Bridle and Timberlake, 1997). Substituting synthetic colorants by less stable natural pigments is one of the major challenges in the food industry (Aguilera et al., 2016). The global market for food colorants in 2008 was U.S. $1.2 Bn, with natural colorants accounting for 31% with an annual growth rate of 5% versus only 1% for artificial (Bamfield and Hutchings, 2010). Anthocyanins are the most commonly found natural pigments and are already widely used in the food industry. Anthocyanins are responsible for the major red, purple and blue pigments in flowers and fruits (Petroni and Chiara, 2011). This gamut of colours is due to their ability to form resonance structures through variation of pH (Mazza and Brouillard, 1987). Normally, anthocyanins are red in acid solutions and blue in basic ones (Tsao, 2010). The degree of hydroxylation, methylation and glycosylation also affect the colour of anthocyanin compounds (Tsao, 2010). The European Union (EU) approved the use of anthocyanins (EU code: E 163) as natural colorants in *quantum satis* (European Commission, 2011) which implies no limit to the amounts that may be added since they are considered safe.

The colour-structure relationships of molecules were probably first studied by Witt in 1876 (Christie, 2015). Witt proposed that dyes contain two types of group that are responsible for their colour, i.e., the chromophore, which is defined as a group of atoms responsible for the colour of the dye; and the auxochromes, which are 'salt-forming' groups of atoms that provide certain colour enhancement (Christie, 2015). Chromophores are typically electron-withdrawing molecular groups containing π (or double) bonds (Owen, 1996), while auxochromes are usually electron-releasing molecular groups linked to one another through a conjugated system (Figure 1.7) (Christie, 2015). The colour of the chromophoric anthocyanidin (anthocyanin without carbohydrate or "aglycon anthocyanin") depends on the number of hydroxyl groups and their orientation in the molecule (Cacelli et al., 2016). Generally, as the number of phenolic hydroxyls increases, the colour changes from pink to blue (Mazza and Brouillard, 1987).

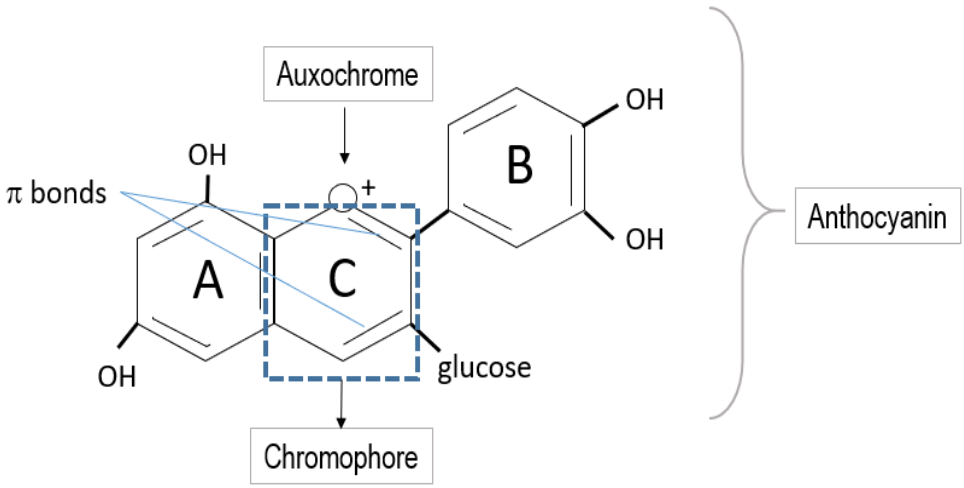

Figure 1.7 Chromophore and auxochrome of an anthocyanin molecule.

Several research groups have tried to stabilise anthocyanins to be used as natural colorants under different conditions (Chung et al., 2016, Cortez et al., 2017). Possible stabilization mechanisms include co-pigmentation, hydrogen bonding, hydrophobic interactions, intermolecular stacking, encapsulation, and complex formation with proteins (Cortez et al., 2017). Substances used to stabilise them include polyphenols, pectin, casein, gum Arabic, agar, potato starch, and aluminium (Chung et al., 2016, Rein, 2005, Considine and Considine, 1982, Asen et al., 1969, Cortez et al., 2017). The use of xanthan gum as anthocyanin stabiliser was studied in this thesis.

1.9 Interactions between polyphenolic compounds and foaming agents

Some studies on the interaction between polyphenolic compounds and proteinaceous foaming agents have been reported. Rodriguez et al. (2015) studied the foaming and interfacial properties of β-lactoglobulin and casein macropeptide affected by green tea polyphenols. They concluded that polyphenols improved the foam stability: the interfacial properties and drainage were worse than in foams without polyphenols. In another study, foams made with catechin and a Tween 20/β-lactoblobulin mixture, foamability and foam stability was improved (Sarker et al., 1995). Moreover, Delgado-Sanchez et al. (2017) showed that foams prepared with tannins were very stable and rigid after drying. They also mentioned that temperature is a crucial parameter not only because it affects foam stability but because it triggers the crosslinking process that ends with rigid foam (Delgado-Sánchez et al., 2017). However, anthocyanins have not received much attention with regards to foam formation and stability despite the fact that anthocyanin-rich fruits such as strawberries, blueberries

and blackcurrants are widely used along with proteinaceous bases to produce foams (e.g., mousses, baked goods, ice creams, macaroons and meringue).

1.9.1 Polyphenol-protein separation methods

Because proteinaceous foaming agents tend to bind with polyphenols, determination of the concentration of anthocyanins in a foam typically requires a method to separate them from the foaming agent. Methods for the anthocyanin separation/extraction from complex food matrices include the use of ammonium sulphate (AM) (Wu et al., 2011, Chen et al., 2013), trichloroacetic acid (TCA) (Han et al., 2006), methanol/hydrochloric acid (metOH-HCl) (Rosales-Soto et al., 2012, Awika et al., 2004), and C18 cartridges (Pace et al., 2014, Scibisz et al., 2012). Anthocyanins can be separated from protein matrices via protein digestion, using cathepsin B for ovalbumin (Han et al., 2011) or porcine pepsin for many proteins (Uzunovic and Vranic, 2008, Chen et al., 2013). The latter has been reported to have low anthocyanin affinity. However, traces of either porcine pepsin or egg albumin can increase the turbidity of samples and modify the spectrophotometric readings. Studies suggest that anthocyanins present in a commercial blackcurrant (Uzunovic and Vranic, 2008) and blueberry juice (Chen et al., 2013) remain stable after acid pepsin digestion.

1.10 Spectroscopy

In this study, light, colour and fluorescence spectrometry were used to quantify the apparent anthocyanin content of samples, characterise the colour of anthocyanin in dried samples during storage, and to identify traces of protein in anthocyanin solutions. When light interacts with matter, it may be reflected,

absorbed, scattered or transmitted (Martelo-Vidal and Vazquez, 2016). Absorption/reemission (fluorescence/phosphorescence) or absorbance and bond breaking (photochemical reaction) can also occur (Owen, 1996).

Absorption, which can be detected in the visible and ultraviolet region, is the process in which an increase to a higher energy level (excited state) happens after applying to a molecule an electromagnetic radiation with a given wavelength. Electromagnetic radiation that is not absorbed by the molecule is either reflected, scattered or transmitted. Absorption by anthocyanins depends on a variety of structural configurations of their C ring (see Figure 1.7), number of hydroxylated groups, and the type and quantity of sugars.

1.10.1 Light spectroscopy

Light spectroscopy is a widely used technique to quantify anthocyanins (Lee et al., 2008, Aguilera et al., 2016, Ahmed et al., 2004, Han et al., 2006, Jakobek et al., 2007, Abbasi and Azizpour, 2016, Azima et al., 2014, Bobbio et al., 1994, Laleh et al., 2006, Lee et al., 2002). To determine the concentration of one or more molecules (also called analytes) via light spectroscopy, the amount of radiation that transmits through the sample is measured and compared to a reference sample (Martelo-Vidal and Vazquez, 2016). This quantitative analysis relies on Beer's law describing a correlation between the light absorbed and the number of absorbing molecules or analyte concentration (Owen, 1996).

An important point to consider in the quantitative analysis of anthocyanins by light spectroscopy is that the relationship between light absorbed and concentration is not always linear. In the case of anthocyanins, negative or positive deviations from Beer's law can be observed at pH <2 (Bridle

and Timberlake, 1997) and pH >3.5 (Margalit, 2016), respectively. This phenomenon is the result of self-association (Bridle and Timberlake, 1997) and ionic dissociation of anthocyanins in solution.

Anthocyanins analysed spectrophotometrically are determined as total monomeric anthocyanins (Lee et al., 2008). This is possible since monomeric anthocyanins undergo pH-driven reversible structural transformations. At pH 1.0, a coloured oxonium form is more predominant than at pH 4.5 where a colourless hemiketal form is more abundant (Lee et al., 2005). This is the basis for "the pH differential method" included in the standard procedure of the Association of Official Agricultural Chemists (AOAC). Lee et al. (2008) compared high–performance liquid chromatography (HPLC) to the pH differential spectrophotometric method and concluded that the latter is a simple, rapid and economic way to determine the amount of anthocyanins in a sample. In this method, the absorbance of the sample at pH 1 and 4.5 are measured at 520 nm (maximum wavelength of the main pigment) and at 700 nm (to correct for haze). The difference between absorbance measurements at the two pH levels at 520 nm is proportional to the pigment concentration (Equation 1.7). Since cyanidin-3-glucoside with a maximum absorbance at 520 nm is the most abundant anthocyanin, concentrations are normally expressed as anthocyanin equivalents with this anthocyanin as the reference.

Equation 1.7

$$\text{Anthocyanin pigment concentration(cyanidin-3-glucoside equivalents in } \frac{\text{mg}}{\text{L}}\text{)}$$

$$= \frac{\big((A_{520nm} - A_{700nm})pH1.0 - (A_{520nm} - A_{700nm})pH4.5\big)(MW)(DF)(10^3)}{(\varepsilon)(l)}$$

where:

MW = molecular weight of cyanidin − 3 − glucoside (449.2 $\frac{\text{g}}{\text{mol}}$)

DF = dilution factor

ε = molar extintion coefficient

l = pathlenght in cm

An alternative to the sample adjustment to pH 4.5 is the use of sodium metabisulphite (SO_2) to decolour monomeric anthocyanins (Timberlake and Bridle, 1976). Then, total anthocyanin (TA) content (in mg/l) can be calculated directly from the spectrophotometer readings according to Equation 1.8.

Equation 1.8

$$TA = 20\left[A^{HCl}_{(520nm)} - \frac{5}{3}A^{SO2}_{(520nm)}\right]$$

where ($A^{HCl}_{(520nm)}$) is the spectrophotometer reading of the anthocyanins in an HCl solution and ($A^{SO2}_{(520nm)}$) corresponds to the reading in the spectrophotometer of a sample mixed with SO_2. Figure 1.8 shows diagrams of the light spectrophotometer with samples with HCl and SO_2.

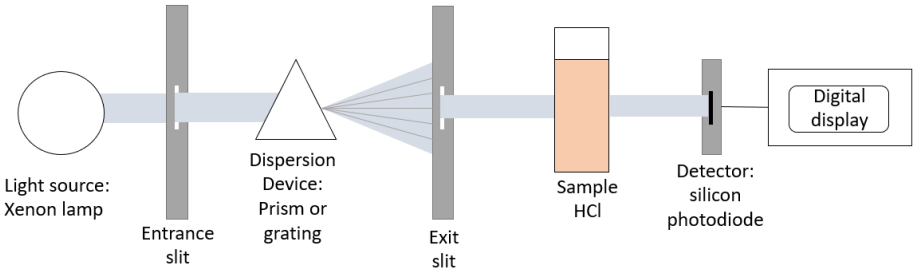

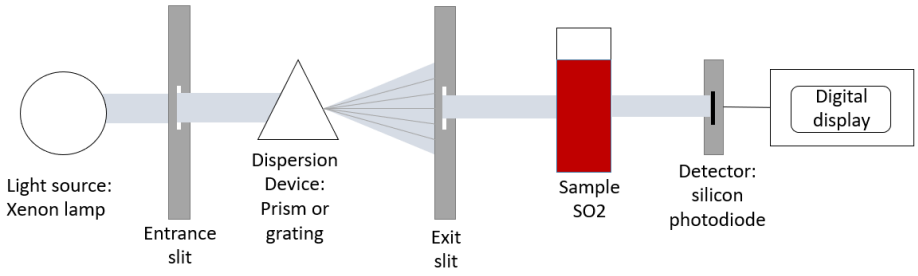

Figure 1.8 Light spectrophotometer with samples in hydrochloric acid (HCl) and sodium metabisulphite (SO_2).

1.10.3 Colour spectroscopy

Colour spectroscopy uses especially designed light spectrophotometers called colorimeters with detector systems comparing samples to a desired or standard colour. The sample reflectance and transmittance are quantified with a colour space system stablished in 1976 by the Commission Internationale de l'éclairage (CIE) expressing readings as the CIE colorimetric coordinates *L, a* and *b* and thus the acronym CIELAB (Berns, 2000). These three coordinates represent the lightness "*L*" (*L* = 0 black; *L* = 100 white), "*a*" for the red/green (+*a* = red; -*a* = green) and "*b*" for the yellow/blue (+*b* = yellow; -*b* = blue) of the sample in the CIE space. Each detection coordinate has spectral sensitivities equal to one of the colour matching functions of a specified CIE standard observer. One of the most commonly used standard observer is the D65/10° illuminant/observer. D65 corresponds to an average midday light in western Europe/Northern Europe and 10° corresponds to the angle of view.

L, a and *b* values are used to calculate 3 parameters: 1) ΔE^*_{ab} (Δ= incremental change, E = Empfindung, from German "sensation", and suffix *ab* corresponds to CIE76), the first and most common manner to express a change in colour sensation; 2) ΔH (change in hue or pure spectrum of colour); and, 3)

ΔC (change in chroma or colour saturation). These parameters describe colour differences between a standard colour and a sample. ΔH and ΔC describe bathochromic and hypsochromic effects in the sample, i.e., a movement of the spectral band position of a sample towards longer wavelengths (red) or shorter wavelengths (blue), respectively. In blackcurrant anthocyanin solutions, red and blue are the most noticeable sample colours. Most importantly, the sample colour does not correspond to the absorbed spectral band position. On the contrary, the observed colour of a sample corresponds to what it transmits, reflects and scatters. If a sample appears to absorb wavelengths in the spectral band corresponding to green, the sample will appear red to our eyes. The circle diagram shows a basic representation of the colour opposition observed (Figure 1.9).

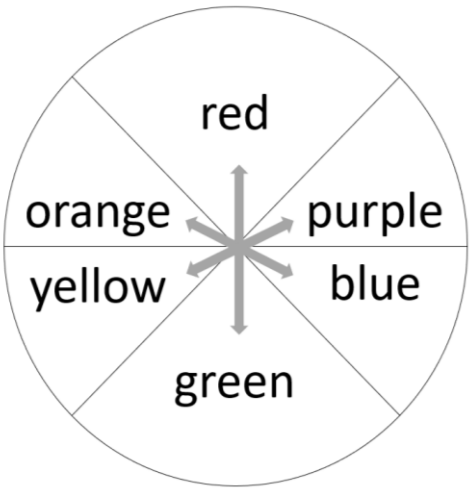

Figure 1.9 Colour circle with arrows indicating colour opposites.

The use of colorimeters for the colour analysis of anthocyanins has been reported for acerola (De Rosso and Mercadante, 2007), pomegranate peel (Mphahlele et al., 2016), blackcurrant and elderberry (Hubbermann et al., 2006),

purple carrot (Chung et al., 2016), plum (Ahmed et al., 2004), purple- and red-flesh potatoes (Reyes and Cisneros-Zevallos, 2007), and in many other applications.

1.10.3 Fluorescence spectroscopy

Luminescence is the phenomenon where molecules exhibit light emission (Perkin-Elmer, 2006). Fluorescence is a type of luminescence in which light at a short wavelength is applied to a molecule called a fluorophore which, in response, emits light at a longer wavelength. Fluorescence intensity (FI) is a measure of this emission of light and it is not an absolute measurement. FI is usually quantified in relative fluorescence units (RFU). FI is detected by the use of a fluorescence spectrophotometer, emitting and detecting different kinds of light wavelengths. Fluorescence spectrophotometers have the same principle of a light spectrophotometer but they need excitation and emission filters (monochromators) in addition to a light source and detector (typically a photomultiplier tube, PMT) (BMGLabtech, 2016). Additional filters and mirrors are used to improve the unit performance (Figure 1.10).

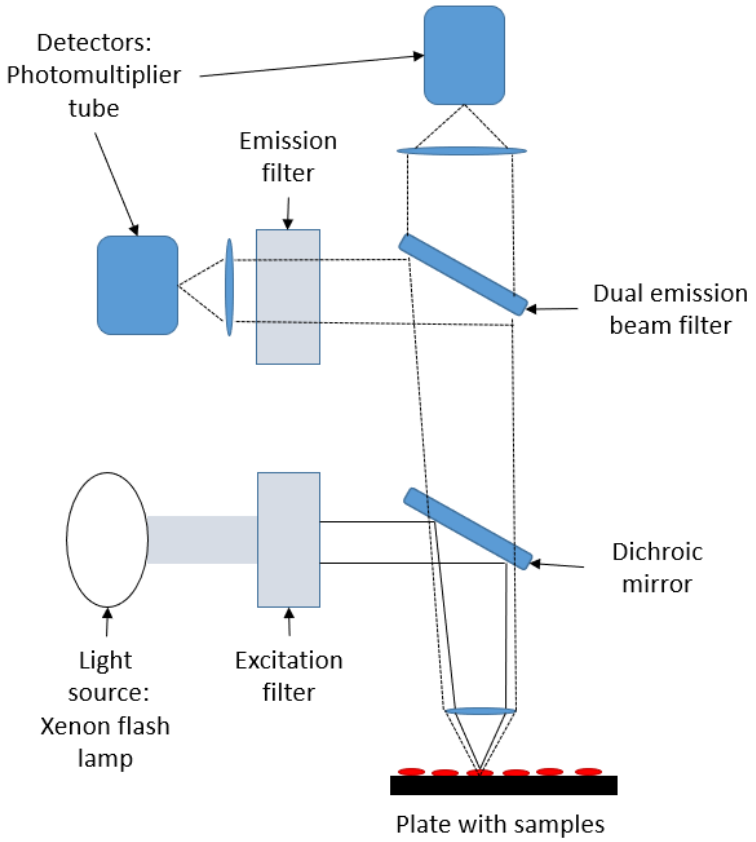

Figure 1.10 Fluorescence spectrophotometer components.

Fluorescence spectroscopy is used to quantify protein unfolding and refolding induced by chemical denaturants, and changes in temperature, pH or pressure (Ferrel, 2015, Royer, 1995). This is possible since the fluorescence properties of protein associated with aromatic amino acids such as tryptophan, tyrosine and phenylalanine are modified by the aforesaid conditions (Lin et al., 2016, Royer, 1995). The presence of quencher molecules such as polyphenols (e.g., anthocyanin) can also decrease the amino acid fluorescence (Hassan, 2012, Lin et al., 2016, Papadopoulou et al., 2005). This phenomenon occurs when anthocyanins and proteins (e.g., egg albumin) interact, forming a non-fluorescent

compound (Papadopoulou et al., 2005). This phenomenon can be used to analyse the effect of the presence of proteins in anthocyanin solutions.

1.11 Analysis of sugars

Sugars are highly hygroscopic and thus widely used to retain moisture to increase the shelf life of bakery and other food products. Sucrose contains one moiety of glucose and one of fructose forming hydrogen bonds with water molecules (Mathlouthi and Genotelle, 1998). Since the hygroscopic property of sugars affects water retention, the blackcurrant juice sugar content needs to be known.

Sugars can be quantified by high performance anion exchange chromatography coupled with pulsed amperometric detection (HPAEC-PAD). HPAEC can separate carbohydrates at very low concentrations (picomole) because at high pH, neutral monosaccharides such as fructose, mannose, and glucose are partially ionized (Rohrer, 2013). The Thermo Scientific™ Dionex™ CarboPac™ PA20 column typically used is a polymeric, hydrophobic, anion exchange resin stable across the whole pH spectrum (Dionex, 2011) and the electrochemical detector Thermo Scientific™ Dionex™ ED40 is a flow-through cell with a silver/silver-chlorine reference electrode, a counter titanium electrode and, a gold electrode. The ED40 measures current resulting from the application of potential (voltage) across the electrodes in the flow-through cells (Dionex, 1995). The ED40 has several detection modes. Pulsed amperometry detection (PAD) works by measuring the current resulting from the oxidation or reduction of the analyte molecules on the surface of the working electrode during a portion of time by applying a repeating (pulsed) potential (Dionex,

1995). The oxidation or reduction of the analyte molecules happens when a potential is applied between the gold (working) and the silver (reference) electrodes. A constant potential difference is assumed between the reference electrode and the sample. Therefore, changes in the potential difference detected are assumed to arise between the working electrode and the sample.

The Thermo Fisher™ DX500 (Dionex™ Corporation, Sunnyvale, California) depicted in Figure 1.11 shows all system components including the gradient pump, injector, column, and detector. The sample, e.g. blackcurrant juice, is treated prior to injection into the chromatograph to remove fibres and other compounds that could interfere with the analysis of sugars, and it is also diluted to a concentration in the range of the standard curve.

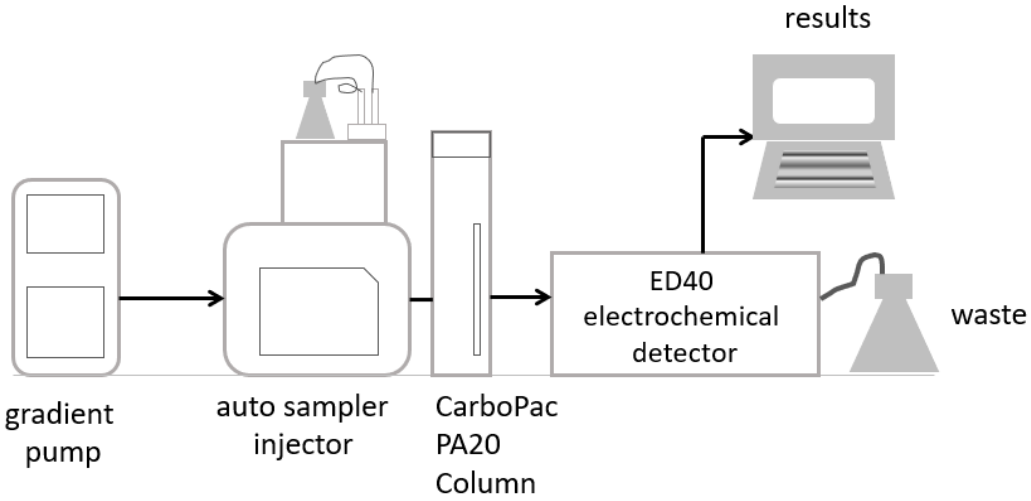

Figure 1.11 Diagram of Chromatograph

1.12 Mathematical models of foams during freeze-drying

Several mathematical models have been proposed for the study of freeze-drying (Mascarenhas et al., 1997, Sadikoglu and Liapis, 1997, Figueiredo-Borgognoni et al., 2012, Nastaj and Witkiewicz, 2009, Sheehan and Liapis, 1998,

Schoen et al., 1995, Boss et al., 2004, Chakraborty et al., 2006). However, mathematical models for foam-mat freeze-drying are relatively new. The challenges of designing these models include the increase in void spaces associated with the air bubbles in the sample. Sochanski et al. (1990) proposed a model in which the bubbles of foamed milk were assumed to be open pores that allow free circulation of air and water vapour in the entire volume of the foam throughout the drying process. These pores or void spaces increase the total porosity of the sample which is equivalent to the air volume fraction in foams. Both porosity and air volume fraction are the ratio of total void space per total volume of sample (Rahman, 2008). Furthermore, the size of the bubbles may affect the drying rate. In a study of egg white foamed apple juice, it was observed that a small pore size increased heat and mass transfer which are the basis of the drying rate analysis (Raharitsifa and Ratti, 2010a, Raharitsifa and Ratti, 2010b).

Mathematical models proposed hitherto do not relate the air volume fraction and the density of the samples to the drying rate of freeze-dried foams, which is an easy way to predict the latter. This is important because when designing a food product, these relationships need to be considered to reduce production costs and final product characteristics. Therefore, there is a need for a mathematical model that shows differences in drying rate between foams and non-foamed juice during the first stage of freeze-drying (sublimation) and reflecting the sample characteristics. This model should also show how the presence of anthocyanin affects the drying rate in freeze-dried foams.

1.13 Aims and objectives

The main aim of this research was to characterise blackcurrant foams used widely in the food industry and to show how their formulations affect the drying rate during freeze-drying, anthocyanin retention and the colour of the powders obtained. In order to achieve this aim, the following work was required:

- The anthocyanin retention after foam-mat freeze-drying was analysed by light and fluorescence spectrophotometry after a proposed separation method of the anthocyanin-egg albumin complex via porcine pepsin.
- Foams with and without anthocyanin were prepared in order to elucidate differences given by the polyphenols in a macroscopic scale and how they influence the freeze-drying rate.
- A mathematical model was developed to help understand the differences in drying rate between samples.
- Sample colour differences of the anthocyanin-egg albumin complex were analysed over 5 months after freeze-drying.

Chapter 2 Experimental Materials and Methods

2.1 Preparation of juice and zero anthocyanin samples

Three samples of bottled concentrated blackcurrant juice (SKU # 521105, Ribena®, Lucozade Ribena Suntory Ltd., Stockley Park, Uxbridge, UK) differing in anthocyanin content were purchased locally and used as stock samples. Juice foams were prepared from juice as is (J100) or diluted 1:4 with water (J25). The pH of juice as is, and after dilution, was measured with a pH meter previously calibrated with pH 4 and 7 buffers (Jenway Model 3520, Cole Parmer Ltd, Staffordshire, UK).

A zero anthocyanin (ZA or model) solution with the same sugar profile determined for the commercial blackcurrant juice samples and the ascorbic acid content declared by the juice manufacturer but without anthocyanins was also used to prepare foams. In a 200 ml volumetric flask placed on a Stuart™ magnetic hotplate stirrer (Model SB162, Sigma-Aldrich, Darmstadt, Germany), 2.6 g D(-)-fructose (98%, Product # 161350025, Acros Organics, Geel, Belgium), 14.8 g D(+)-glucose monohydrate (heavy metals <10 ppm as Pb, Maltose <0.5%, Moisture 7-9.5 % wb, Product # 24371.297, VWR Chemicals, Oud-Heverlee, Belgium), 11.6 g D(+)-sucrose (>99.5%, Product # 84097, Sigma Aldrich), and 11 ml of a 22.5 g l^{-1} L-ascorbic acid stock solution (99%, Sigma-Aldrich) were added and brought to volume with water acidified to pH 2.8-3 with 1 M HCl (Hach Co., Loveland, CO). Foams were prepared from the model solution as is (ZA100s) or diluted 1:4 with water (ZA25s).

2.2 Preparation and characterization of foams

2.2.1 Preparation of foam samples

Blackcurrant juice and model solution foam samples were prepared in a stand mixer with the whisk attachment (Model KM336, Kenwood™ Classic Chef, Havant, UK) using 100 ml of juice or model solution, 4 g albumin (No. 400451000, Acros Organics, Thermo Fisher Scientific, Geel, Belgium), and 0.05 g xanthan gum from *Xanthomonas campestris* (CAS Number 11138-66-2, Sigma-Aldrich Co., St. Louis, USA). After 30 min (speed no. 6), duplicate foam samples (10 g) were poured into two aluminium dishes (8.1 cm diameter, 2.2 cm height) and stored overnight at -30 °C.

2.2.2 Characterization of foams

The foam bubble size distribution (*BSD*) was determined by placing foams in a slide ring (3 mm height, 15 mm diameter). Foam pictures (800x600 pixels RGB) were taken under a light microscope (Bresser LCD Micro, Bresser GmbH, Rhede, Germany) with a 4x magnification. Bubbles (1010 for each foam sample) were measured using ImageJ calibrated to 611 pixels/mm according to a graticule (100 x 0.01 = 1 mm) photographed with the same magnification and pixel size (Kröner and Doménech Carbó, 2013). Cumulative frequency and frequency density graphs for the bubble diameter (0.005 to 0.83 mm range and 0.0125 mm bin width) were used to compare the four foam types. The Sauter mean bubble diameter D_{32} was determined as follows (Raharitsifa et al., 2006):

Equation 2.1

$$D_{32} = \frac{\sum d_n^3}{\sum d_n^2}$$

where d_n is the diameter of the nth bubble and the summation is over all bubble measurements. The standard deviation (σ) of the diameter of bubbles for each sample was calculated in Excel.

The air volume fraction (*AVF*) was obtained based on the solution (ρ_L) and foam (ρ_F) density for each sample and expressed as follows (Raharitsifa et al., 2006):

Equation 2.2

$$\phi = 1 - \left(\frac{\rho_F}{\rho_L}\right)$$

Solution and foam density values were determined by weighing a brand-new 115 ml crystallizing dish fully-filled with the sample (Raharitsifa et al., 2006) in an analytical balance (readability = 0.0001 g. Ohaus Explorer Analytical Balance, UK).

To quantify foam drainage, the amount of liquid drained from 20 ml foam samples poured into a wide-mouth graduated cylinder was measured after 90 min.

Finally, viscosity was measured in a Malvern rheometer (Kinexus Ultra, Worcestershire, UK) using cone–plate geometry CP2/60:PL65 (60 mm diameter, 2^o angle cone over a 65 mm plate). The operating gap was 70 μm, and the shear rate ranged from 0.1 to 10 s^{-1} at 25 °C. Viscosity was analysed immediately after whipping and 1.5 hours after whipping.

2.3 Freeze-drying of foam samples

Frozen samples were placed the next day on 100 g precision spring scales (Model 10100, precision: max tolerance ± 0.3% of load. Pesola A.G., Schindellegi,

Switzerland) (Nastaj and Witkiewicz, 2009) and freeze-dried at -50 °C, 0.04 mbar in a freeze-drier (Alpha 1-4 LSC, Martin Christ Gefriertrocknungsanlagen GmbH, Osterode am Harz, Germany). Sample weight was recorded every hour until reaching constant weight after about 6-8 h. The change in mass (ΔM) was calculated as the initial weight (m_i) minus the weight after an hour (m_{t+1}) and plotted against the square root of time. The slope of the curve corresponds to the drying rate (DR) of the samples. The same procedures were repeated for undiluted and diluted juice and model solution samples. Freeze-dried foams prepared from J100, J25, ZA100s and ZA25s will be referred to as FJ100, FJ25, ZA100sf and ZA25sf, respectively. The moisture content of wet and dried samples was determined at 140°C for 4.5-5 min and at 115°C for 11-12 min, respectively, using an HB43-S Halogen Moisture Analyzer (Mettler-Toledo AG Laboratory & Weighing Technologies, Greifensee, Switzerland).

2.4 Sugar content in blackcurrant juice

The sucrose, glucose and fructose content of blackcurrant juice was determined by high-performance anion-exchange chromatography coupled with pulsed amperometric detection (HPAEC-PAD) with a 65 µeq/column anion exchange capacity (Thermo Fisher Model DX500 with an AS500 autosampler, GP40 gradient pump, LC20 column oven at 30 °C, ED40 electrochemical detector with gold working and silver reference electrodes, 3 x 150 mm CarboPac PA20 analytical column with 3 x 30 mm guard). Blackcurrant juice (1 ml), first diluted with 4 ml MilliQ water (Millipore Inc.), was added (1 ml) to 4 ml absolute ethanol (CAS Number 64-17-5, Merck KGaA, Darmstadt, Germany), and centrifuged at 3000 rpm for 10 min at 20 °C in a Thermo Scientific™ Heraeus™ Megafuge™ 16R

(Thermo Electron LED GmbH, Osterode, Germany). Supernatant diluted 50 times with MilliQ water, was well mixed, filtered (300 μL) using 0.45 μm PTFE membrane filters (Chromacol Ltd., Welwyn Garden City, UK), and then transferred directly into autosampler vials. Autosampler-injected samples (10 μl) were eluted following the program reported by Karim et al. (2017) with some modifications: 0.4 ml/min isocratic elution of 60 mM NaOH for 10 min, increased to 200 mM NaOH at a rate of 28 mM min^{-1}, held constant for 2 min, then reduced back to 60 mM at a rate of 46.7 mM min^{-1}, and finally held constant for 5 min.

Standard curves with concentrations of 0.02, 0.04, 0.06, 0.08, 0.1, 0.12 and 0.14 ug/10ul in MilliQ water were prepared using D(-)-fructose for biochemistry (99%, Prod. 161350025, Acros organics, Geel, Belgium), D(+)-glucose monohydrate for biochemistry (Prod. 24371.297, VWR Chemicals, Leuven, Belgium), and sucrose for molecular biology (≥99.5%, HPLC, code 84097, Sigma Aldrich, Darmstadt, Germany).

2.5 Anthocyanin analysis: spectroscopy

2.5.1 Anthocyanin quantification

The anthocyanin content of blackcurrant juice was determined spectrophotometrically (Jenway Model 6715, Cole-Parmer Inc., Stone, Staffordshire, UK) as described by Zoecklein et al. (1995). Total anthocyanin (TA) content expressed as cyanidin-3-glucoside equivalents (mg/l) was determined using Equation 1.8, i.e., TA =20 $\left[A^{HCl}_{(520nm)} - \frac{5}{3}A^{SO2}_{(520nm)}\right]$. The first term, ($A^{HCl}_{(520nm)}$) was obtained by mixing 200 μl sample with 10 ml HCl acid (1 N, Cat. 23213-53, HACH Company, Loveland, CO). After 3 h at 25°C, the solution was

read at 520 nm in a light spectrophotometer Jenway Model 6715 (Bibby Scientific Ltd, Staffordshire, UK). To account for dilution, actual values of ($A^{HCl}_{(520nm)}$) were obtained by multiplying readings by 10/0.2. The second term, ($A^{SO2}_{(520nm)}$) corresponds to the reading in the spectrometer of the sample in the cuvette (10 mm path length, 3.5 ml PMMA, dimension of 12.5 x 12.5 x 45 mm, Brand Gmbh Co, Wertheim, Germany) mixed with 20 μl sodium metabisulphite (mixed by inversion for 1 min), and read at the same wavelength. The sodium metabisulphite solution [20% (w/v)] was prepared by dissolving 2 g sodium metabisulphite (CAS Number 7681-57-4, reagent grade, 97 %, Sigma Aldrich, Darmstadt, Germany) in 10 ml deionized water. Finally, blanks were prepared using a saturated solution of potassium hydrogen tartrate (Item P/5480/60, CAS no. 868-14-4, Fisher Scientific, Loughborough, UK) and 4 g D(+)-glucose monohydrate (Item 24371.297, for biochemistry, VWR Chemicals, Leuven, Belgium) in 20 ml distilled water. Readings were performed in triplicate and pH 2.8 to 3 at 23 °C.

Since foams contained albumin, a pepsin pre-treatment was required to separate anthocyanins from proteins. First, to break foams, 8 ml hydrochloric acid (HCl 1N, Hach Co) was poured on the foam, mixed, and left undisturbed for 1 h. The liquified foams were then transferred to beakers and adjusted to pH 1.2 with HCl. A 0.32% w/v solution of porcine pepsin (CAS Number 9001-75-6, Product # 77160-25G, 600-1200 units/mg, Sigma Aldrich) was added to each beaker and samples were then digested in the dark for 12 h in a 36 °C water bath with continuous agitation. Samples were centrifuged for 40 min at 10000 g and 20 °C (Avanti High-Speed Centrifuge Model J-30I, Beckman Coulter Life Sciences,

Brea, CA). Supernatants were recovered and divided equally in 3 beakers. Sodium hydroxide (NaOH, 2 M) was used to adjust the supernatant pH to that of blackcurrant juice pH (2.8 ± 0.1) and then analysed for anthocyanin content as previously described. In the case of freeze-dried foams, samples were reconstituted to their % water loss, subjected to the same pepsin treatment described above, and then analysed for anthocyanin content.

Finally, 100 ml of each of the three juice samples were whipped for 30 min under the same conditions for foam preparation and analysed for anthocyanin content.

2.5.2 Colour spectroscopy

For determining colour changes of blackcurrant juice after conventional and foam-mat freeze-drying, samples were prepared in the following way: Two new bottles of blackcurrant juice were mixed for this analysis. J25 and FJ25 were prepared as stated before. Also prepared was a solution of J25 with xanthan gum (JX) by adding 0.05 g xanthan gum to every 100 ml J25. All samples were freeze-dried as previously described in aluminium containers (14 cm x 12 cm x 5 cm) in three batches of 48 h each.

Freeze dried samples were divided in two categories: vacuum (Vac) and no vacuum (Air). Before packaging, each sample was finely ground in a mortar. The samples analysed were: J25 vacuum (J25,Vac), J25 no vacuum (J25,Air), FJ25 vacuum (FJ25,Vac), FJ25 no vacuum (FJ25,Air), JX vacuum (Xanthan,Vac) and JX no vacuum (Xanthan,Air). Co-extruded nylon/polyethylene bags filled with each powdered sample were heat-sealed (Model J-V002, The Food Machinery Company Ltd., Rochester, UK) at -15 cm Hg or atmospheric pressure for vacuum

and air samples, respectively. All samples were covered in aluminium foil and stored in a desiccator inside a refrigerator at 6 °C. Two unopened bags of each treatment were analysed after 5 months storage.

Non-freeze-dried samples (liquid) J100 and J25 were prepared as stated in section 2.1; FJ25 was prepared as stated in section 2.2.1 and was left to stand until the foam had broken. Non-freeze-dried J100, J25 and FJ25 samples were stored in six bottles containing 30 ml of each sample and stored inside a refrigerator at 6 °C for 5 months. Also, the pH of the J25 sample was modified with HCl and NaOH *quantum satis* to obtain pHs from 1 to 6.

The analysis of colour was performed in the following way. Each month, spectral % transmittance and % reflectance values were measured for liquid and solid (powders) samples, respectively. Measurements were performed from 400 to 750 nm according to the CIELAB colour scale relative to the standard D65/10° illuminant/observer using a Color-Eye 7000A spectrophotometer (Gretag Macbeth, New Windsor, NY) and 10 mm quartz cuvette (internal dimensions 10 x 26 x 58 mm, external dimensions 14 x 31 x 62 mm, part number A-OC/T7, photometric resolution 0.001%). Liquid samples were read in the internal compartment of the spectrometer. Powder samples (without dissolving) were read in the external holder of the spectrometer covered with a black cloth.

Freeze-dried and non-freeze-dried J25 samples (at month 0) were used as standard colour for all dried and liquid samples, respectively. ΔE^*_{ab} was calculated as follows:

Equation 2.3

$$\Delta E^*_{ab} = \sqrt{(L^*_2 - L^*_1)^2 + (a^*_2 - a^*_1)^2 + (b^*_2 - b^*_1)^2}$$

where subscript 1 corresponds to the standard colour and suffix 2 corresponds to the sample to be compared.

The change in hue (ΔH) was calculated as:

Equation 2.4

$$\Delta H = \sqrt{(\Delta E^*_{ab})^2 - (\Delta L^*)^2 - (\Delta C^*_{ab})^2}$$

where ΔE^*_{ab} was calculated according to the previous equation and ΔL^* and ΔC^*_{ab} were calculated with the following equations:

Equation 2.5

$$\Delta L^* = L^*_2 - L^*_1$$

Equation 2.6

$$\Delta C^*_{ab} = C^*_{sample} - C^*_{standard}$$

where

Equation 2.7

$$C^*_{sample} = \sqrt{(a_2)^2 - (b_2)^2}$$

Equation 2.8

$$C^*_{standard} = \sqrt{(a_1)^2 - (b_1)^2}$$

2.5.3 Fluorescence spectroscopy

Liquid samples (300 µl of juice and supernatants) were poured directly with manual pipette (Catalog No. 3124000113, Eppendorf Research Plus, Hamburg, Germany) into three fluorescence plate wells. Solid samples (0.022 ± 0.002 g) were carefully weighed (balance Ser. No. 131195007, Kern&Sohn,

Balingen, Germany) and mixed with 150 μl of MilliQ water with a pipette (Catalog No. 3123000055, Eppendorf Research Plus, Hamburg, Germany) into three other wells and mixed thoroughly. J100 and J25 were used as the corresponding blanks to correct background fluorescence. Samples were tested as shown in Table 2.1. The fluorescence intensity of samples was measured in a spectrometer PHERAstar FS (BMG Labtech, Germany) with an excitation wavelength of 350 nm and emission at 460 nm, at an average temperature of 25 °C. Digested samples and foams had an average pH = 1.2 and pH = 4, respectively.

Table 2.1 Experiment design of samples tested in the fluorescence spectrophotometer. ● indicates a tested sample.

				After Pepsin treatment		
Sample	Untreated (blank)	After foaming (no freeze-drying)	After foam-mat freeze-drying	Untreated	After foaming (no freeze-drying)	After foam-mat freeze-drying
J100	●	●	●	●	●	●
J25	●	●	●	●	●	●

The quenching effect of blackcurrant anthocyanin on egg albumin was determined by mixing 2 g untreated egg albumin and 0.025 g of xanthan gum mixed with solutions of J100/distilled water: 0 ml/100 ml (used as blank), 25 ml/75 ml, 50 ml/50 ml and 100 ml/0 ml. Also, the stock solution was diluted 1 part in 4 parts with distilled water, foamed and treated with pepsin. Then, the solids were mixed with different concentrations of anthocyanin solutions as follows (J100/distilled water): 100 ml/0 ml, 80 ml/20 ml, 60 ml/40 ml, 40 ml/60 ml, 20 ml/80 ml and 0 ml/100 ml; the last one was used as blank. These were prepared as stated before for solid samples in the fluorescence spectrometer. Three different batches were tested with the same juice. The complete foam-mat

freeze-drying and analysis process for the samples for blackcurrant juice is described in the diagram below (Figure 2.1).

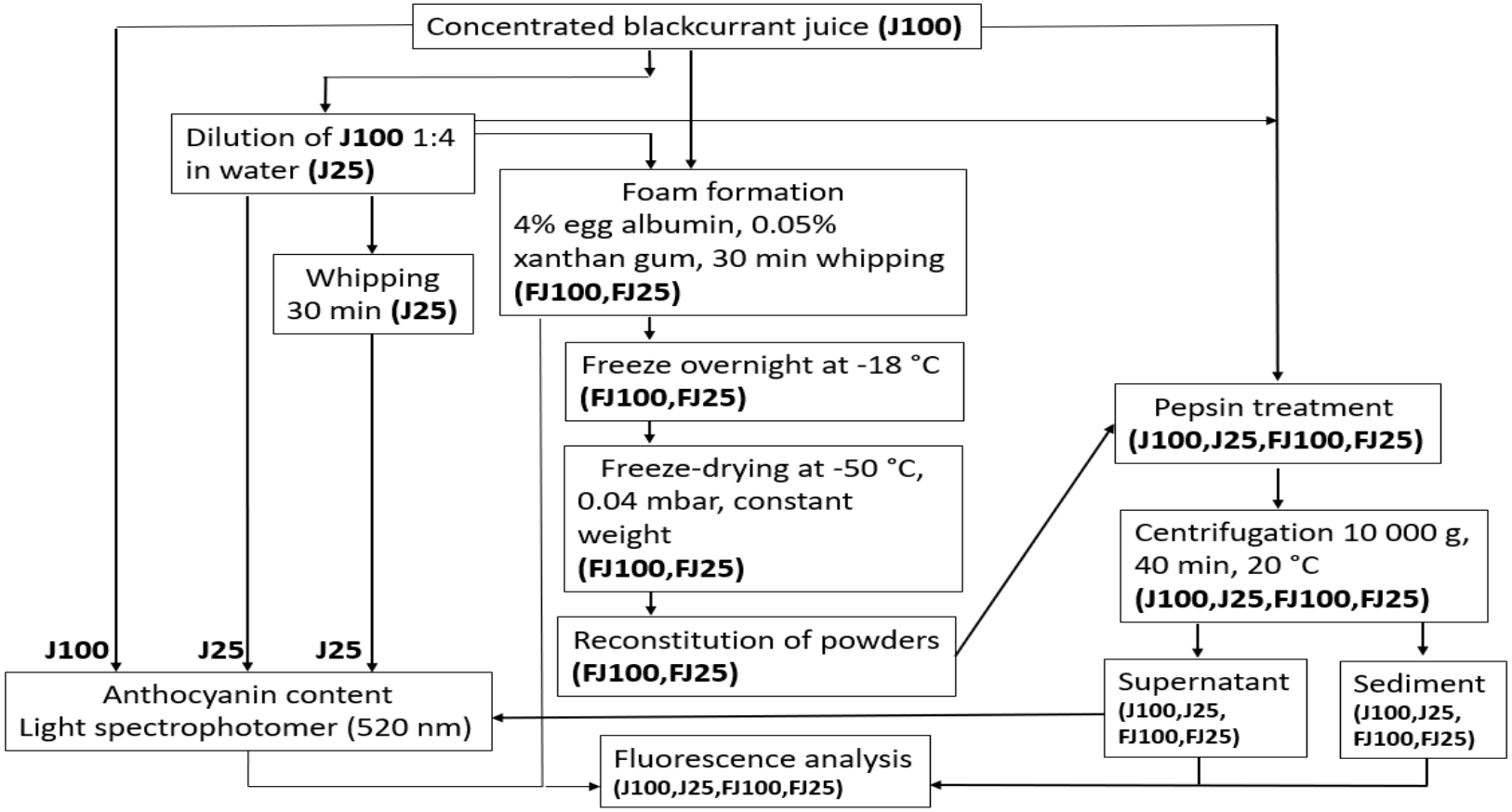

Figure 2.1 Flowchart of methodology used to analyse the anthocyanin survival after conventional (J100,J25) and foam-mat (FJ100,FJ25) freeze-drying blackcurrant juice.

2.6 Mathematical model

In simple freeze-driers with no heating plates and accurate weight measurements over short times such as the one used in this study, it is only possible to obtain data to describe and model in steady state the first freeze-drying stage. The second drying stage normally involves heating the sample to desorb bound water. Thus, the drying process (Figure 2.2) was mathematically modelled assuming: 1) the sublimation process occurs at the dry/wet sample interface (suffix s); 2) the sublimation interface is located at a distance r from the top of the container in a sample with thickness l; 3) during sublimation, the interface moves down towards the bottom of the container; 4) the change in mass (ΔM) corresponds to sample moisture losses; 5) the sublimed water leaves the product through the foam bubbles or the pores (left by ice) in the dried layer without interacting with it; 6) heat flows from the exterior of the freeze-drier to the sample via radiation; 7) heat (q) and mass (J) fluxes have opposite directions; 8) the surface of the sample (A) corresponds to the internal area of the aluminium container; 9) pressure and temperature of the condenser are referred to as P_o and T_o, respectively.

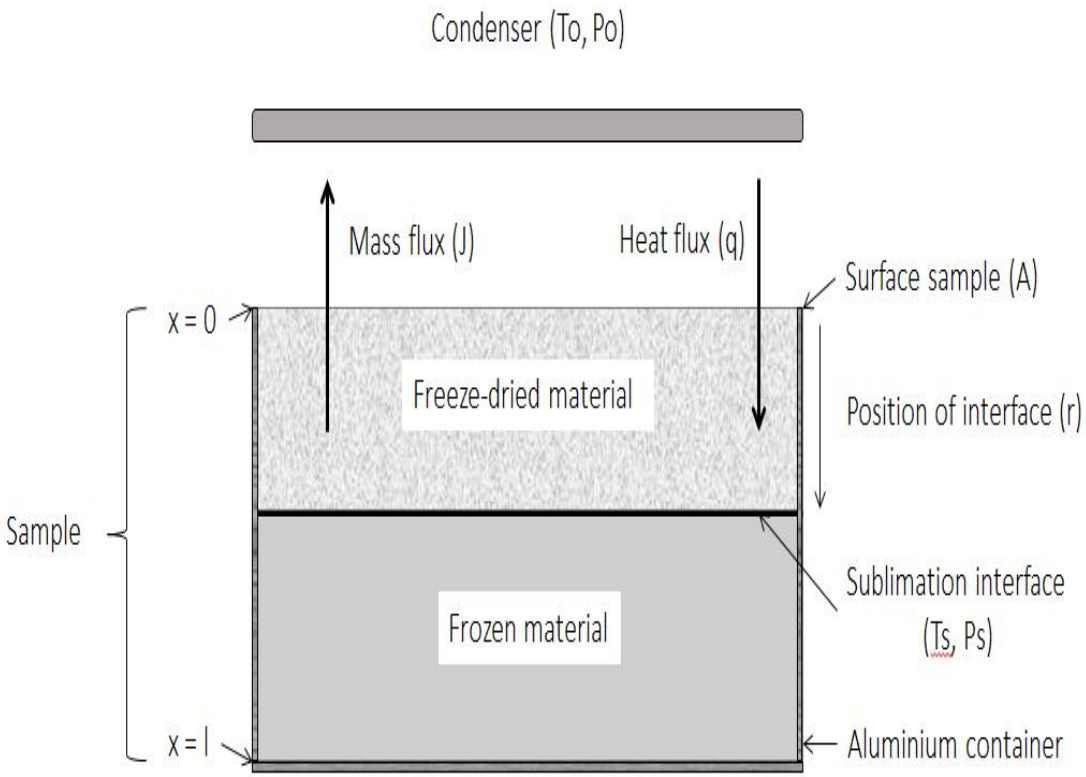

Figure 2.2 Freeze-drying diagram. See text for further description.

2.6.1 Simultaneous heat and mass transfer

Freeze drying involves simultaneous heat and mass transfer (Muthukumaran, 2007). Thus, to describe the first stage of freeze-drying, the coupled mass and heat balance laws of Fick and Fourier were used and considered together with the ideal gas and Clausius-Clapeyron equations. The former describes the water vapour concentration in the sample at a particular temperature T_s and pressure P_s. At the same time, T_s and P_s can be related to the change of phase from ice to vapour using Clausius-Clapeyron. Thus, the

mathematical model was constructed based on Mascarenhas et al. (1997) and Prakotmak et al. (2010) as follows:

1) **Fourier's law:**

Equation 2.9

$$q = -kA\frac{dT}{dr}$$

or alternatively

$$\int_o^l q\, dr = -k\, A \int_o^l dT$$

where the steady state condition assumption implies q to be the same everywhere along the sample thickness. Integrating and rearranging leads to:

Equation 2.10

$$\frac{q}{A} = \frac{-k(T_s - T_o)}{l}$$

The various symbols in the above equation are defined as follows:

q is heat flow [W m^{-2}]

k is thermal conductivity of the sample [W m^{-1} K^{-1}]

A is area of contact [m^2]

T_s is temperature of the sublimation interface [sample, K]

T_o is temperature of the condenser [K]

r is the thickness of the layer of dried sample material [m]

l is the thickness of the sample [m]

2) Ideal Gas Equation:

Equation 2.11

$$PV = nRT$$

where:

P is pressure [Pa]

V is volume [m^3]

n is number of moles

R is the gas constant [461.5 J kg^{-1} K^{-1}]

T is temperature [K]

Rearranging Equation 2.11 to obtain $\frac{n}{V}$, the number of moles per volume, (i.e. concentration, C) we have:

Equation 2.12

$$C = \frac{n}{V} = \frac{P}{RT}$$

This concentration C can now be substituted in Fick's equation to recast the equation in terms of pressure variation for the ideal gases.

3) Fick's law:

Equation 2.13

$$J = -D\frac{dC}{dr}$$

where:

J is mass flux [kg m^{-2} s^{-1}]

D is diffusivity [m^2 s^{-1}]

Substituting Equation 2.12, we get,

Equation 2.14

$$J = -\frac{D}{R}\frac{d\left(\frac{P}{T}\right)}{dr}$$

Rearranging and integrating Equation 2.14 yields:

$$\int_o^l dr\, J = -\frac{D}{R}\int_o^l d\left(\frac{P}{T}\right)$$

Assuming a uniform mass flux, J, at steady state, and solving the integrals leads to:

Equation 2.15

$$J = \frac{D}{Rl}\left(\frac{P_s}{T_s} - \frac{P_o}{T_o}\right)$$

where P_o and T_o are the pressure and temperature of the condenser plate.

Although T_s and P_s are unknown, it is possible to obtain one of them as follows. Considering that Equation 2.15 and Equation 2.10 describe a simultaneous energy and mass balance, both sides of Equation 2.15 were multiplied by the latent heat L of water. This relates the incoming heat flux (left side of Equation 2.16) with the energy required to sublime ice (for mass flux to happen, right side of Equation 2.16).

Equation 2.16

$$\frac{q}{A} = \frac{k(T_s - T_o)}{l} = JL = \frac{DL}{R\,l}\left(\frac{P_s}{T_s} - \frac{P_o}{T_o}\right)$$

and solving Equation 2.16 for P_s yields:

Equation 2.17

$$P_s = \frac{kR}{LD}(T_s - T_o)T_s + \frac{P_o}{T_o}T_s$$

4) Clausius-Clapeyron equation:

Equation 2.18

$$\ln\left(\frac{P^*}{P_s}\right) = -\frac{L}{R}\left(\frac{1}{T^*} - \frac{1}{T_s}\right)$$

In this equation T_s and P_s are the pressure and temperature interface values previously defined, whereas P^* and $T^*$are the pressure and temperature of water at its triple point, respectively. Thus, expressing P_s in terms of T_s.

Equation 2.19

$$P_s = P^* e^{\left(-\frac{L}{R}\left(\frac{1}{T^*} - \frac{1}{T_s}\right)\right)}$$

Now, equating P_s as given by (2.17) and (2.19), we have an equation to obtain T_s, at any stage during the process:

Equation 2.20

$$\frac{kR}{LD}(T_s - T_o)T_s + \frac{P_o}{T_o}T_s = P^* e^{-\frac{L}{R^*}\left(\frac{1}{T^*} - \frac{1}{T_s}\right)}$$

Equation 2.20 was computed numerically in MATLAB (see Appendix A for details) for each sample. The value of diffusivity (D) was estimated by least squares fitting the model values to the experimental data. The estimation process for D values was repeated for 3 experimental datasets for each sample. The solution for T_s (Equation 2.20) was also used to estimate the sample water vapour concentration over time which will be referred to as a change in moisture content (ΔM in Equation 2.21) from now on.

Equation 2.21

$$\Delta M = \left(\sqrt{2}\, A \left(\frac{k\, \emptyset\, \rho}{L} (T_s - T_o) \right)^{\frac{1}{2}} \sqrt{t} \right) - B$$

Equation 2.21 was derived from the relationship between the change of position of the interface Δr according to T_s, T_o and the characteristics of the sample $(A, k, \emptyset, \rho, L)$ at a time t, by the following equation:

Equation 2.22

$$L\, \emptyset\, \rho\, \Delta r = \frac{k\, (T_s - T_o)}{r}\, \Delta t$$

where:

ρ is density of sample [kg m^{-3}]

L is latent heat of water [2835036.09 J kg^{-1}]

k is thermal conductivity of sample: 0.407 W m^{-1} K^{-1} for foams (Coimbra et al., 2006), and 2.1 W m^{-1} K^{-1} for juice (Figura and Teixeira, 2007). The thermal conductivity of egg albumin was used for the foams since it was their main structural and organizational component (Miettinen et al., 2012).

$\emptyset$ is the porosity. Porosity is the fraction of volume of void space over the total volume of the sample and approximately describes the abundance of available pathways for vapour to leave the sample. Therefore, porosity in foams can be approximated by their air volume fraction (AVF), while in the case of juices, it can be approximated by their fraction of volume of water content over the total volume of the sample.

B is a constant for the model that is explained below.

Equation 2.22 was solved for r in the following manner:

Equation 2.23

$$\int_o^r r' dr' = \frac{k}{L \emptyset \rho} \int_o^r (T_s - T_o)\, dt$$

Since T_s does not change much, then the difference $T_s - T_o$ can be assumed to remain constant during the freeze-drying process. Therefore, when solved, the equations obtained refer to the position of the interface (r):

$$r^2 = \left(2 \left(\frac{k}{L \emptyset \rho} \right) * (T_s - T_o) \right) t$$

Or

Equation 2.24

$$r = \sqrt{\left(2 \left(\frac{k}{L \emptyset \rho} \right) * (T_s - T_o) \right) t}$$

Since the thickness of the dried layer as a function of time $r(t)$ is described by Equation 2.24, the amount of sublimed water after time t is then:

Equation 2.25

$$\Delta M = r(t) A \emptyset \rho$$

Substituting Equation 2.24 into Equation 2.25 yields:

Equation 2.26

$$\Delta M = (A \emptyset \rho) \sqrt{2 \frac{k}{L \emptyset \rho} (T_s - T_o)\, t}$$

Reorganizing and adding a constant (B) to this last equation yielded Equation 2.21. This was computed in MATLAB for each sample with $\emptyset$ *and* ρ values corresponding to each sample. The constant B was added to improve the fit of predicted to experimental values (Figure 2.3). This was needed because

heat and mass fluxes are not in steady state during the very early stages of freeze-drying. The value of B can be interpreted as the amount of mass already removed before reaching the steady state condition.

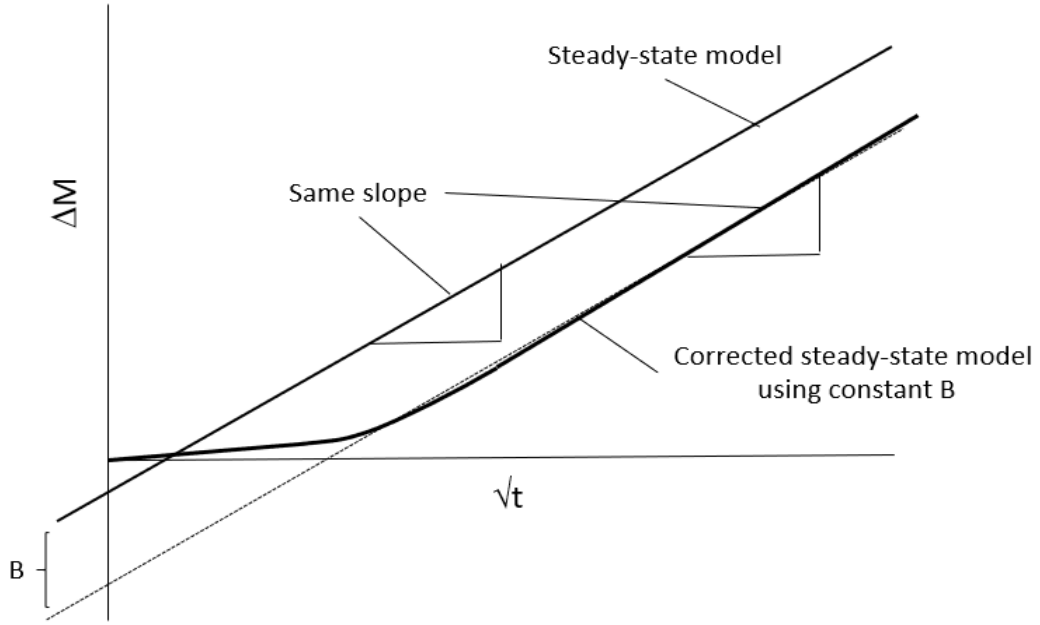

Figure 2.3 Steady-state mathematical model plus constant (B) fit to the experimental data

The experimental $\Delta M(t)_e$ and predicted ΔM change in mass were plotted for each sample using average values of four experimental replicates. The confidence limit of each data set was calculated at 95% by multiplying 1.96 by the standard error. The $\%\, error$ between the experimental drying rate $(DR)_e$ and the predicted one DR was obtained with Equation 2.27.

Equation 2.27

$$\%\, error = \frac{\left(\frac{1}{n}\sum(DR)_e - \frac{1}{n}\sum DR\right)}{\frac{1}{n}\sum(DR)_e}$$

where $\frac{1}{n}\sum(DR)_e$ corresponds to the average drying rate of the experimental values ($n = 4$) and $\frac{1}{n}\sum DR$ to the average drying rate of the predicted values.

A chart for each sample was made with 100 predicted drying rate values over the rank observed (from minimum to maximum) of air volume fraction/porosity of a sample. Three values for the density observed (minimum, average and maximum) in each sample were used for the calculation. Appendix A contains details of the way in which this was done in MATLAB. These charts show the relationship between the drying rate and the characteristics of the sample.

2.7 Statistical analysis of foam characteristics, drying rate and colour for foam-mat freeze-dried vs conventional freeze-dried samples.

In order to analyse the effect of anthocyanin and sugars contents on the foam characteristics and drying rate, statistical models were used. For Sauter Mean (SM), a simple general linear model was used. For each of the following responses: drainage, density, air volume fraction (AVF) and drying rate (DRexp), multiple readings were made for each batch and so mixed effects models were used with Batch as a grouping factor. All models were fitted in MINITAB using 95%, two-sided confidence intervals and allowing anthocyanin*sugars, anthocyanin*foam and sugars*foam interactions (Appendix B). The treatment design was foam/juice, high/low sugars content and anthocyanin quantity as a covariate.

In the colour analysis, a mixed effects model was used to analyse colour differences between foam-mat freeze-dried and conventional freeze-dried

blackcurrant juice (powders) for each of these responses: ΔE, ΔC and $(\Delta H)^2$. The model design was the same as that used for mixed effects models described previously. ΔH data were transformed into $(\Delta H)^2$ to allow a better interpretability of the results (see equation 2.4). Fisher pairwise comparisons were made for ΔE, $(\Delta H)^2$ and ΔC to perform null hypothesis tests for the equality of means between each of the samples and also for the effect of vacuum in the bags (Appendix B).

Chapter 3 Effect of foam-mat freeze-drying on the anthocyanin content of blackcurrant juice

3.1 Introduction

This chapter focuses on anthocyanin recovery after foam-mat freeze-drying blackcurrant juice with added egg albumin and xanthan gum. It also shows that some anthocyanin remains linked to egg albumin after the separation process and describes how whipping affects the apparent content of anthocyanin in juice. The methodology used is described in Chapter 2 sections 2.2, 2.3, 2.4, 2.5.1 and 2.5.3.

3.2 Results

3.2.1 Anthocyanin content

The total anthocyanin content of blackcurrant juice before and after freeze-drying is presented in Table 3.1. These results were in accordance with previous reports showing that the recovery of anthocyanins remains stable after freeze-drying fruits (Michalczyk et al., 2009), and also after digesting with pepsin a commercial blackcurrant juice at low pH (Uzunovic and Vranic, 2008). Interestingly, Figure 3.1 depicts an increment of the apparent anthocyanin content after whipping blackcurrant juice for 30 min, the same time used for foaming (See the end of section 2.5.1). Anthocyanin content of non-whipped juice was 51.0 ± 1.4 mg l^{-1} and of whipped juice was 60.3 ± 1.7 mg l^{-1}, n = 3 (Figure 3.1).

Table 3.1 Total anthocyanin content of blackcurrant juice after foam-mat freeze-drying and conventional freeze-drying for low concentration of anthocyanin+sugars ([F]J25) and high concentration of anthocyanin+sugars ([F]J100). Experimental values, mean ± standard error based on replicate readings of each sample, n = 3.

	Original content [mg l^{-1}]	Freeze-drying [mg l^{-1}]	Foam before freeze-drying [mg l^{-1}]	Foam-mat freeze-drying [mg l^{-1}]
J25			**FJ25**	**FJ25**
Juice 1	33.78 ± 0.05	31.98 ± 0.34	31.10 ± 1.15	22.88 ± 3.02
Juice 2	33.56 ± 0.02	33.70 ± 0.35	27.82 ± 0.04	26.52 ± 0.99
Juice 3	64.58 ± 0.21	53.69 ± 0.59	51.08 ± 1.21	40.67 ± 3.54
Average	43.97 ± 10.54	39.79 ± 6.97	36.67 ± 7.27	30.02 ± 5.43
% recovery	-	92.7	84.7	69.9
J100			**FJ100**	**FJ100**
Juice 1	309.26 ± 1.02	256.68 ± 1.93	225.49 ± 3.24	120.07 ± 0.37
Juice 2	352.67 ± 0.71	279.23 ± 0.34	215.36 ± 3.61	109.07 ± 2.33
Juice 3	328.22 ± 0.88	261.34 ± 0.82	222.20 ± 3.23	114.00 ± 0.92
Average	330.05 ± 12.56	265.75 ± 6.87	221.01 ± 2.98	114.38 ± 3.18
% recovery	-	83.0	72.9	38.8

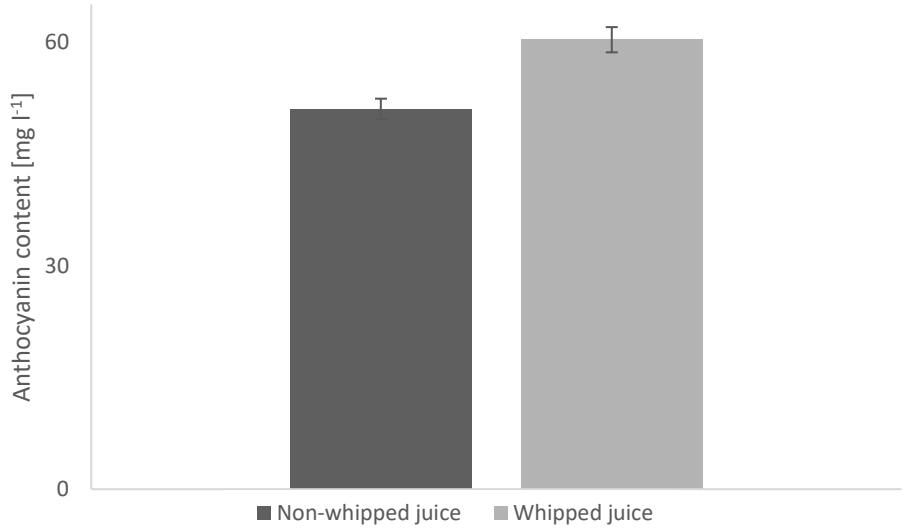

Figure 3.1 Increment of the apparent anthocyanin content in blackcurrant juice after whipping.

The 18% increase in the apparent anthocyanin content in whipped samples (Figure 3.1) is likely to be due to browning of anthocyanins. Aeration during whipping blackcurrant juice oxidised anthocyanins and resulted in higher spectrophotometer absorbance readings. Browning of anthocyanin due to air contact has been observed in wine (Timberlake and Bridle, 1976).

3.2.2 Fluorescence spectroscopy

The quenching effect of blackcurrant anthocyanin on egg albumin for untreated samples and treated samples (after foaming and pepsin treatments) is depicted in Figure 3.2. An increase of the quenching effect of anthocyanins on untreated egg albumin was observed with increasing anthocyanin content. However, the quenching effect of anthocyanins on treated egg albumin had a tendency to decrease with increasing anthocyanin content. Table 3.2 shows the

different anthocyanin concentrations used to observe the quenching effect of blackcurrant anthocyanins in untreated and treated egg albumin.

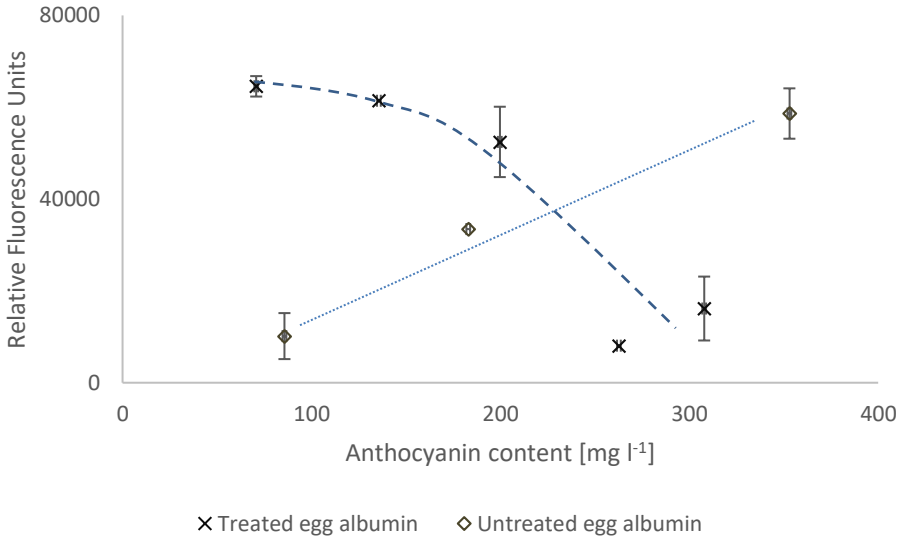

Figure 3.2 Relative fluorescence units (RFU) as function of anthocyanin content showing the quenching effect of blackcurrant anthocyanin on untreated and treated egg albumin (n=3). Lines are shown only to guide the eye.

Table 3.2 Anthocyanin content in different dilutions of blackcurrant juice.

J100 ml/H_2O ml	**Anthocyanin content (mean ± standard error, n=3) mg l^{-1}**
20/80	70.8 ± 1.0
25/75	85.7 ± 0.7
40/60	135.7 ± 2.0
50/50	183.0 ± 0.3
60/40	199.7 ± 0.3
80/20	262.8 ± 1.5
100/0 (for treated egg albumin)	307.9 ± 0.1
100/0 (for untreated egg albumin)	353.0 ± 0.7

The relative fluorescence units (RFU) of FJ100 (high anthocyanin+sugar content) and FJ25 (low anthocyanin+sugar content) before and after freeze-

drying and pepsin pre-treatment are depicted in Figure 3.3 and 3.4. Freeze-dried samples yielded lower RFU values when compared to non-freeze-dried ones.

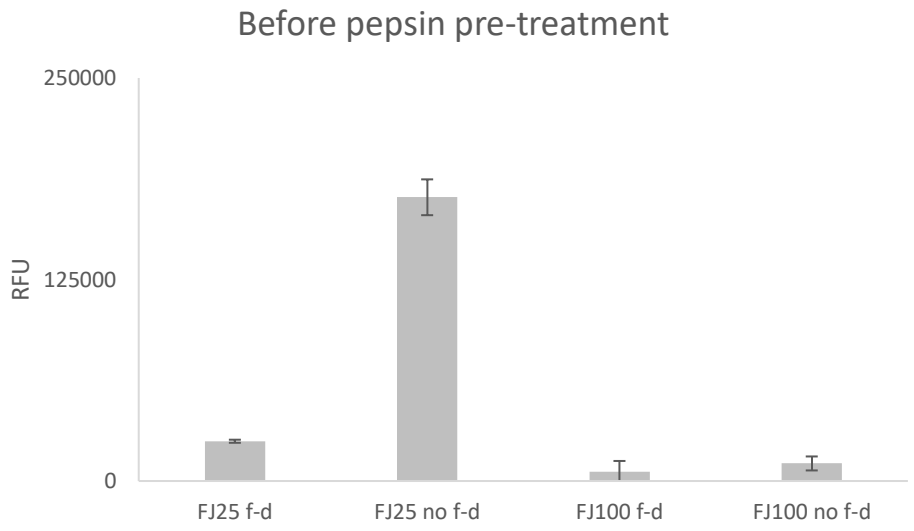

Figure 3.3 Relative fluorescence units (RFU) before pepsin treatment of freeze-dried (f-d) and non-freeze-dried (no f-d) samples foams with two different anthocyanin concentrations (FJ25 and FJ100, n=3).

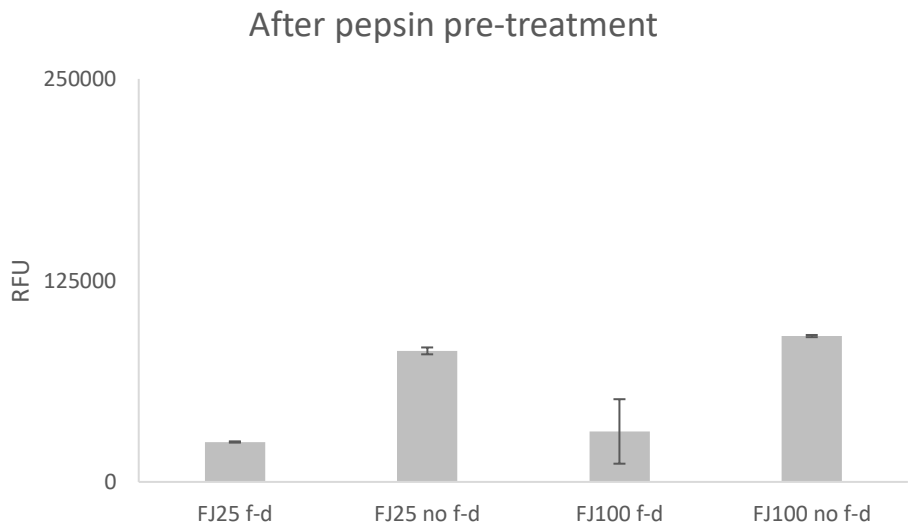

Figure 3.4 Relative fluorescence units (RFU) after pepsin treatment of freeze-dried (f-d) and non-freeze-dried (no f-d) samples foams with two different anthocyanin concentrations (FJ25 and FJ100, n=3).

Figure 3.5 depicts increments in RFU of J100 and J25 after pepsin pre-treatment. This shows the effect of pepsin on two different concentrations of blackcurrant juice (J100 and J25) when egg albumin is not mixed with the latter.

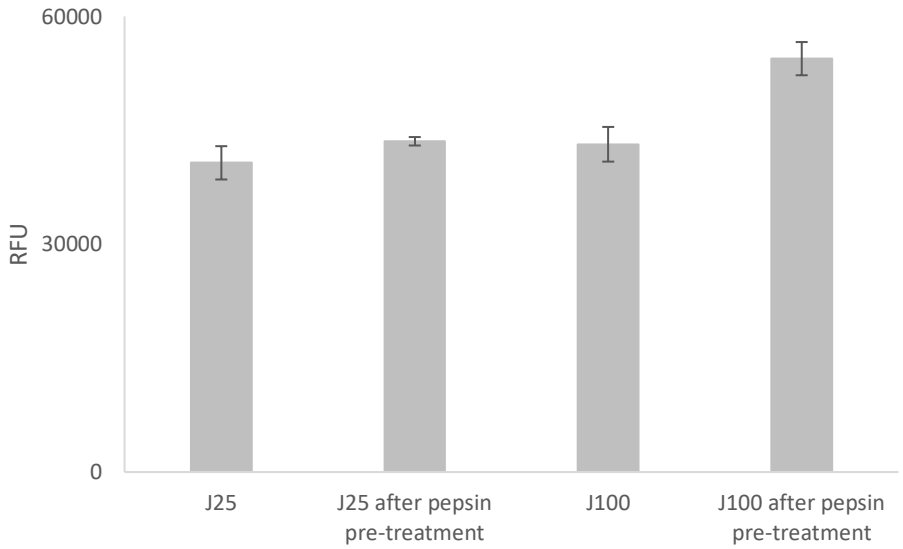

Figure 3.5 Relative fluorescence units (RFU) of J100 and J25 before and after pepsin pre-treatment (n=3).

The figures that follow depict foams without anthocyanin at low sugar content before and after freeze-drying and pepsin pre-treatment (analysed as stated in section 2.5.3) to quantify changes in the RFU of egg albumin due to freeze-drying. Contrary to what was observed in Figures 3.3 and 3.4, higher egg albumin RFU values were obtained after foam-mat freeze-drying than in non-freeze-dried samples.

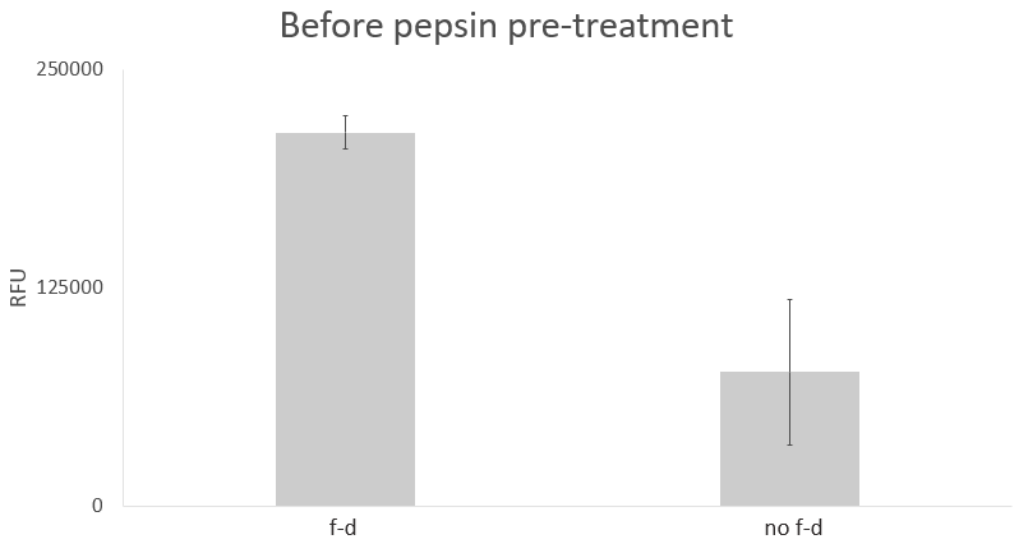

Figure 3.6 Relative fluorescence units (RFU) before pepsin pre-treatment of freeze-dried (f-d) and non-freeze-dried (no f-d) foam samples without anthocyanin and with low sugar content (n=3).

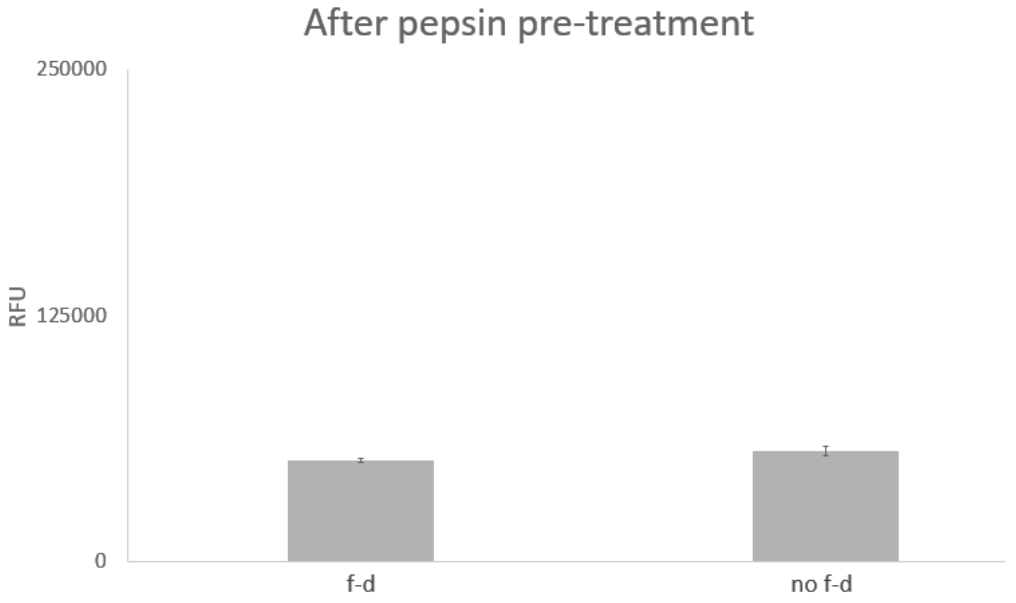

Figure 3.7 Relative fluorescence units (RFU) after pepsin pre-treatment of freeze-dried (f-d) and non-freeze-dried (no f-d) foam samples without anthocyanin and with low sugar content (n=3).

3.2.3 Sugar content

HPAEC-PAD analysis showed three main peaks of sugars in blackcurrant juice corresponding to the same elution times observed for the glucose (3.96 min), fructose (4.34 min) and sucrose (6.68 min) standards (Figure 3.8). Peaks 1 and 2 were assumed to be column contaminants since multiple samples were injected in the chromatograph for over two days of analysis.

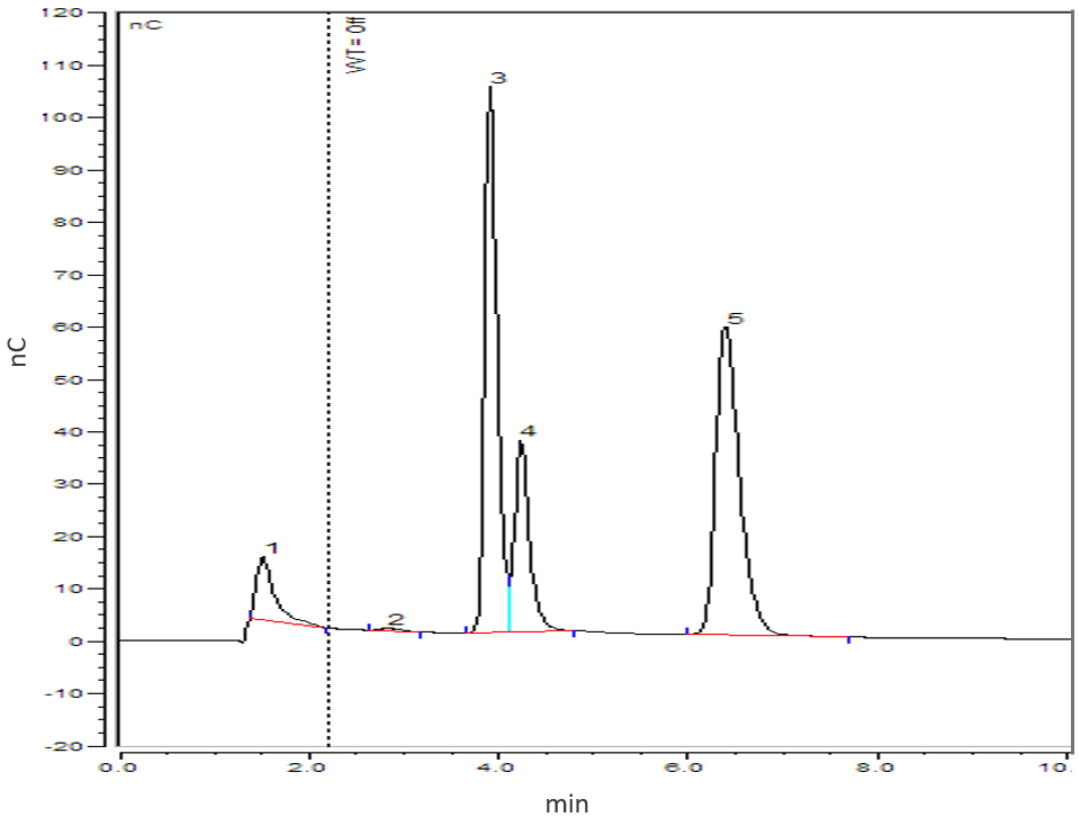

Figure 3.8 Chromatogram depicts electric charge in nanocoulombs (nC) versus elution time (min) showing glucose (peak 3), fructose (peak 4) and sucrose (peak 5) present in blackcurrant juice Ribena™. Peaks (1) and (2) were assumed to be sample or column contaminants.

Standard curves for glucose, fructose and sucrose are presented in Figures 3.9 a, b and c.

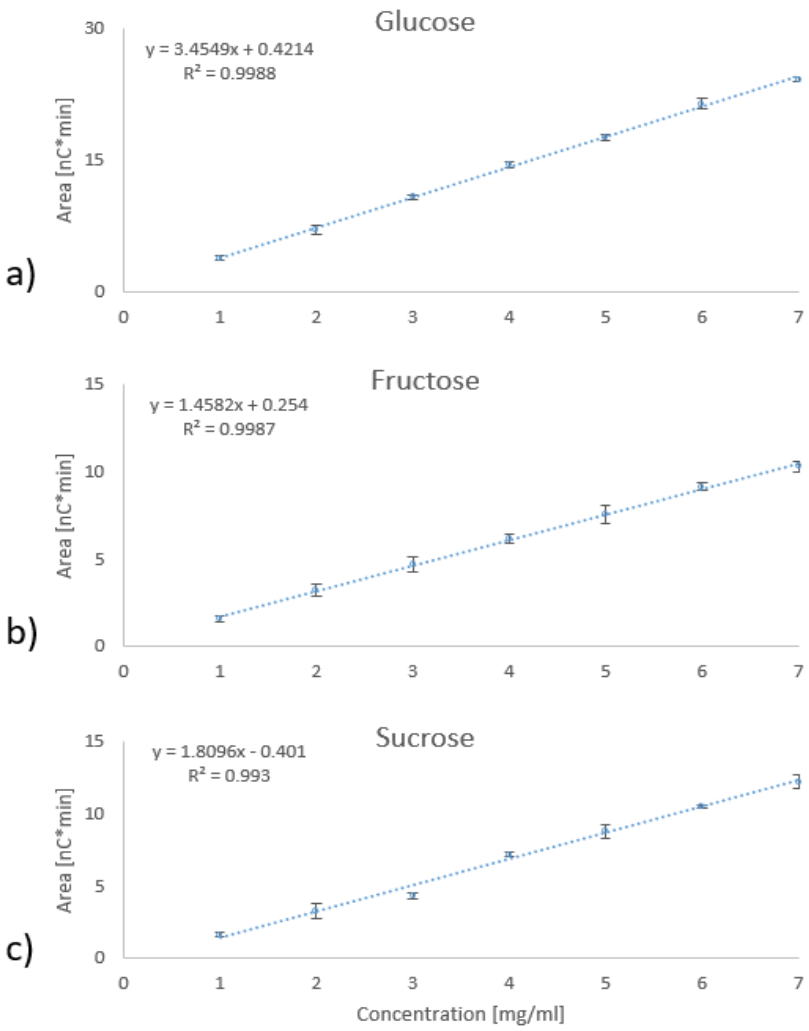

Figure 3.9 Concentration curves for a) glucose, b) fructose and c) sucrose (n=3).

These curves were used to calculate the sugar contents of blackcurrant juice: 74 .1 ± 2.3 g l^{-1} of glucose, 13.0 ± 2.8 g l^{-1} of fructose and 58.0 ± 1.7 g l^{-1} of sucrose (mean ± std error, n=3).

3.3 Discussion

3.3.1 Anthocyanin losses after foam-mat freeze-drying

After foam-mat freeze-drying of samples FJ25 and FJ100, the average anthocyanin content decreased by 31 and 65 %, respectively (Table 3.1). The

apparent losses of the total anthocyanin content in samples after foam-mat freeze-drying (Table 3.1) were presumably the result of several mechanisms including the formation of anthocyanin-egg albumin complexes (or binding of anthocyanins [BA] to egg albumin), auto-association of anthocyanins, foam dehydration, poor sample reconstitution, and anthocyanin oxidation after whipping. Part of the original anthocyanin content may remain attached to the unfolded egg albumin in the continuous phase of the foam, some with the folded egg albumin in the interface, another part with the free water of the foams, and the rest may participate in auto-association. Since polyphenolic compounds auto-associate, some of them may have settled out during centrifugation and thus not be quantified during the spectrophotometric analysis of the supernatant (Le Bourvellec and Renard, 2012). Such auto-associated anthocyanins would remain mixed with the egg albumin-anthocyanin complex in the sediment at the bottom of the centrifuge tube, making them difficult to wash and retrieve.

Phenolic compounds, including anthocyanins, bind to proteins because phenolic groups are excellent hydrogen donors forming hydrogen bonds with the unionized carboxyl amine and OH groups of the protein (Mulaudzi et al., 2012, Viljanen et al., 2005, Van Buren and Robinson, 1969). This is consistent with the observation that proportionally less anthocyanin was retrieved in samples with higher anthocyanin content. In a similar study, Chen et al. (2013) observed that a smaller anthocyanin fraction was retrieved when the concentration of anthocyanin in bovine serum albumin and blueberry anthocyanins mixtures was augmented. This suggests that stronger anthocyanin-egg albumin complexes were formed under the conditions tested.

Anthocyanin auto-association may be responsible in part for a stronger attachment to egg albumin and thus an inhibition of pepsin, hampering the separation of egg albumin from anthocyanin. Two anthocyanin-egg albumin complex formation mechanisms can be visualized, one via egg albumin unfolding during foaming, and one during blackcurrant foam drying. During foaming, egg albumin unfolding exposes hydrophobic groups which can bind anthocyanins (Le Bourvellec and Renard, 2012, Asano et al., 1982, Siebert, 1999). Figure 3.10 shows the interaction of anthocyanin with the hydrophobic proline residue of the unfolded protein. This hydrophobic interaction stabilises the egg albumin-anthocyanin complex (Viljanen et al., 2005).

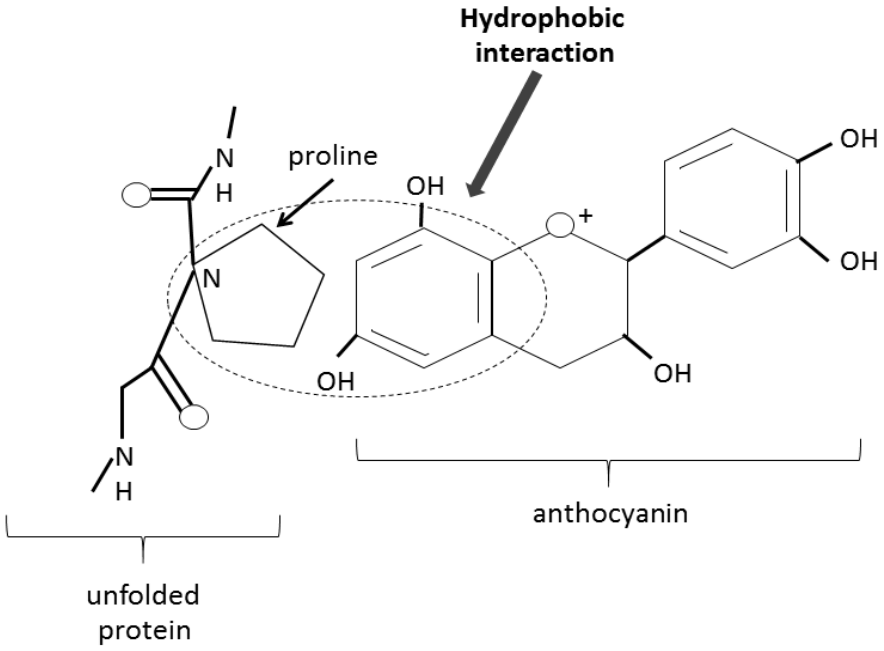

Figure 3.10 Hydrophobic interactions between proteins and polyphenols. Image modified from Bourvellec (2012).

It has been suggested that covalent bonds are formed between proteins and phenolic compounds when the latter are oxidised (Le Bourvellec and

Renard, 2012). This is consistent with Figure 3.1 showing the oxidation of anthocyanin alone when whipping due to air overexposure. Therefore, covalent bonds could have been formed in the foams.

Oxygen affects the degree of anthocyanin ionisation (Timberlake and Bridle, 1976) and can thus modify how anthocyanin-egg albumin complexes are formed. Also, it has been suggested that in ovalbumin, the phenolic-protein interaction might occur not only via hydrophobic or hydrogen-bonding but also via ionic bonding since ovalbumin contains several ionic residues (Lu et al., 2009). Ionic bonding of anthocyanin and egg albumin can occur between positively charged groups of proteins (i.e., lysine) and the negatively charged hydroxyl groups of the anthocyanin (Asano et al., 1982).

During freeze-drying, both protein and anthocyanin dehydrate bringing these molecules into closer proximity. Water molecules can bind to polar protein side chains via hydrogen bonds and form highly ordered water molecule cages, or clathrates, around hydrophobic residues (Zdzislaw and Haard, 2006). When sublimation occurs, the protein hydrogen bonding and hydrophobic residues sites are exposed leaving them available for the anthocyanin to react with them and thus enhancing the formation of anthocyanin-egg albumin complexes. It has been observed that sublimation also changes the structure of proteins (Roy and Gupta, 2004), which may have influenced the sample rehydration capacity and reconstitution. Thus, the apparent reduction of the anthocyanin content between blackcurrant foam before and after freeze-drying could also reflect poor reconstitution of the freeze-dried sample powder.

Past research on reactions between proteins and anthocyanins suggest two additional mechanisms for the apparent reduction in anthocyanin content after freeze-drying. First, the more hydrophobic the phenolic compound is, the stronger its affinity towards proteins will be, regardless of the sample pH (Papadopoulou et al., 2005). Therefore, the fewer hydroxyl groups (OH) the phenolic compound has, the greater the binding to the protein will be. However, in a high–performance liquid chromatography (HPLC) analysis of four anthocyanins (cyanidin-3-glucoside, delphinidin-3-glucoside, cyanidin-3-rutinoside and delphinidin-3-rutinoside) mixed with 4 and 6 g egg albumin per 100 ml stock solution (1.3 mg/ml ascorbic acid, pH 2.8), foam-mat freeze-dried, and then digested with pepsin under the same conditions as used in this work, it was observed that delphinidin-3-glucoside (which contains five OH) was less well retrieved than cyanidin-3-glucoside (four OH) (Jingyu, 2016). This suggested that foam-mat freeze-drying aided the protein-anthocyanin binding.

A second mechanism for the apparent reduction in anthocyanin content after freeze-drying could be that anthocyanin can also bind to the surface of the unfolded egg albumin in the continuous phase. In other studies, the binding sites of phenolic compounds with proteins like bovine serum albumin (BSA) showed that phenolic compounds bonded within the hydrophobic pockets of BSA surrounding the protein molecule (Zhou et al., 2014, Papadopoulou et al., 2005). These studies suggested that phenolic compounds with high protein affinity had a particular size which allowed the penetration into the inter-fibrillar protein regions and the cross-linking of peptide chains at more than one point (Mulaudzi et al., 2012).

3.3.2 Fluorescence of egg albumin in the presence of blackcurrant anthocyanins after foam-mat freeze-drying

Foam-mat freeze-dried FJ100 exhibited the lowest egg albumin fluorescence (in relative fluorescence units, RFU) before pepsin treatment (Figure 3.3). This suggested a higher presence of non-fluorescent complexes corresponding to anthocyanin-egg albumin interactions per mass at high anthocyanin concentrations. Lower egg albumin RFU values were also observed for foam-mat freeze-dried FJ25 samples when compared to non-freeze-dried ones. Reduced egg albumin RFU after freeze-drying foams FJ100 and FJ25 suggested the influence of freeze-drying on the formation of the non-fluorescent anthocyanin-egg albumin complex. This also meant that the anthocyanin was more attached to and surrounding the egg albumin in samples with high anthocyanin content. This observation is in accordance with similar studies where RFU of protein decreased due to the presence of phenolic compounds (Hassan, 2012, Lin, 2016). Interestingly, the opposite effect was observed when the egg albumin was first foamed and subjected to the pepsin pre-treatment and then mixed with different anthocyanin concentrations in the present study, the opposite effect was observed (Figure 3.2). This suggested that the formation of the anthocyanin-egg albumin complex took place during the unfolding of the egg albumin during foaming. Future microscope imaging studies are suggested to elucidate whether changes in the structure of egg albumin due to foaming, freeze-drying, and/or pepsin treatment affect its anthocyanin interaction.

After pepsin pre-treatment, foams yielded similar egg albumin RFU values according to the treatment (foam-mat freeze-dried and non-freeze-dried)

(Figures 3.4 and 3.7). This suggested that pepsin worked in similar protein residues in each treatment and according to the anthocyanin content. Foam-mat freeze-dried FJ100 and FJ25 showed lower RFU in egg albumin than the non-freeze-dried ones after pepsin pre-treatment, and therefore higher presence of the anthocyanin-egg albumin complex (Figure 3.4). These similar values of RFU in egg albumin after foam-mat freeze-drying and pepsin pre-treatment suggested a saturation of anthocyanin on egg albumin to form the anthocyanin-egg albumin complex. However, the anthocyanin recovery fraction in foam-mat freeze-dried FJ100 after pepsin pre-treatment was lower than in FJ25. This can be explained by observing Figure 3.5 where differences in RFU of (liquid samples) J100 and J25 after pepsin pre-treatment produced an average increase in RFU of 26 % and of 7 %, respectively, when compared to their similar levels before pepsin pre-treatment. Higher RFU in J100 and J25 after pepsin pre-treatment suggested an interaction of pepsin with anthocyanin that could be reflected in samples depicted in Figure 3.4. Traces of pepsin when quantifying anthocyanin in the light spectrometer could have also increased the absorbance of the samples, yielding higher calculated anthocyanin contents (Table 3.1). Thus, part of the non-quantified anthocyanin in FJ100 and FJ25 may have remained interacting with egg albumin (anthocyanin-egg albumin complex) and pepsin. In contrast to Figure 3.3, Figure 3.6 depicts higher RFU in egg albumin after foam-mat freeze-drying than in non-freeze-dried samples without anthocyanin (Figure 3.6). This suggested that the arrangement of fluorescent residues of egg albumin was affected by the anthocyanin and also by freeze-drying. An overexposure of fluorescent residues in egg albumin after foam-mat

freeze-drying increased the RFU showed in Figure 3.6. At the same time, this overexposure of fluorescent residues bound to anthocyanin, quenched the egg albumin fluorescence as shown in Figure 3.3.

3.4 Conclusions

The high affinity between anthocyanins and egg albumin made it difficult to achieve their complete separation and thus a full quantification of anthocyanins. Anthocyanin retention in foam-mat freeze-dried blackcurrant juice was quantified using a pepsin pre-treatment. However, high anthocyanin concentration appears to have inhibited the pepsin. RFU of liquid samples (juice) after pepsin pre-treatment increased slightly compared to non-treated samples suggesting a pepsin-anthocyanin interaction. The percentage anthocyanin recovery after foam-mat freeze-drying blackcurrant juice was larger in samples with lower anthocyanin concentration than in those with higher anthocyanin concentration, reflecting a reduction in anthocyanin sedimentation and anthocyanin-protein (egg albumin and pepsin) interaction. Additionally, the percentage anthocyanin recovery before freeze-drying foams was higher than after freeze-drying foams since protein dehydration promoted anthocyanin-egg albumin interaction. Foam-mat freeze-drying promoted the formation of the anthocyanin-egg albumin (non-fluorescent) complex due to the exposure of hydrophobic sites and hydrogen bonds of egg albumin during foaming (protein unfolding) and then freeze-drying (dehydration), both fostering anthocyanin binding. Anthocyanin quenched egg albumin fluorescence, except when egg albumin was foamed and treated with pepsin previous to being mixed with anthocyanin, confirming the enhancement of anthocyanin-egg albumin

interaction due to foam-mat freeze-drying. Finally, foam-mat freeze-drying blackcurrant foams can be used to attach strongly blackcurrant anthocyanins to egg albumin. Thus anthocyanin-egg albumin powder could be used as an anthocyanin carrier in food supplements.

Chapter 4 Influence of anthocyanins on foam characteristics.

4.1 Introduction

The previous chapter focused on anthocyanin-protein interactions and their role on anthocyanin extraction and protein fluorescence in the foam-mat freeze-drying of blackcurrant juice. This chapter describes how the anthocyanin-protein interaction manifests itself in the characteristics of the foam and whether anthocyanins affect the bubble size, density, air volume fraction (AVF), viscosity and drainage (Methodology in Sections 2.1 and 2.2). Experiments were designed to allow comparisons of blackcurrant foams with and without anthocyanins. Statistical models were used to analyse differences of means of the characteristics of foams between samples with and without anthocyanins (Section 2.7). The importance of this research focus lies in the different uses of the blackcurrant foam in the development of products with novel textures or marketed as functional or "free from" (lactose, casein, soya) foods. The production of these foods requires the application of additional foam processing steps such as drying, cutting, and toppings. Foams need to be able to allow these and other manipulations.

4.2 Results

The characteristics of the four foams studied (FJ100 = high anthocyanin/high sugars contents; ZA100sf = zero anthocyanin/high sugars contents; FJ25 = low anthocyanin/low sugars contents and ZA25sf = zero anthocyanin/low sugars contents), and those of the corresponding solutions used before foaming, are presented in Table 4.1. FJ100 obtained a rather small bubble size (as Sauter mean, SM) compared to the other foams. AVF was greater in foams with diluted solutions. Foams with anthocyanin were more stable (lower drainage) than zero anthocyanin ones. Zero anthocyanin solutions obtained similar values for density (ρ) and pH as the juices (Table 4.1). These results indicate similarity in solid content and acidity between juices and model solutions.

Table 4.1 Characterization of foams. Mean ± standard error, n=3. Further information about the bubble size distributions is given in Fig 4.1 and 4.2.

Sample	***Sauter mean, [mm**, n=2]*	***Density, [g/ml]***	***Air volume fraction***	***Drainage (%)***	***Concentration of sugars, [g/l]***	***Concentration of ascorbic acid, [mg/ml]*** ǂ	***pH***
J100	-	1.247 ± 0.009	-	-	145.2 ± 3.4	0.32	3 at 25°C
FJ100	<0.085 ± 0.004*	0.128 ± 0.007	0.711 ± 0.006	0	145.2 ± 3.5	0.32	4 at 25°C
J25	-	1.130 ± 0.001	-	-	48.4 ± 2.3	0.1	2.8 at 25°C
FJ25	0.26 ± 0.07	0.130 ± 0.006	0.771 ± 0.006	0	48.4 ± 2.3	0.1	4 at 25°C
ZA100s	-	1.230 ± 0.005	-	-	4:4	0.32	3 at 25°C
ZA100sf	0.17 ± 0.01	0.172 ± 0.003	0.680 ± 0.003	7	4:4	0.32	4 at 25°C
ZA25s	-	1.131 ± 0.002	-	-	4:1	0.1	2.8 at 25°C
ZA25sf	0.28 ± 0.05	0.146 ± 0.009	0.768 ± 0.007	8	4:1	0.1	4 at 25°C

*Many bubbles <0.01 mm were not counted. ǂ This characteristic was experimentally controlled (0.5% error).

Viscosities after whipping were (in descending order, at a shear rate of 0.1 s^{-1}) 1000 Pa s for FJ100, 582.4 Pa s for FJ25, 478.5 Pa s for ZA25sf and 179.8 Pa s for ZA100sf. Viscosities after 90 min were (in the same order, at 0.1 s^{-1}) 856.3 Pa s for FJ100, 643.9 Pa s for FJ25, 608.1 Pa s for ZA25sf and 429.1 Pa s for ZA100sf.

For bubble size distributions, Figure 4.1 depicts a large peak of frequency density around 0.03 mm diameter in FJ100 and a standard deviation (σ) of 0.024 mm. In FJ25, the maximum of frequency density was observed around 0.08 mm with σ = 0.085 mm. In ZA100sf, two peaks were observed, one around 0.10 mm and another around 0.14 mm diameter with σ = 0.039 mm. ZA25sf showed a plateau over several bubble sizes around 0.15 mm and obtained σ = 0.082 mm. Figure 4.2 shows that foams with anthocyanin had higher % cumulative frequencies around small diameters than their zero anthocyanin counterparts. FJ100 (high anthocyanin/high sugar contents) has a more pronounced slope than ZA25sf (zero anthocyanin/low sugars contents). The % cumulative frequency of FJ100 reached almost 100 % under a bubble size diameter of 0.1 mm. ZA100sf reached almost 100 % under a bubble size of 0.2 mm. In FJ25, a less abrupt curve was observed and virtually all bubble diameters were <0.4 mm like in ZA25sf. The main difference between FJ25 and ZA25sf was that the latter obtained a uniformly increasing slope while the shape of the curve FJ25 showed a kink at around 0.15 mm.

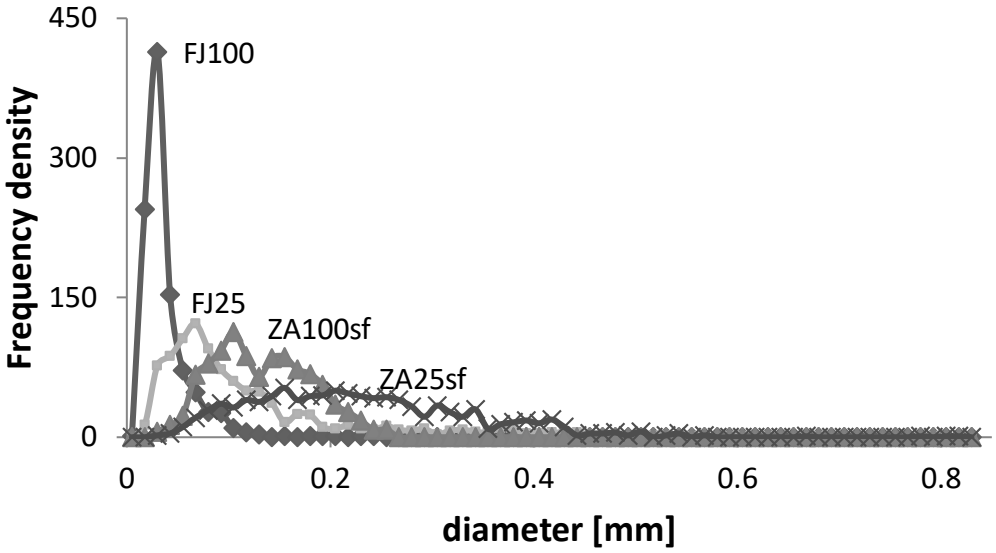

Figure 4.1 Frequency density of the bubble diameter (mm) in foams.

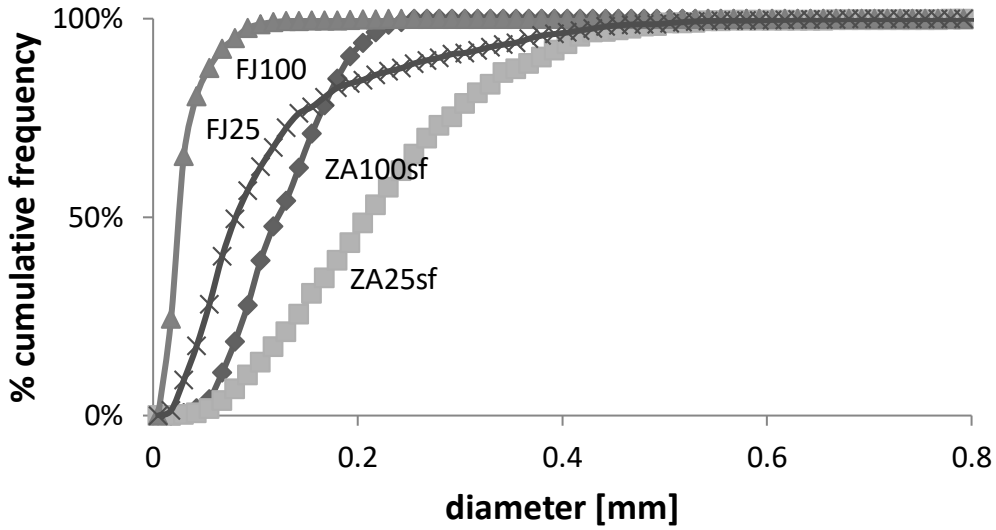

Figure 4.2 Cumulative frequency distribution for the bubble diameter (mm) of foams.

Figure 4.3 shows pictures of the four foams under the microscope. Pictures are arranged from smallest to largest bubble size from a to d. The bubble size of (a) FJ100 (the more concentrated anthocyanin and sugar foam) was

considerably smaller than (d) ZA25sf (the foam with zero anthocyanin content and less sugar content). Bubble size of ZA100sf looked slightly smaller than FJ25.

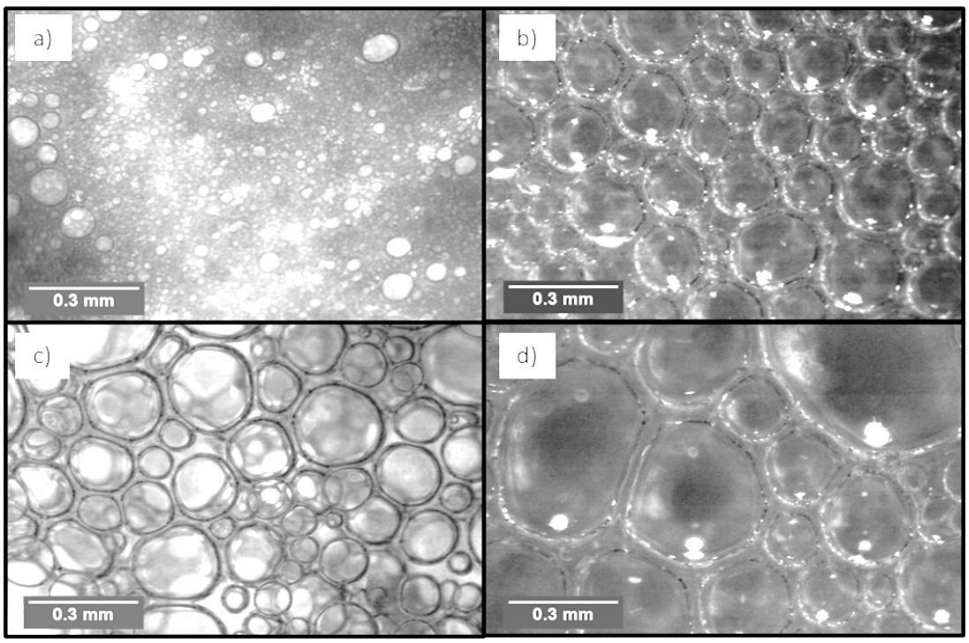

Figure 4.3 Light microscope pictures of foams: a) FJ100; b) ZA100sf; c) FJ25 and d) ZA25sf.

Figure 4.4 shows a picture of foam-mat freeze-dried blackcurrant juice (FJ25). Strings of the internal structure of the foam, involving egg albumin-anthocyanin-sugars, appeared forming a network around air pockets after dehydration.

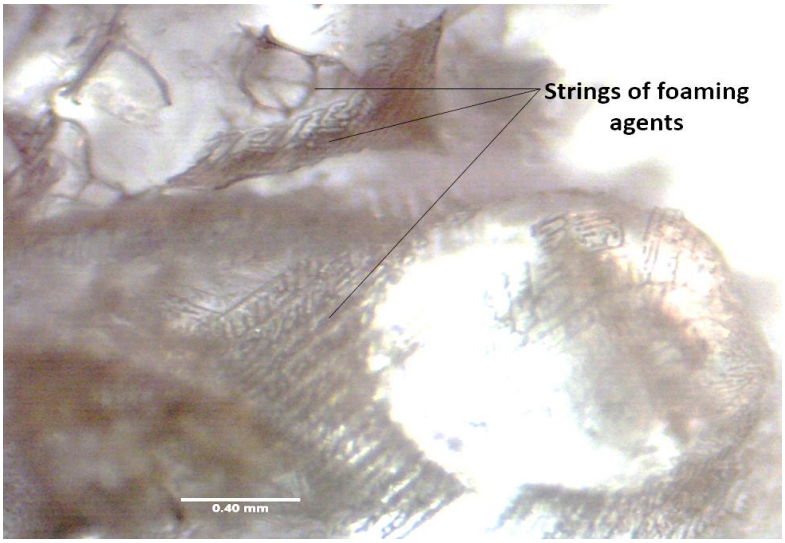

Figure 4.4 Light microscope (4x) picture of foam-mat freeze-dried blackcurrant juice (FJ25).

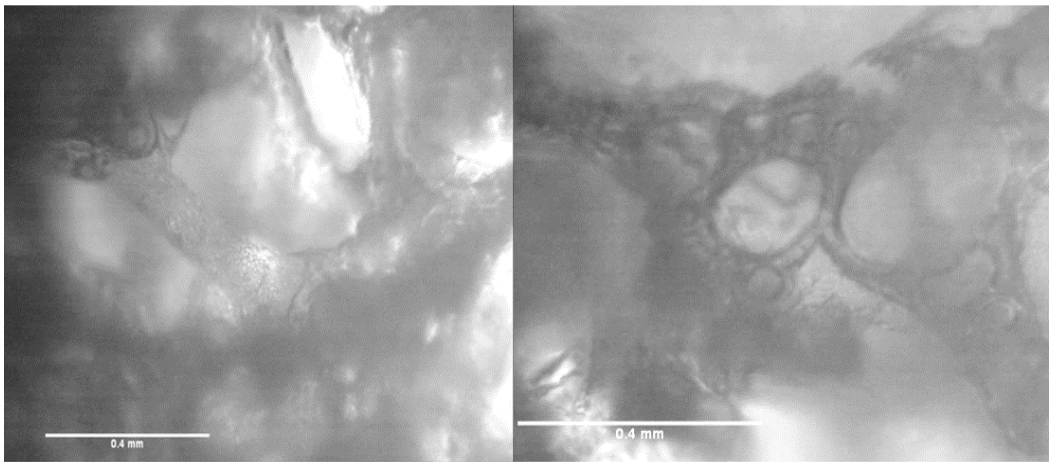

Figure 4.5 Light microscope (4x) pictures of foam-mat freeze-dried concentrated blackcurrant juice (FJ100).

The statistical model suggests that in foams:

1) The air volume fraction (AVF) increases by 0.008 ± 0.002% per mg l^{-1} of anthocyanin (p-value 0.007). AVF decreases by 0.044 ± 0.003 per mg ml^{-1} of total sugars content (SC) (p-value <0.0005).
2) The density decreases by 0.013 ± 0.003% per mg l^{-1} of anthocyanin (p-value 0.002) and increases by 0.017 ± 0.004 per mg ml^{-1} of total SC.

3) The drainage decreases by 0.004 ± 0.001 per mg l^{-1} of anthocyanin (p-value 0.016). SC did not modify significatively the drainage in foams (p-value 0.709).
4) The Sauter mean (SM) was not affected significatively by the presence of anthocyanins (p-value 0.152), but the coefficient obtained in the model suggests that SM decreases by 0.0003 ± 0.0002 per mg l^{-1} of anthocyanin. High SC was significant (p-value 0.048) for SM. SM decreases by 0.056 ± 0.022 per mg ml^{-1} of total SC added to the sample.

4.3 Discussion

In diluted samples, the presence of anthocyanin did not produce such large differences in the foam characteristics as it did in concentrated samples. Table 4.1 shows that the foam with the highest density (ZA100sf) obtained the lowest air volume fraction (AVF). The statistical model suggests that the air volume fraction (AVF) of foams increases by 0.008 ± 0.002% per mg l^{-1} of anthocyanin added to the sample (p-value 0.007), and decreases by 0.044 ± 0.003 per mg ml^{-1} of total sugars content (SC) added to the sample (p-value <0.0005). Foam density tended to decrease with more bubbles (high AVF) in the sample. A special case was observed with FJ100, which obtained the lowest mean density but not the highest AVF. Foams with anthocyanin obtained lower density values than their zero anthocyanin counterparts. The statistical model suggests that density in foams decreases by 0.00013 ± 0.00003 per mg l^{-1} of anthocyanin added to the sample (p-value 0.002) and increases by 0.017 ± 0.004 per mg l^{-1} of total SC added to the sample. Consequently, the AVF of foams with anthocyanin was higher than their zero anthocyanin counterparts. The presence of

anthocyanin aided the air retention in foams by 4 and 1 % in the high and low anthocyanin concentrations tested respectively.

The smallest mean bubble size and the highest viscosity were observed in FJ100. Viscosity of FJ100 at a shear rate of 0.1 s^{-1} was similar to that reported for egg albumin-gelatin marshmallow (Miquelim and Caetano da Silva-Lannes, 2009). However, the decrease of viscosity in FJ100 after 90 min suggested that its structure was not very stiff. An increment of viscosity of 22 % was observed between FJ25 (low anthocyanin/low sugars) and ZA25sf (zero anthocyanin/low sugars) and of 456 % between FJ100 (high anthocyanin/high sugars) and ZA100sf (zero anthocyanin/high sugars). The increase of viscosity of ZA100sf, FJ25 and ZA25sf after 90 min suggested loss of air, leaving a more concentrated solution which produces more resistance between the plates of the viscosimeter.

The effect of anthocyanin can be seen by comparing FJ100 with ZA100sf. The lowest viscosity was observed in ZA100sf where the mean bubble size was about 2-fold that of its counterpart FJ100. This suggests that viscosity of foams not only depends on small bubble size but also on the composition of the continuous phase. The anthocyanin content affected the bubble size only in highly concentrated sugars samples. The Sauter mean decreased 53% from ZA100sf to FJ100. Although the statistical model suggests that the presence of anthocyanins was not significant (p-value 0.152) with regards to the mean bubble size (SM), the coefficient obtained for the latter suggests that SM might decrease by 0.0003 ± 0.0002 per mg l^{-1} of anthocyanin added to the sample (more repetitions might produce statistical significance). Smaller bubbles were found in highly concentrated sugar solutions than in diluted ones. This was in

accordance with other publications where bubble size was reduced when adding sucrose to egg white foams (Raikos et al., 2007). High sugars content (SC) was significant (p-value 0.048) for SM and the latter mentioned decreases by 0.056 ± 0.022 per mg ml^{-1} of total SC added to the sample.

The effect of anthocyanins on bubble size distribution can be seen from Figures 4.1 and 4.2. Foams with anthocyanins yielded more asymmetric curves (Figure 4.1), positive skewed. In other words, the mode of such samples tended to be around smaller bubble sizes (modes: FJ100 = 0.012 mm and FJ25 = 0.081mm) than zero anthocyanin foams (modes: ZA100sf = 0.120 mm and ZA25sf = 0.178 mm).

Differences in foam characteristics can be attributed to the following five points:

1) As mentioned before, formation of bubbles in proteinaceous mixtures happens when the protein unfolds and is adsorbed at the air-liquid interface (Wierenga and Gruppen, 2010). The reorganization of the protein happens within and between molecules (Murray et al., 1999). This orientation of protein creates a network of almost straight and parallel polymer chains at the interface (bubble surface). Such a network can be seen in Figure 4.4 showing FJ25 after freeze-drying. In addition, Figure 4.5 shows FJ100 after freeze-drying where on the left picture, a strand connecting two parts of the foam structure appeared to be shaped by very small circles (where bubbles were, see Figure 4.3a). The two pictures of Figure 4.5 show larger circular holes left by the dehydration of foam.

2) Anthocyanin fosters cross-links with unfolded and folded egg albumin (Ozdal et al., 2013) at the air-liquid interface and in the bulk phase of foams,

respectively. It has been suggested that if each polyphenol molecule has a fixed number of binding ends and each protein contains a fixed number of polyphenol binding sites, each polyphenol molecule should be able to bridge between two protein molecules (Siebert et al., 1996, Van Buren and Robinson, 1969). This property presumably conferred major capacity to retain air in foams with anthocyanin in the present study (Table 4.1). Also, this interaction was reflected in high viscosity and low drainage (more stability) in foams with anthocyanin. The statistical model suggests that the presence of anthocyanin decreases the drainage by 0.004 ± 0.001 per mg l^{-1} of anthocyanin added to the sample (p-value 0.016).

3) The presence of sugars like sucrose in the samples aids foam stability since they strengthen hydrophobic interactions between proteins, increase the density of the continuous phase, aid protein hydration, promote compact molecular conformations of the protein, slow down adsorption at air-water interphases (Yang, 2008) and their large number of equatorial-OH groups decrease the mobility of water (Ochi et al., 2000). However, foams without anthocyanin did not depict as much stability as the anthocyanin foams with the same concentration of sugars, suggesting foam improvement due to anthocyanin. The statistical model also suggests that the presence of sugars (high/low content) did not modified the drainage in the foams tested (p-value 0.709).

4) When mixing both the model solutions and the blackcurrant juice (both at pH 2.8 - 3) with the egg albumin, the pH obtained was around 4. pH 4 was very close to the isoelectric point of the major protein constituent of egg albumin ovalbumin (pH(I) = 4.5) (Huntington and Stein, 2001, Carraro-Alleoni,

2006). Foaming properties have been reported as optimal for a range of proteins near their isoelectric points (Foegeding et al., 2006). It is known that adsorption of proteins is faster around the isoelectric point (Wierenga and Gruppen, 2010, Foegeding et al., 2006) because the electrostatic repulsion for the net neutrally charged proteins is minimal, improving foam stability. Also, some surface rheological properties that improve interfacial stability are maximized at the isoelectric point for many proteins because at this point solubility tends to a minimum (Carraro-Alleoni, 2006).

5) Ovalbumin at its isoelectric point can coagulate. Coagulation is the random aggregation of already denatured (unfolded) protein molecules (Hermansson, 1979). Proteins with higher percentages of hydrophobic amino acids are classified as coagulation-type proteins and concentration dependent (Gossett et al., 1984). This is the case of egg albumin (Shimada and Matsushita, 1980). The formation of disulphide bonds and the exposure of hydrophobic amino acid residues are involved in the first step of coagulation (Gossett et al., 1984). Thus, the presence of anthocyanin presumably links to the denatured egg albumin (disulphide bonds and hydrophobic amino acid residues) to form packed aggregates in the continuous phase of foam.

The presence of high contents of anthocyanin and sugars during protein coagulation with prolonged whisk time (30 min) produced a very stable continuous phase, especially in FJ100. Figure 4.6 depicts a proposed interaction between the major components of foam with anthocyanin, where anthocyanin acted as “cement” in the bubble interphase and in the continuous phase of foam linking the components of foam and strengthening the structure. This also

affected the anthocyanin retrieval, as seen in the previous chapter, because after freeze-drying, anthocyanin presumably ended up trapped in the creases of the dehydrated egg albumin hindering the anthocyanin retrieval. The egg albumin coagulation (also reflected in the high viscosity value) and the high anthocyanin and sugars contents were the main reasons why the concentrated blackcurrant foam (FJ100) was one of the most stable foams and also why the anthocyanin recovery decreased. In foam processing, coagulating egg albumin by mechanical forces may be better than adding additives or heating if a more solid-like foam with anthocyanin is required.

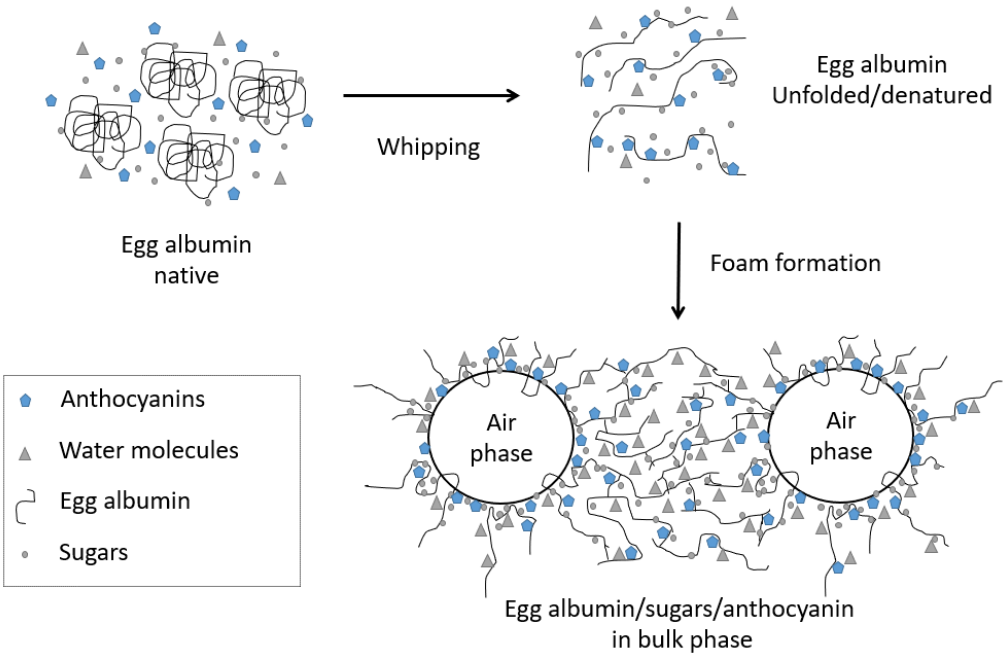

Figure 4.6 Diagram of foam formation in the presence of anthocyanin.

Finally, since after a certain period of time, proteins regenerate to their original conformation (Ptaszek et al., 2014), the presence of different molecules during foaming (i.e. anthocyanin, sugars) improves the stability of foams due to the delay of the regeneration of the protein.

4.5 Conclusions

While sugars promoted the formation and stability of foams, the presence of anthocyanin further improved their characteristics. High anthocyanin and sugars concentrations aided the formation of a viscous continuous phase with small bubble sizes, similar to marshmallow. Density decreased in foams with anthocyanin as air volume fraction and stability increased. Coagulation of egg albumin occurred at the pH tested in the continuous phase which resulted in stable foams, especially the ones containing anthocyanin.

Foam FJ100 could be a good topping substitute in lactose-, casein- and soya-free bakery products due to its low drainage and high viscosity.

Chapter 5 Drying rate modelling of freeze-dried foams.

5.1 Introduction

As seen in the previous Chapter, foams made with different concentrations of anthocyanin and sugar yielded different bubble size distributions, density, air volume fraction, viscosity and drainage. This chapter investigates the influence of the characteristics of samples (both foamed and non-foamed) on the drying rate during freeze-drying, using both experimental observations and a mathematical model. The model can be found in Chapter 2 Section 2.6 of this thesis and describes the change of mass of a sample in terms of temperature and pressure, and the density and the air volume fraction (AVF) of the sample. Density and AVF carry information about the composition of the sample, but mathematical models of drying do not usually incorporate the influence of anthocyanin and sugars in a sample due to the difficulty of doing this. Therefore, a statistical model was fitted to the anthocyanin and sugar content of a sample to analyse their effect on the drying rate.

To validate the mathematical model, the % error was calculated as mentioned in Chapter 2 with the observed and the predicted average values of the drying rate of a sample. Section 2.3 describes how the observed (experimental) drying rate values were obtained.

5.2 Results

Table 5.1 presents the experimental and predicted drying rates and the % error between each of five samples (in ascendant order): foam: high

anthocyanin/high sugars content (FJ100), foam: zero anthocyanin/high sugars content (ZA100sf), foam: low anthocyanin/low sugars content (FJ25), foam: zero anthocyanin/low sugars content (ZA25sf) and (non-foamed) blackcurrant juice: low anthocyanin/low sugars content (J25). The freezing point of J100 (high anthocyanin/high sugars content) was not reached at -30˚C and thus the drying rates were impossible to analyse with the equipment of the laboratory; the samples were bubbling and spilling from the containers during the reduction of pressure in the chamber.

The highest drying rate observed was for the juice (J25) and the slowest was for the concentrated foam (FJ100). These data suggested that the more concentrated and complex is the sample, the slower the dehydration will occur.

Table 5.1 Experimental and predicted drying rates of blackcurrant juice and four different foams. Each value is the mean, % error, n = 4.

	Drying rate [g/√s]		
Sample	**Experimental**	**Predicted**	**% error**
FJ100	0.0319	0.0309	2.9042
ZA100sf	0.0456	0.0452	0.7135
FJ25	0.0517	0.0510	1.3540
ZA25sf	0.0567	0.0541	4.7996
J25	0.1514	0.1513	0.0165

Figure 5.1 depicts the water loss (change in mass, ΔM) in 10 grams of foam per $\sqrt{s}$ for the four foams tested. The graphs are presented from high (ZA25sf) to low (FJ100) drying rates from left to right. Figure 5.2 depicts change in mass in 56 g of juice (which was equivalent in volume to 10 g of foam) per $\sqrt{s}$. Figures 5.3 and 5.4 depict the experimental values during freeze-drying foams

and juice. A steady sublimation rate in foams was observed after 1 h of freeze-drying and lasted for around 4 h. In juice, a steady sublimation rate was observed after 3 h of freeze-drying and lasted for at least the 12 h of the experiment.

Table 5.2 shows the calculated values for diffusivity (D), temperature of the interface (T_s) and constant B of Equation 2.21. Values for diffusivity reported for microwave assisted freeze-dried ice spheres (D = 2.2x10^{-3} m^{2}s^{-1} at -15˚C, 20 Pa) by Wu et al. (2004), turkey breast (D = 1.5x10^{-3} m^{2}s^{-1} at -15 ˚C, 38 Pa) and beef (D = 1.0x10^{-3} m^{2}s^{-1} at -15˚C, 38 Pa) by Ma and Peltre (1975) were slightly smaller than the samples studied here at much lower temperatures and pressures, which make them plausible.

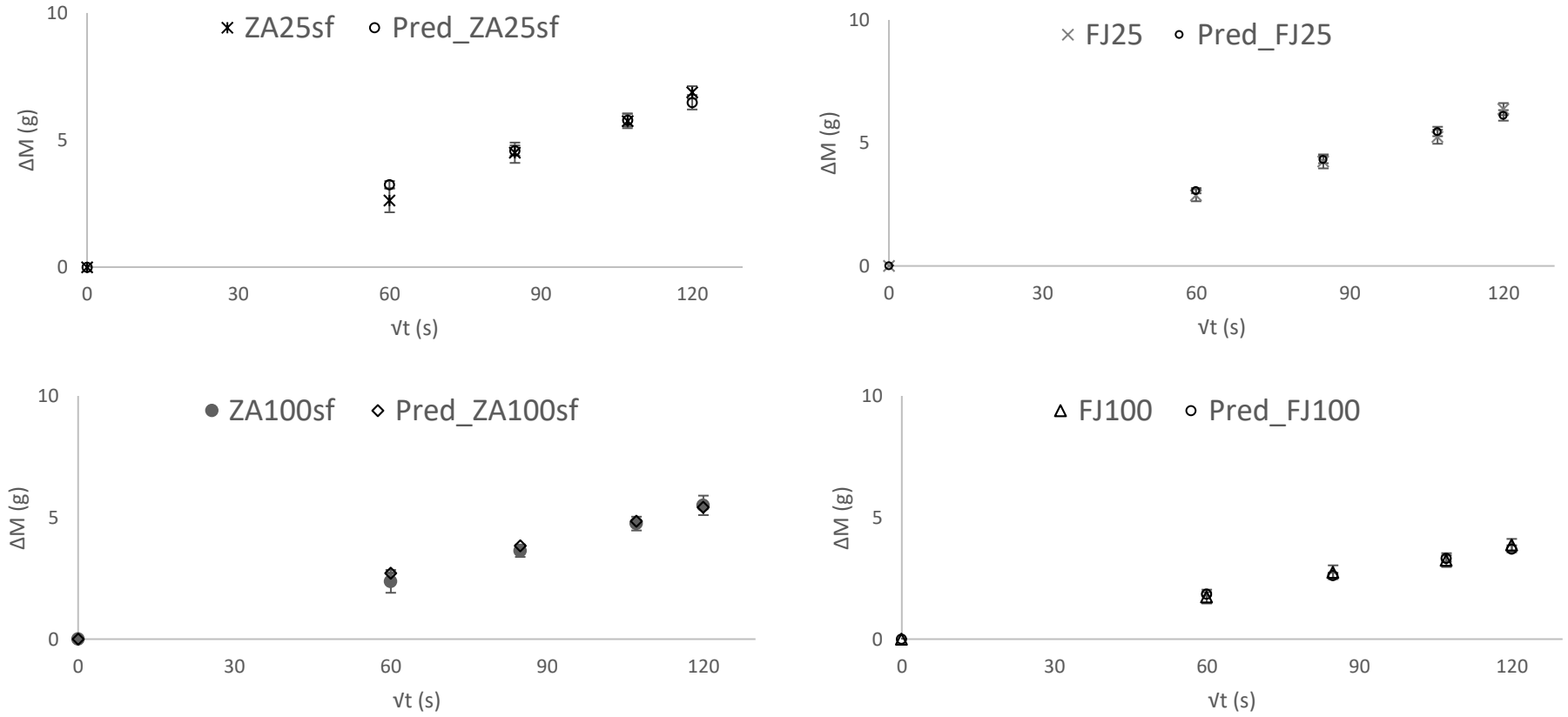

Figure 5.1 Change in mass (ΔM) vs √t (s) foams: zero anthocyanin+low sugars concentration (ZA25sf), low concentration of anthocyanin+sugars (FJ25), zero anthocyanin+high sugars concentration (ZA100sf) and high concentration of anthocyanin+sugars (FJ100). "Pred_" indicate data obtained with the model. Mean, confidence limit 95%, n = 4.

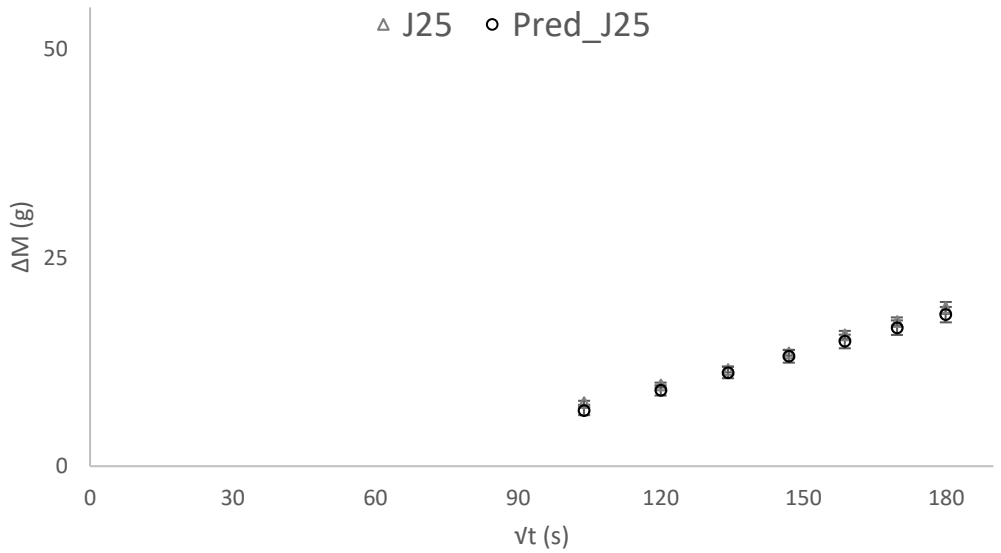

Figure 5.2 Change in mass (ΔM) vs √t of blackcurrant juice (J25). "Pred_" indicate data obtained with the model. Mean, confidence limit 95%, n = 4.

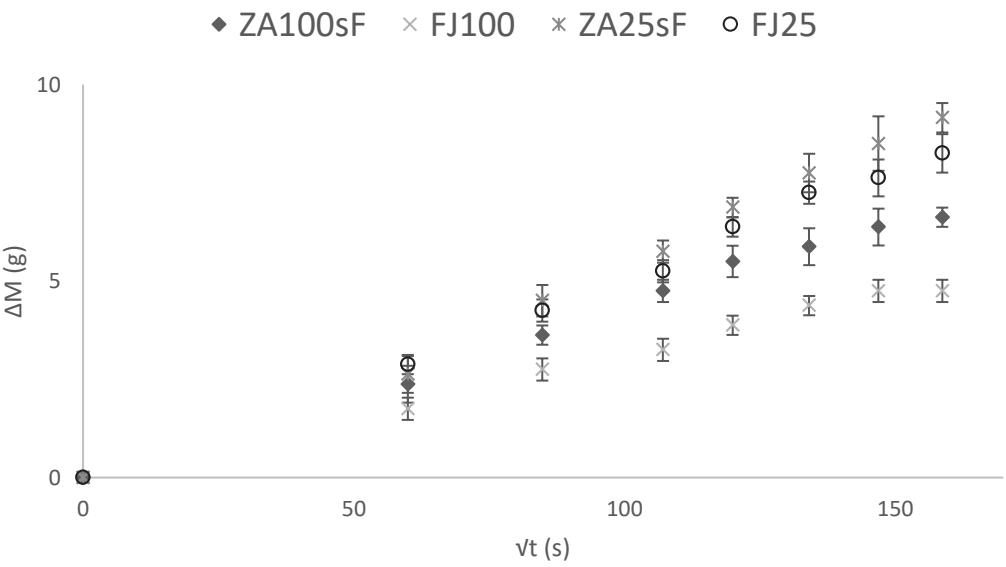

Figure 5.3 Drying behaviour until constant weight of foams (~8 hours). Change in mass (ΔM) vs √t (s), n = 4.

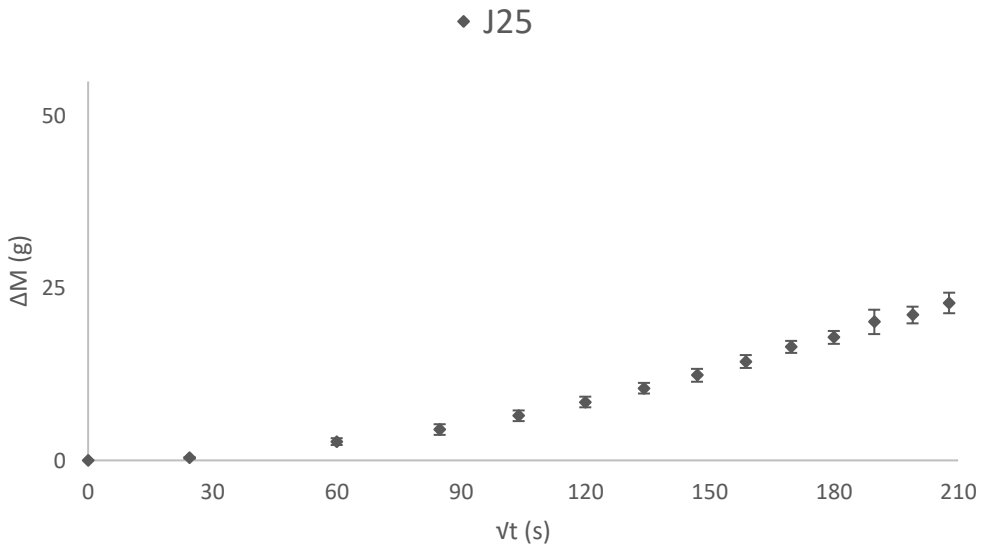

Figure 5.4 Drying behaviour of blackcurrant juice (J25) (12 hours). Change in mass (ΔM) vs √t (s), n = 4.

Table 5.2 Diffusivity (D), Temperature of the interface (T_s) and constant (B) of blackcurrant juice (J25), high concentration of anthocyanin+sugars (FJ100), zero anthocyanin+high sugars concentration (ZA100sf), low concentration of anthocyanin+sugars (FJ25), zero anthocyanin+low sugars concentration (ZA25sf).

	J25	***FJ100***	***ZA100sf***	***FJ25***	***ZA25sf***
$D\ [m^2s^{-1}]$ *at -50˚C, 4 Pa**	0.0218	0.0125	0.0271	0.0688	0.0688
T_s **[K]**	220.84	221.53	222.45	223.08	223.57
B	-9.08	-1.3	-1.3	-1.3	-1.3

*the freeze-drier kept a pressure between 3.6 and 6.3 Pa during the process.

Figures 5.5 and 5.6 depict the model graphically showing the predicted drying rates versus AVF (or porosity) and density, respectively. These figures show the regions where the model was validated,

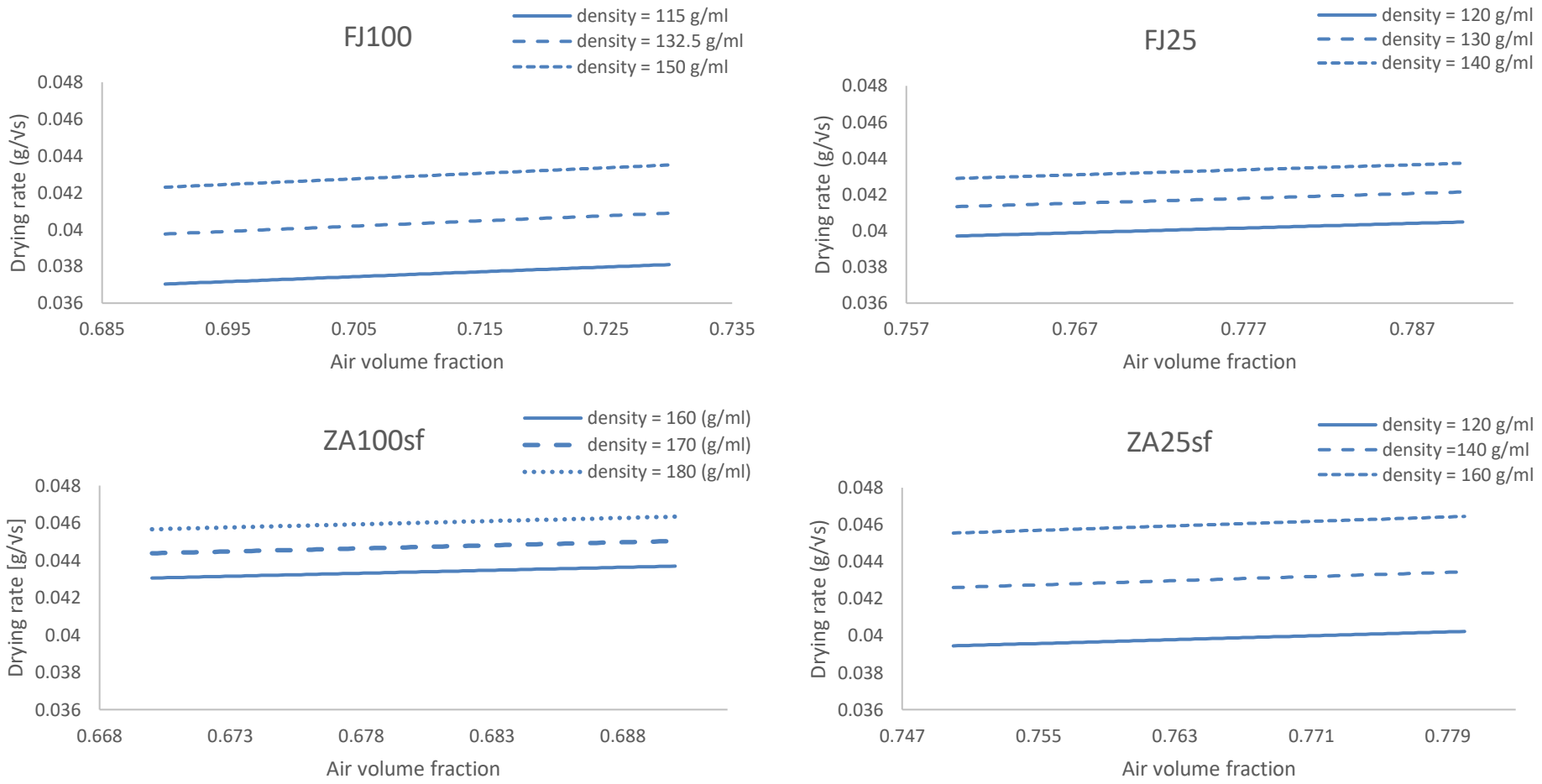

Figure 5.5 Predicted drying rate vs air volume fraction for the minimum, mean and maximum values of density tested in each foam.

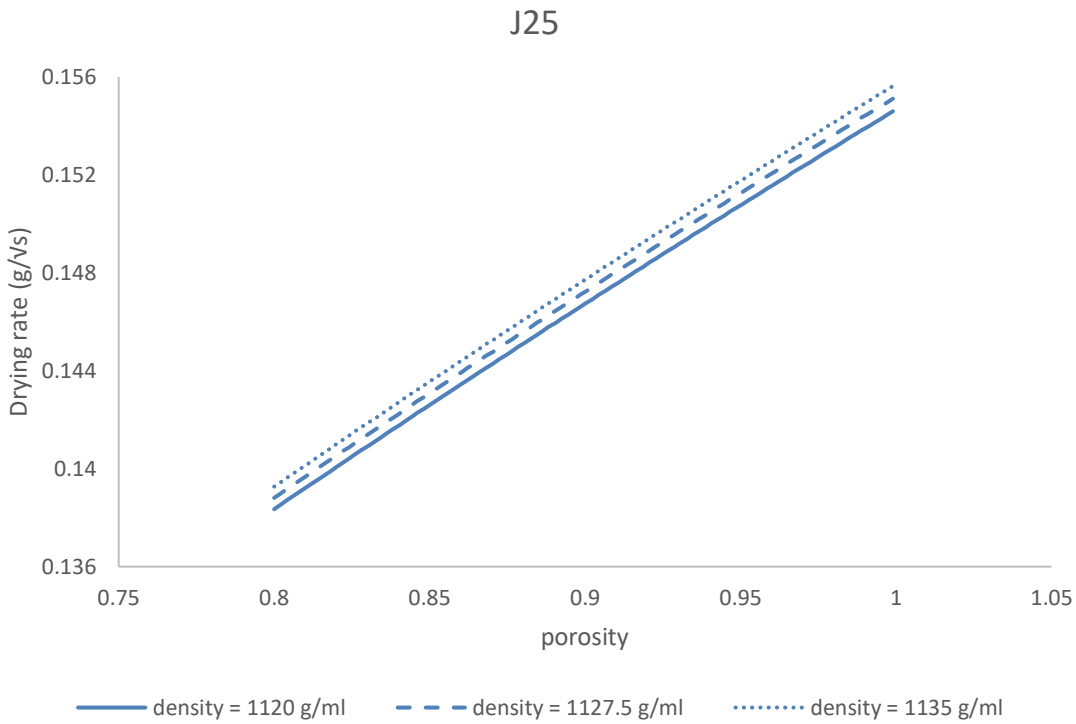

Figure 5.6 Predicted drying rate of blackcurrant juice vs porosity (See section 2.6.1 above) for the minimum, mean and maximum values of density tested.

Table 5.3 Characteristics of samples after drying. Mean value ± standard error, n=4.

	J25	*FJ100*	*ZA100sf*	*FJ25*	*ZA25sf*
time until weight reaches a plateau [h]	24*	6	7	7.5	7
Total water loss [%]	78.0 ± 0.2	46.9 ± 0.1	66.6 ± 0.1	83.3 ± 0.2	86.9 ± 0.1
Moisture content powders [% wet basis]	0.4 ± 0.2‡	2.6 ± 0.3	3.2 ± 0.1	4.8 ± 0.6	3.6 ± 0.4

* Constant weight was not reached but the equipment had no more drying capacity
‡Surface of the sample.

The statistical model suggests foaming decreases the drying rate by 0.041 ± 0.004 g/√s. The quantity of anthocyanin in foamed samples had a small effect on the drying rate (p-value 0.032) decreasing it by 0.00016 ± 0.00007 g/√s per mg l^{-1} of anthocyanin. The presence of sugars in the samples had also a significant effect (p-value 0.002) in the drying rate, decreasing it by 0.005 ± 0.001 g/√s. The anthocyanin alone in the non-foamed samples did not have a significant effect on the drying rate (p-value 0.102) (Model details and residual plots in Appendix B). The statistical model, when comparing means of foams, suggests that the drying rate (DRexp) decreases by 0.009 ± 0.002% g/√s per mg l^{-1} of anthocyanin (p-value = 0.001) and also by 0.56 ± 0.07% g/√s per g l^{-1} of total SC (p-value <

0.0005). The interaction between anthocyanin and high-SC increases the DRexp of foams by 0.006 ± 0.002% g/√s (p-value = 0.023).

5.3 Discussion

The non-foamed blackcurrant juice (J25, 93.6 ± 3.8 % water content, wet basis) presented the fastest drying rate in the period and conditions analysed. Then, in descendent drying rate order: ZA25sf, FJ25, ZA100sf and FJ100 (Table 5.1). This order correlated well with the order of their D (Table 5.2), Sauter mean (See Chapter 4, Table 4.1) and % water loss (Table 5.3). This suggests that foams with high proportions of larger bubbles promoted larger diffusivities and in consequence faster drying rates. Also, large bubbles provide large holes through which water vapour could escape easily. This is in accordance with other publications were it was shown that large bubbles increased the evaporation area in blackcurrant foams (glycerine monostearate and soy protein isolate as foaming agents), accelerating the drying process (Zheng et al., 2011). However, in egg white–apple juice foams, small bubbles favoured heat and mass transfer and therefore increased the drying rate (Raharitsifa and Ratti, 2010a, Raharitsifa and Ratti, 2010b).

As seen in Chapter 4, the anthocyanin reduced the bubble size. Thus, the higher the anthocyanin content, the smaller the bubble size and the slower the drying rate that was detected. The statistical model (comparing only foams) suggests that the anthocyanin and the high sugars content (SC) as well as their interaction had significant effects on the drying rate of foams (p-values: 0.001, < 0.0005 and 0.023, respectively). The model also suggests that the drying rate

(DRexp) in foams decreases by 0.009 ± 0.002% g/√s per mg l^{-1} of anthocyanin and also by 0.56 ± 0.07% g/√s per g l^{-1} of total SC. However, the interaction between anthocyanin and high-SC increases the DRexp of foams (by 0.006 ± 0.002% g/√s). This presumably happened since anthocyanin and sugars react with each other, leaving more free water available to sublimate.

Comparing samples with the same sugars content, the reason why the drying rate of FJ25 was slightly lower (9%) than ZA25sf was presumably because the Sauter mean of the latter was larger (8%). The *D* values of FJ25 and ZA25sf were equal since the difference of AVF between these foams was small (0.4%) indicating similar fractions of dispersed and continuous phases and hence promoting similar rates of mass transfer. Among the main differences between FJ25 and ZA25sf was that, as seen in Chapter 4, the bubble size distribution of ZA25sf appeared to be broad and covering several bubble sizes, while FJ25 showed a high peak in the frequency density of small bubbles and a long tail towards larger bubble sizes. ZA25sf did not show a single peak like the other foams. This characteristic (among others) gave ZA25sf a faster drying rate than the other foams.

The lowest drying rate corresponded to FJ100, having the smallest bubble size amongst all the samples and a bubble size distribution that showed the largest frequency density peak of all foams (at 0.03 mm) while its counterpart, ZA100sf, showed two peaks (0.10 and 0.14 mm). This suggested that foams with these sugars concentrations produced small bubble sizes but more bubble coalescence could have occurred in ZA100sf, increasing the frequency density to larger bubble sizes and thus increasing the drying rate. This

was confirmed because ZA100sf had larger % drainage than FJ100, suggesting foam breakage. A decrease in the drying rate of 30% was observed in FJ100 when compared to ZA100sf, showing the impact of the anthocyanin over the drying rate at these concentrations of sugar and anthocyanin. However, the mean bubble size was not the only characteristic affecting the drying rate.

Another characteristic of the foams affecting the drying rate was the viscosity. Higher viscosity in the foams indicated more 'friction' between molecules, which hindered sublimation. This was mainly observed in FJ100 which had the highest viscosity and the lowest total water loss. However, viscosity in foams also depends on the bubble size (small mean bubble sizes tend to yield higher viscosities), so at larger bubble sizes like those of FJ25 and ZA25sf, similar viscosities and total water loss were obtained. An intermediate value of mean bubble size (ZA100sf) produced an intermediate total water loss and the lowest viscosity compared to the other foams. Although viscosity provided information related to the texture of a foam, it did not capture the internal characteristics of the foam in terms of mass, which in drying has a more important role. Thus, density together with AVF is a better way to capture the relationship of solid, liquid and gas when drying foams, especially those with similar formulations.

A loose positive relationship was observed between the density of pre-foaming liquid (ρ_L) (Table 4.1) and the total water loss in foams (Table 5.3). Despite the fact that the mathematical model (Equation 2.21) did not need ρ_L to predict the drying rate, ρ_L can be a good starting point to know how fast samples will dry. In foams, it was observed that the higher and lower % water loss values

corresponded to the less (ZA25sf) and more (FJ100) concentrated foams, respectively. The difference observed was of 46% in water loss between FJ100 and ZA25sf. When comparing the effect of anthocyanin in foams with equal sugar concentrations, a 30% decrease of water loss was observed between FJ100 and ZA100sf and a 4% decrease between FJ25 and ZA25sf. This showed a larger effect of anthocyanin with higher sugar concentration. These differences were presumably because lower solute concentrations in foam promoted higher free water content in ZA25sf than in the more concentrated foams. This affected the drying rate since the vapour pressure of water decreases with solutes (Vaclavik and Christian, 2014) and more energy is required to convert water (ice) to vapour (see Equation 2.17, where P_s decreases if LD increases which corresponds to the amount of heat needed to change the water phase by a specific sample diffusivity). This is because when solutes interact with water, there are fewer water molecules in the same volume available for vaporization and therefore fewer molecules in the vapour state (Vaclavik and Christian, 2014). Thus, the more solids the sample contained, the more water interacted with them forming bound water, and thus less free water (ice) sublimed. The quantity of free water in samples was then the total water loss (in %) of the samples measured at the time when constant weight was reached (Table 5.3). Furthermore, the lower the free water content of foams, the faster the time to constant weight observed. Nevertheless, faster time to constant weight is not the same as drying rate. The drying rate accounts for the characteristics of the sample that affect the loss of water (Equation 2.21) over time and can be used when drying large batches, whilst the time to constant weight is a simple

measure of a specific sample and might not be accurate when drying large batches.

In these terms, the loss of water as described in Equation 2.21 relates to how effectively heat and mass transfer occur in the sample. Mass transfer, as mentioned before, was enhanced by large mean bubble size and higher AVF which also enlarged the porosity of the sample. However, foams are known to be insulating materials since air (bubbles) transmit heat slowly. Thus, the more air (bubbles) or the higher the AVF, the slower the heat transfer will occur through the sample. Also, the less concentrated the continuous phase of foam, the slower the heat transfer will occur. Interestingly, the foam with the largest mean bubble size and the largest AVF, and lowest solute content (ZA25sf) obtained the largest drying rate (and % water loss) among the foams. This supports the idea that drying in foams is not limited by mass transfer (Raharitsifa and Ratti, 2010a); and suggests that heat transfer relies on the free water content in the continuous phase.

Equation 2.21 then, accounts for the subtle differences over T_s for different free water, sugar, anthocyanin and air contents of the foams (expressed as ρ_F and AVF). As seen in Table 5.2, the calculated T_s for all samples decreased with lower solute concentration. This means that more energy was required in the sublimation for drying FJ100 (and also J25) than ZA25sf.

Thus, FJ100 reached constant weight faster than any other sample, suggesting lower free water content. This happened since, as mentioned in the previous chapter, high anthocyanin and sugar concentrations along with long enough whipping times aided the hydration and coagulation of egg albumin,

increasing the bound water in the sample. Also, the high % moisture content of the foam-mat freeze-dried powders compared to the non-foamed juice powders supported the hypothesis of more water retention (less free water) in the foams. Ptaszek et al. (2014) reached a similar conclusion in egg white foams. They also suggested that the high water content in the structure of egg white foams did not make them suitable for drying. Also, the % moisture content of the final powders was higher in the foams than in the juice, which can compromise the shelf life of the product. Nevertheless, the use of egg albumin as foaming agent to dry samples can indeed shorten drying processes since less free water is available to be removed.

The mathematical model predicted the shape of the DRexp curve at steady state. Figures 5.1 and 5.2 show good agreement between the experimental ($\Delta M(t)_e$) and predicted (ΔM) change of mass (moisture content loss) for foams and juice (J25), respectively. Figure 5.4 ($\Delta M(t)_e \; vs \; \sqrt{s}$) shows a delay in J25 reaching steady state when freeze-drying but afterwards it shows a straight line predicted by the model. By contrast, foams entered into a steady state faster than J25 since the free water content was lower (Figure 5.3). Thus, constant B was settled at -9.08 for J25 while in foams it was settled at -1.3 for all the repetitions to account for the aforementioned delay. Diffusivity (D) was estimated using the mathematical model by tuning the parameter (D) to fit the experimental data. In future work, knowing the diffusivity of a foam a priori would allow the model to be tested more rigorously.

The difference between the predicted and experimental DR could be due to the lack of accurate values for the specific samples analysed i.e. we did not

have temperatures recorded at different times and zones of the sample nor very precise weights at very short time intervals. Future research could improve the comparison between the two by adding thermocouples into the sample at different distances throughout its thickness and by using more sophisticated balances and drying equipment. However, the % error between experimental and predicted drying rates was < 5 % in all cases (Table 5.1).

Drying times until constant weight obtained in this study (Table 5.3) were in accordance with other studies, where foamed samples needed ~6 h to dry and non-foamed samples needed nearly 15 h to remove 50% of ice in the same volume (Muthukumaran, 2007). These certainly suggest that foams dry at least 3 times faster than non-foamed samples in the same volume. However, in this study, the mass of J25 in the same volume was at least 5 times larger than in foams. This affected the capacity of the condenser because of the formation of an ice layer around it. This layer insulates the condenser, increasing T_o towards T_s, which reduces the gradient of vapour concentration between the sample and condenser.

Nevertheless, it has to be mentioned that the weak structure left behind by the dried juice (J25) could collapse in some parts of the dried layer, blocking the passage of water vapour. This phenomenon was reduced in foams because of the increased structural strength that foaming agents provide, especially those containing polyphenols as demonstrated by (Wu et al., 2007, Rodriguez et al., 2015).

Finally, the mathematical model was tested with the data from a published study of freeze-dried skim milk (Sadikoglu and Liapis, 1997). The

conditions of their study were inferred from the above paper and two others (Liapis and Bruttini, 1994, More and Prasad, 1988). Their drying curve was approximately linear but its slope was equal to that predicted by the mathematical model at a certain time point around 2.5 h into the first stage of freeze-drying (See Appendix A).

5.4 Conclusions

Short drying time has been one of the main points used in favour of drying foams. However, short time to constant weight is not the same as fast drying rate. Foams analysed here did reach constant weight faster than non-foamed samples but foams had slower drying rates than non-foamed samples because differences in the total amount of water loss. Also, the characteristics of foams modified the drying rate. The effect of the bubble size and bubble size distribution on improving the drying rate depended on the bulk phase and were not the only, or indeed the main factors affecting the drying process. Producing different bubble sizes via modifying the formulation of foams also affected the foams density, AVF, drainage and viscosity. The result was that low solutes concentrations increased the drying rate. Anthocyanin decreased the drying rate only in highly concentrated sugars foams.

Finally, the mathematical model served two purposes: 1) it predicted the shape of the drying curve at steady state and 2) it estimated the diffusivity of both foamed and non-foamed samples. In future studies, it could predict the drying rate of a sample if the following parameters were known: the process

conditions (P and T), the area of the container, the diffusivity, the porosity or air volume fraction (in the case of foam) and the density of a sample.

Chapter 6 Colour change of foam-mat freeze-dried and conventional freeze-dried blackcurrant powders during five months storage.

6.1 Introduction

Colour changes of edible products containing anthocyanin, like food or medicines (e.g., cough syrups), are important since appearance is one of the major characteristics the consumer judges when buying or disposing a product (Bridle and Timberlake, 1997). The shelf life of a product also depends on colour changes. In this chapter, the change in colour of blackcurrant juice (as it can be found in nature, not concentrated) was analysed after foam-mat freeze-drying and compared to conventional freeze-dried blackcurrant powders using a colorimeter (Methodology in section 2.5.2). Measurements were taken at monthly intervals during five months storage with or without vacuum. Xanthan gum was also tested as a colour stabiliser in the juice.

Since the foaming agent (egg albumin) was found to change the pH of the sample and the colour of anthocyanin depends on pH, tests of colour in a modified pH blackcurrant juice were run to observe changes in colour due to pH. This can also be used as a guide of how blackcurrant juice change colour after processing.

6.2 Results

Colour changes occurred during storage for all treatments, but especially the powders obtained via foam-mat freeze-drying. Results are presented here for

% reflectance of powders obtained via freeze-drying and foam-mat freeze-drying with their respective pH, % moisture contents (wet basis) and densities. Pictures of both conventional freeze-dried and foam-mat freeze-dried samples are shown before and after five-month storage. Charts of differences of means (statistical analysis) between conventional freeze-dried powders versus foam-mat freeze-dried powders are also presented. Finally, the % transmittance and colour profile of non-freeze-dried samples (liquid samples) are presented.

To understand the role of pH in the change of colour of blackcurrant juice, Figure 6.1 shows the % transmittance of blackcurrant juice at six different pH levels (1 to 6). Samples with pH 1 to 3 presented low transmittance (high absorbance) over the wavelengths corresponding to green, meaning they had a more intense red colour than samples with pH 4 to 6, all with the same apparent anthocyanin content (40.4 ± 0.1 mg l^{-1}).

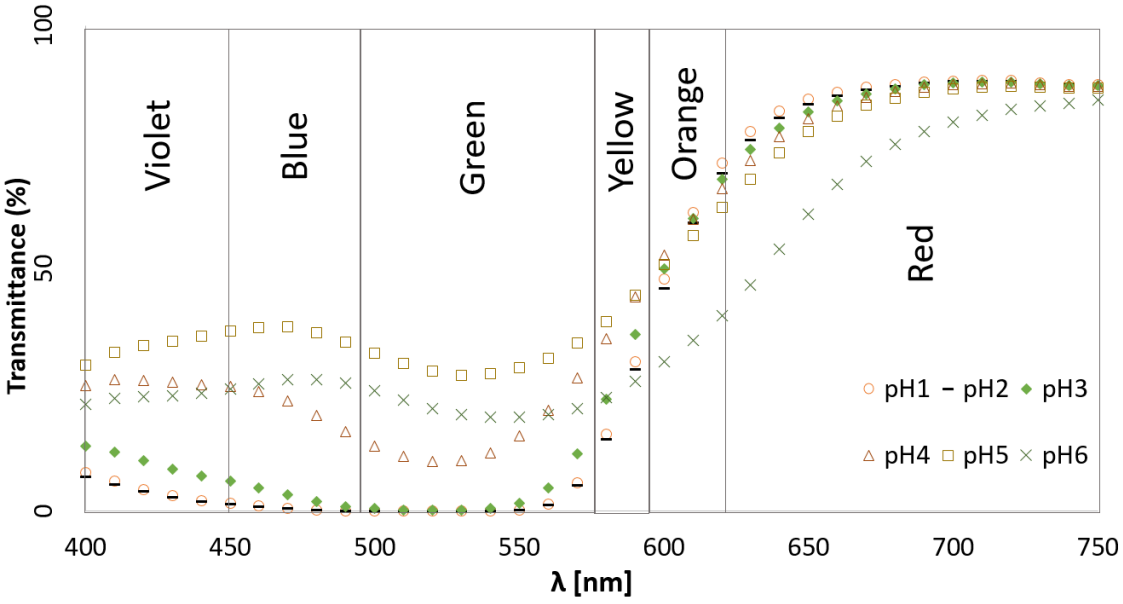

Figure 6.1 % Transmittance of different pH in blackcurrant juice. Colours shown over the corresponding wavelengths (λ) in nanometres (nm). Average std error = 0.01, n=3.

Figures 6.2 and 6.3 depict the % reflectance of powders produced via foam-mat freeze-drying (FJ25) and conventional freeze-drying of blackcurrant juice (J25) and from blackcurrant juice with xanthan gum (Xanthan). Foam-mat freeze-dried samples showed higher % reflectance (%r) in the wavelengths (λ) corresponding to green compared to the freeze-dried samples, suggesting that the first ones will look less red. J25 and Xanthan powders showed low %r of green, suggesting more red intensity than FJ25.

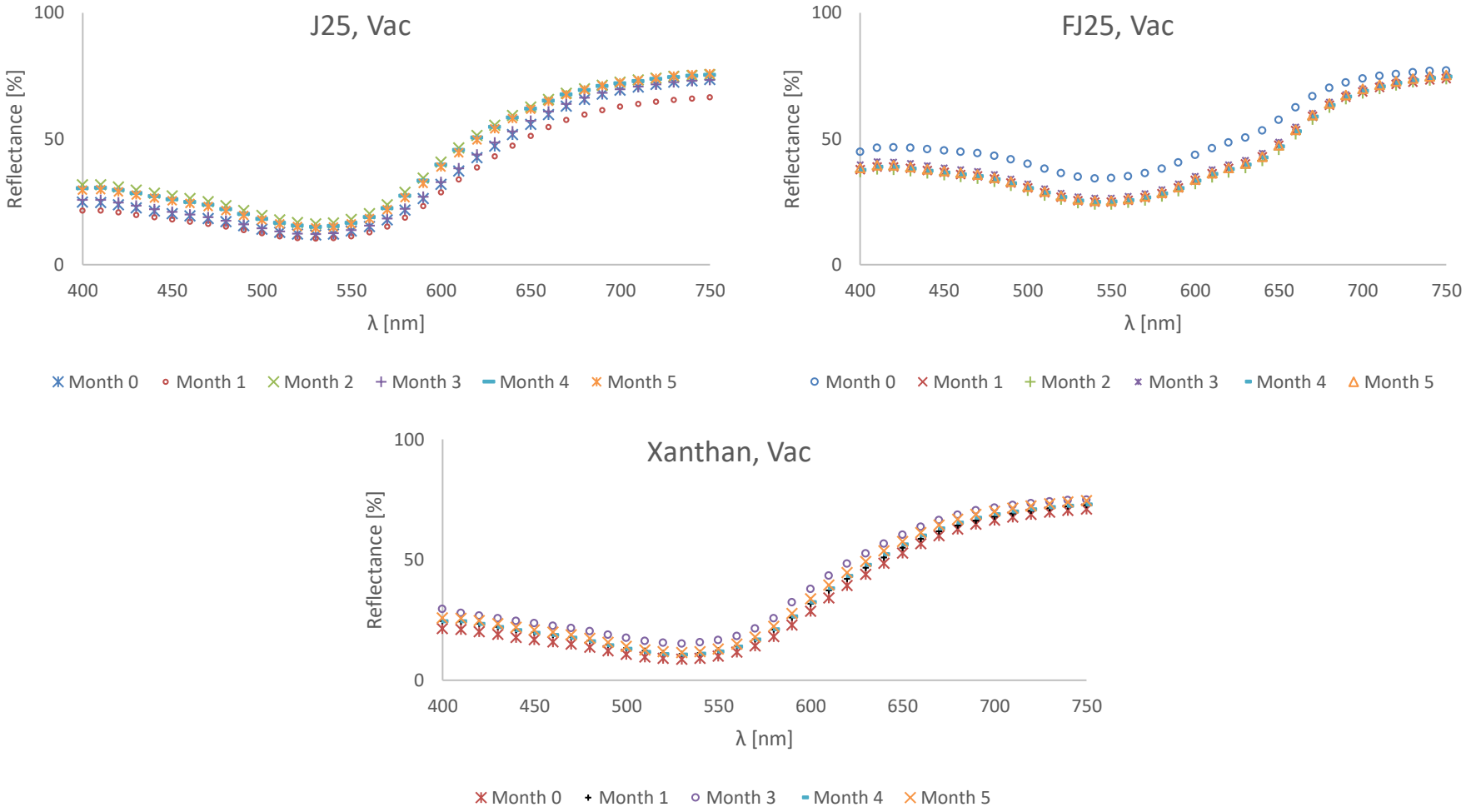

Figure 6.2 Reflectance [%] vs wavelength [nm] of samples stored with vacuum (Vac). Average std error: J25 = 0.26, FJ25 = 0.09,Xanthan = 0.39,n=3.

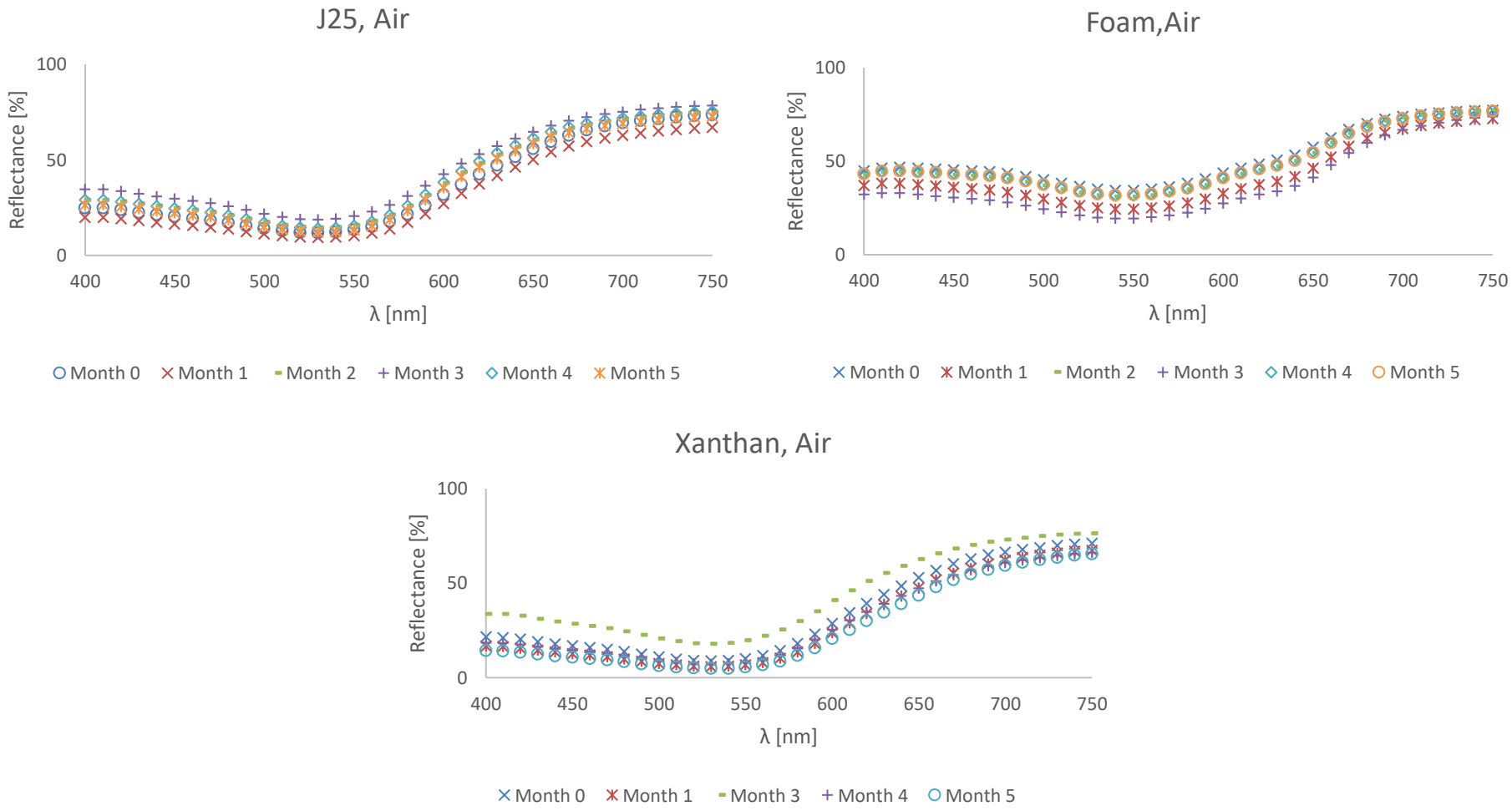

Figure 6.3 Reflectance [%] vs wavelength [nm] of samples stored without vacuum (Air). Average std errors: J25 = 0.08,FJ25 = 0.11,Xanthan = 0.23,n=3.

Table 6.1 shows the pH, the % moisture content and the density of powders obtained via foam-mat freeze-drying (FJ25) and conventional freeze-drying of blackcurrant juice (J25 and Xanthan). FJ25 had larger values of pH and % moisture content (%mc) than conventional freeze-dried powders (J25 and Xanthan). Stable %mc was observed in unopened bags of all samples. Density of powders (ρ) was lower in FJ25 than in J25 and Xanthan samples.

Table 6.1 Characteristics of foam-mat freeze-dried blackcurrant powder (FJ25), conventional freeze-dried blackcurrant powder (J25) and conventional freeze-dried blackcurrant juice with xanthan gum powder (Xanthan). Air and Vac refer to non-vacuum and vacuum storage, respectively. Mean ± standard error, n = 3.

	pH	Moisture content (%, wet basis)	Density (g ml^{-1})
FJ25, Air	4.2	2.64 ± 0.13	0.72 ± 0.01
FJ25, Vac	4.2	3.11 ± 0.07	0.71 ± 0.02
J25, Air	3.3	0.90 ± 0.06	0.96 ± 0.04
J25, Vac	3.4	0.51 ± 0.07	1.03 ± 0.01
Xanthan, Air	3.4	0.84 ± 0.06	1.26 ± 0.04
Xanthan, Vac	3.4	1.03 ± 0.13	1.10 ± 0.04
unopened bags			
FJ25, Air	4.2	2.60 ± 0.19	0.82 ± 0.04
FJ25, Vac	4.2	2.63 ± 0.12	0.72 ± 0.01
J25, Air	3.3	0.96 ± 0.11	0.97 ± 0.05
J25, Vac	3.3	0.63 ± 0.05	0.95 ± 0.01
Xanthan, Air	3.4	0.86 ± 0.05	0.84 ± 0.02
Xanthan, Vac	3.4	1.10 ± 0.06	0.88 ± 0.02

Conventional freeze-dried J25 and Xanthan looked red/pink while foam-mat freeze-dried blackcurrant juice (FJ25) looked purple (Pictures in Figure 6.4).

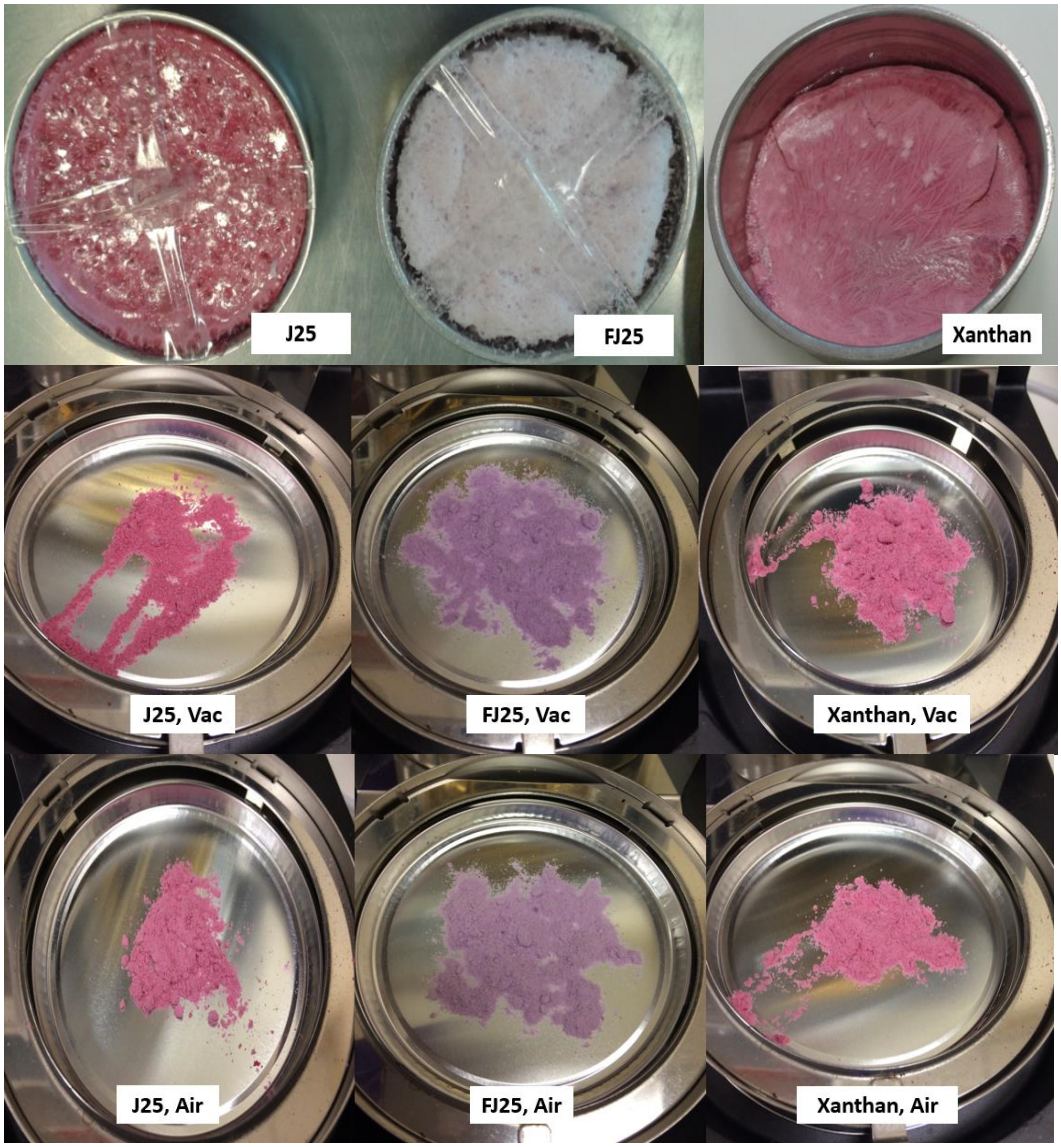

Figure 6.4 Pictures of samples at the beginning (3 top pictures) and at the end of the experiment (6 bottom pictures).

Figure 6.5 shows differences of means of ΔE (noticeable change in colour), $(\Delta H)^2$ (change in hue or pure spectrum of colour) and ΔC (change in chroma or colour saturation) between samples. Samples (J25, FJ25 and Xanthan) were significantly different from each other for all responses (ΔE, $(\Delta H)^2$ and ΔC) except $(\Delta H)^2$ between J25 and Xanthan.

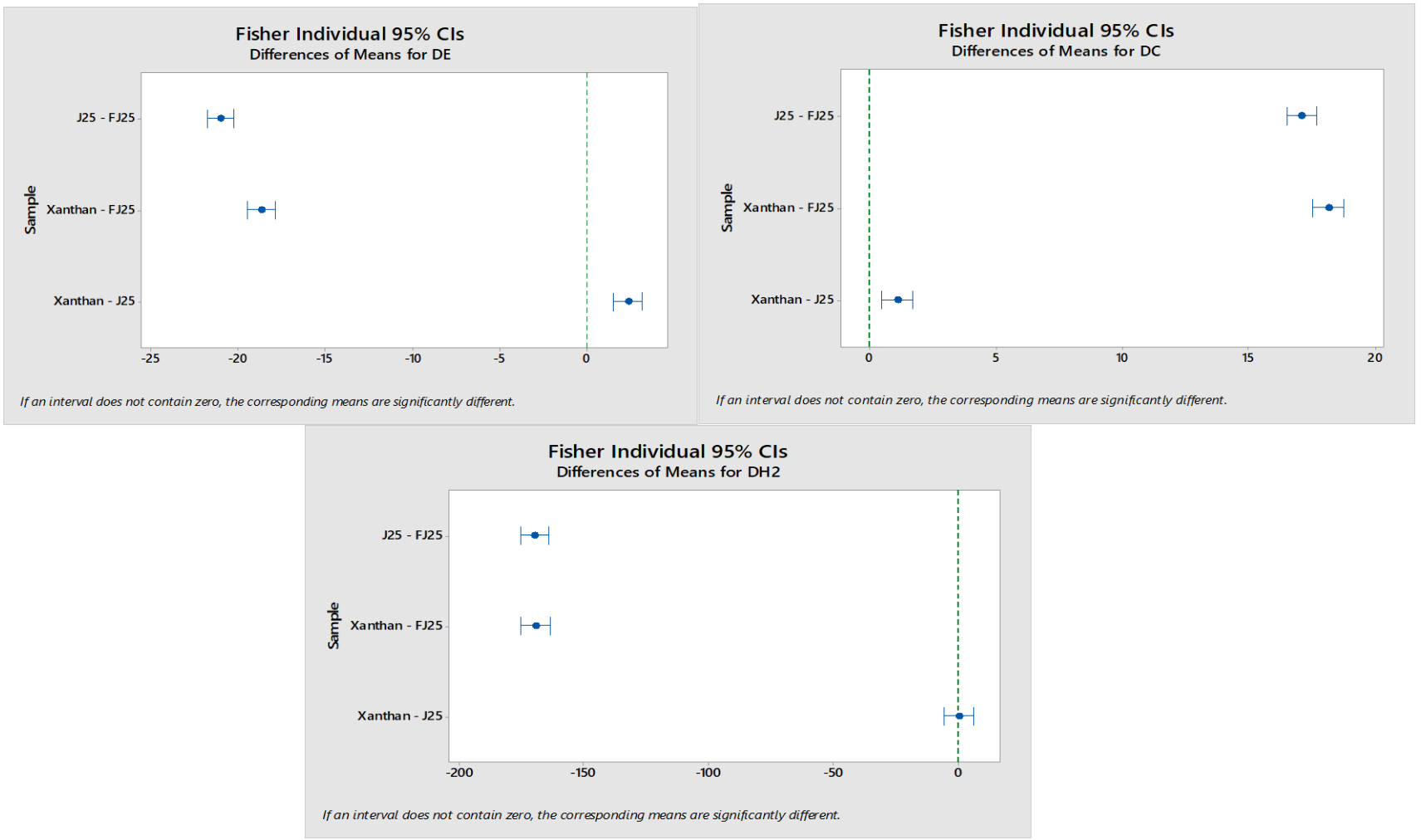

Figure 6.5 Differences of means of ΔE, ΔC and $(\Delta H)^2$ between J25, FJ25 and Xanthan (powders).

The following tables present the *L* (*L*–lightness: Darkest black = 0. Brightest white = 100), *a* (+*a* = redness. -*a* = greenness) and *b* (+*b* = yellowness. -*b* = blueness) values of foam-mat freeze-dried and conventional freeze-dried blackcurrant juice and xanthan-blackcurrant juice powders stored with (Vac) and without (Air) vacuum. Unopened bags were analysed at the end of the experiment. Foam-mat freeze-dried powders yielded lower values in *a* and more negative *b* values than freeze-dried ones, suggesting that the first ones had less red and more blue hues. ΔE, ΔH and ΔC values are also depicted in tables 6.2 showing larger differences between FJ25 powders compared to the standard colour (J25,to).

Tables 6.2 Colour profile of powders dried via conventional freeze-drying (Juice and Xanthan) and foam-mat freeze-drying (Foam) blackcurrant juice. Juice,to = standard colour. Mean ± standard error, n=3.

	Juice,to	Juice, Air					
Month / Parameter	0	1	2	3	4	5	unopened
L	52.00 ± 0.08	47.78 ± 0.13	56.05 ± 0.01	60.42 ± 0.02	55.90 ± 0.19	53.47 ± 0.09	60.66 ± 0.10
a	32.42 ± 0.01	33.04 ± 0.02	32.14 ± 0.14	29.51 ± 0.03	33.36 ± 0.09	34.25 ± 0.04	29.34 ± 0.07
b	-0.02 ± 0.02	0.61 ± 0.04	-1.02 ± 0.01	-1.19 ± 0.03	-0.90 ± 0.04	-0.73 ± 0.05	-1.22 ± 0.08
ΔC	0.00 ± 0.00	0.61 ± 0.03	-0.26 ± 0.15	-2.87 ± 0.03	1.14 ± 0.05	0.83 ± 0.08	-0.19 ± 0.01
ΔE	0.00 ± 0.00	4.20 ± 0.23	4.19 ± 0.06	8.98 ± 0.07	3.78 ± 0.22	4.34 ± 0.09	2.46 ± 0.04
ΔH	0.00 ± 0.00	0.58 ± 0.06	1.00 ± 0.02	1.22 ± 0.02	0.80 ± 0.07	0.92 ± 0.02	0.70 ± 0.02
	Juice, Vac						
L	51.92 ± 0.10	49.30 ± 0.14	58.21 ± 0.31	52.59 ± 0.13	57.12 ± 0.12	56.48 ± 0.10	53.85 ± 0.04
a	32.23 ± 0.05	32.25 ± 0.13	31.51 ± 0.37	32.76 ± 0.09	32.71 ± 0.06	32.69 ± 0.01	32.14 ± 0.05
b	-0.04 ± 0.02	0.10 ± 0.08	-1.22 ± 0.02	-0.17 ± 0.02	-1.16 ± 0.03	-1.01 ± 0.02	-0.43 ± 0.09
ΔC	-0.02 ± 0.04	0.01 ± 0.19	-0.71 ± 0.42	0.38 ± 0.17	0.51 ± 2.57	0.38 ± 0.16	0.46 ± 2.32
ΔE	0.16 ± 0.07	0.54 ± 0.09	8.82 ± 0.30	8.00 ± 0.29	7.80 ± 0.07	7.43 ± 0.25	7.04 ± 0.06
ΔH	0.04 ± 0.04	0.12 ± 0.05	1.32 ± 0.06	1.23 ± 0.05	1.23 ± 0.05	1.25 ± 0.05	1.09 ± 0.05

.

	Foam, Air						
Month / **Parameter**	0	1	2	3	4	5	unopened
L	68.95 ± 0.10	60.78 ± 0.03	66.55 ± 0.02	55.89 ± 0.14	67.10 ± 0.09	67.08 ± 0.05	58.97 ± 0.05
a	11.21 ± 0.02	13.26 ± 0.04	12.19 ± 0.05	15.14 ± 0.02	11.99 ± 0.01	11.70 ± 0.05	13.63 ± 0.01
b	-6.77 ± 0.01	-9.36 ± 0.02	-7.83 ± 0.02	-10.21 ± 0.02	-7.57 ± 0.02	-7.56 ± 0.06	-9.43 ± 0.03
ΔC	-19.32 ± 0.02	-16.09 ± 0.04	-17.93 ± 0.06	-14.12 ± 0.05	-18.27 ± 0.03	-18.23 ± 0.03	-18.49 ± 0.01
ΔE	27.98 ± 0.09	23.10 ± 0.04	26.11 ± 0.06	20.46 ± 0.03	26.61 ± 0.05	26.44 ± 0.09	26.71 ± 0.05
ΔH	11.05 ± 0.01	13.86 ± 0.02	12.20 ± 0.02	14.19 ± 0.02	11.90 ± 0.02	11.92 ± 0.04	12.01 ± 0.01
	Foam, Vac						
L	66.54 ± 0.10	61.37 ± 0.10	60.43 ± 0.02	62.71 ± 0.04	61.30 ± 0.09	61.73 ± 0.12	69.12 ± 0.08
a	12.08 ± 0.02	13.41 ± 0.04	13.31 ± 0.03	13.03 ± 0.02	13.21 ± 0.04	13.12 ± 0.09	10.65 ± 0.07
b	-7.78 ± 0.01	-9.28 ± 0.04	-9.56 ± 0.02	-9.36 ± 0.02	-9.28 ± 0.04	-9.39 ± 0.11	-6.88 ± 0.05
ΔC	-17.55 ± 0.02	-15.87 ± 0.13	-15.86 ± 1.03	-16.15 ± 0.10	-16.11 ± 0.15	-16.09 ± 0.11	-16.11 ± 0.09
ΔE	23.82 ± 0.08	24.28 ± 0.16	23.88 ± 0.12	25.14 ± 0.12	24.22 ± 0.17	24.27 ± 0.14	24.59 ± 0.12
ΔH	10.13 ± 0.01	13.70 ± 0.09	14.14 ± 0.05	14.04 ± 0.06	13.82 ± 0.09	13.80 ± 0.06	14.01 ± 0.05

	Xanthan, Air						
Parameter \ **Month**	0	1	2	3	4	5	unopened
L	48.11 ± 0.12	42.62 ± 0.62	-	59.23 ± 0.07	44.94 ± 0.29	39.83 ± 0.04	60.54 ± 0.02
a	35.61 ± 0.04	38.26 ± 0.08	-	29.56 ± 0.06	35.61 ± 0.08	37.84 ± 0.01	29.49 ± 0.07
b	0.53 ± 0.02	1.25 ± 0.13	-	-1.26 ± 0.01	0.22 ± 0.06	1.72 ± 0.04	-1.29 ± 0.06
ΔC	3.23 ± 0.07	3.16 ± 0.05	-	-2.90 ± 0.12	3.09 ± 0.02	3.27 ± 0.13	5.46 ± 0.01
ΔE	5.00 ± 0.06	5.10 ± 0.14	-	7.80 ± 0.10	7.32 ± 0.06	8.05 ± 0.49	13.44 ± 0.06
ΔH	0.44 ± 0.02	0.52 ± 0.02	-	1.28 ± 0.02	0.16 ± 0.02	0.27 ± 0.11	1.61 ± 0.02
	Xanthan, Vac						
L	56.43 ± 0.12	51.30 ± 0.11	-	57.27 ± 0.20	51.13 ± 0.21	52.47 ± 0.01	56.82 ± 0.05
a	30.63 ± 0.04	33.64 ± 0.22	-	30.04 ± 0.10	35.19 ± 0.14	34.49 ± 0.01	31.33 ± 0.01
b	-0.98 ±0.02	-0.39 ± 0.02	-	-1.12 ± 0.02	-0.11 ± 0.01	-0.38 ± 0.04	-0.83 ± 0.04
ΔC	-1.77 ± 0.01	3.41 ± 0.12	-	-2.28 ± 0.24	3.04 ± 0.10	2.84 ± 0.34	2.24 ± 0.09
ΔE	4.88 ± 0.08	3.68 ± 0.12	-	3.26 ± 0.37	3.56 ± 0.10	3.18 ± 0.46	3.72 ± 0.00
ΔH	1.00 ± 0.02	0.41 ± 0.04	-	0.29 ± 0.05	0.19 ± 0.06	0.20 ± 0.04	0.46 ± 0.05

Figure 6.6 shows the % transmittance (%T) of the non-freeze-dried (liquid) samples during five-month storage: juice (J25), the concentrated juice (J100) and liquid foam (FJ25). The very low %T of J100 from 400 to 600 nm suggests potential as a light protector over those wavelengths (λ). Furthermore, J100 obtained very stable readings over the time tested. The %T of J100 decreased at month 5. J25 obtained small %T in λ corresponding to green and an increment was observed in %T at shorter λ corresponding to yellow and orange when compared to J100. J25 decreased its %T at month 5. FJ25 at month 0 had a similar %T than J25. During the next months, the %T of FJ25 became linear and began to decrease with every month. The %T of FJ25 at month 5 was almost 0; possibly an effect given by the turbidity of the sample.

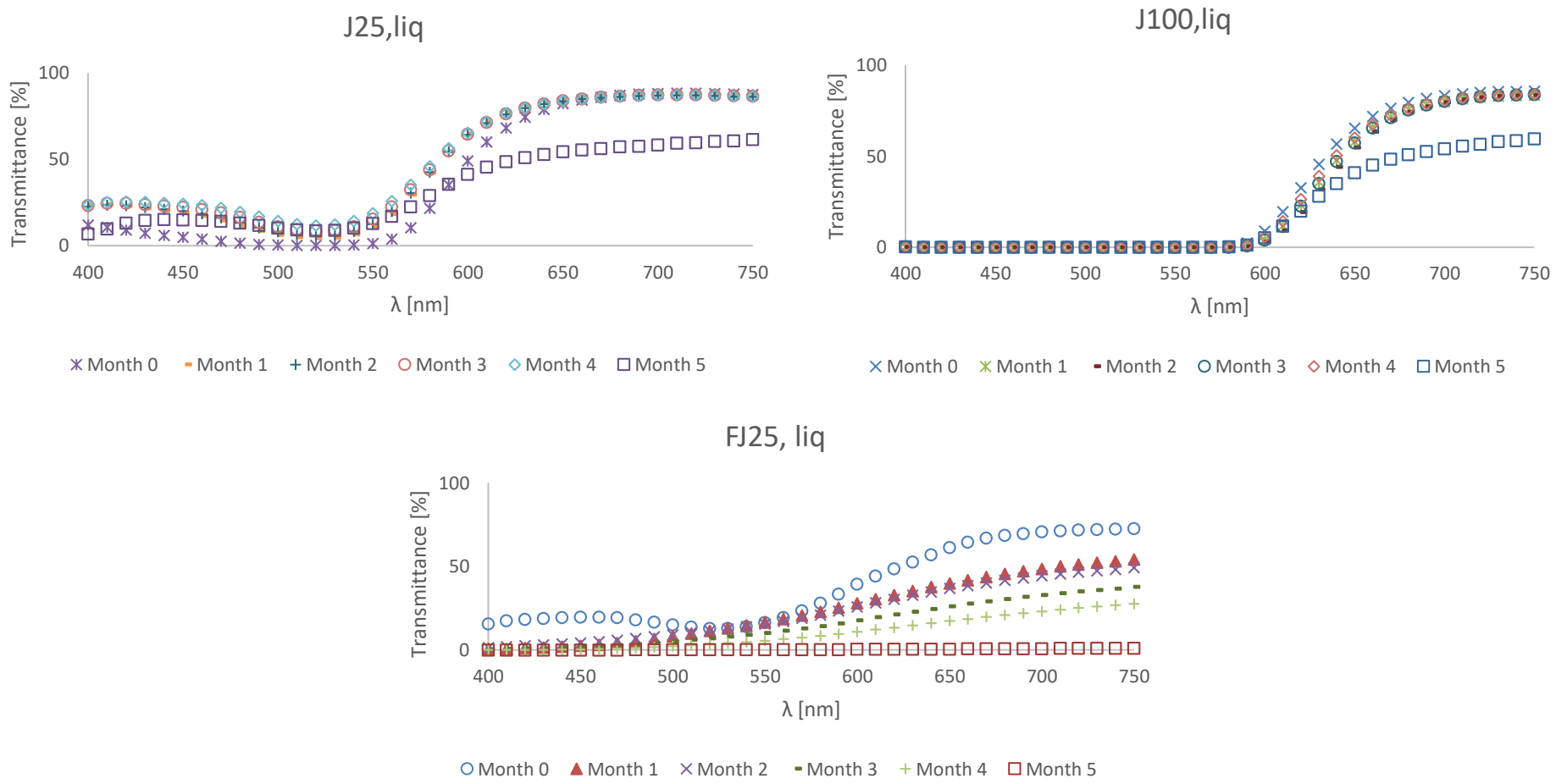

Figure 6.6 % Transmittance of juice (J25), concentrated juice (J100) and liquid pre-foaming (FJ25). Average std error: J25 = 0.01,J100 = 0.01,FJ25 = 0.01,n=3.

The following tables show the *L, a* and *b* values and ΔE, ΔH and ΔC of the liquid samples. FJ25 obtained the lowest *a* value and the highest *b* value suggesting hues towards yellow and green in the CIELab colour space. The *L, a* and *b* values of FJ25 at month 5 compared to month 4 decreased 95, 86 and 94%, respectively. Thus, a decrease of 86% in ΔH was observed in FJ25 from month 4 to month 5. J25 and J100 were similar in the *a* value but in the last two months, the *a* value of J25 decreased 9 and 19% compared to the previous month. This suggested that more concentrated anthocyanin conserved better the red hue. J25 obtained lower *b* values than J100 suggesting blue hues in the first mentioned. The *L* values of J25 and J100 remained stable during the time of the experiment.

Tables 6.3 Colour profile of blackcurrant juice (J25), liquid pre-foam (FJ25) and concentrated blackcurrant juice (J100). J25,to(liq) = std colour. Mean ± std error, n=3.

	J25					
Month / Parameter	J25,to(liq)	1	2	3	4	5
L	49.268 ± 0.020	58.843 ± 0.015	59.765 ± 0.002	61.576 ± 0.010	63.656 ± 0.001	52.999 ± 0.017
a	67.968 ± 0.051	57.824 ± 0.015	54.841 ± 0.003	50.796 ± 0.004	46.358 ± 0.002	37.358 ± 0.005
b	34.394 ± 0.053	16.852 ± 0.005	16.189 ± 0.004	14.917 ± 0.011	14.511 ± 0.004	15.207 ± 0.019
ΔC	0.001 ± 0.085	-15.945 ± 0.060	-18.994 ± 0.060	-23.233 ± 0.060	-27.599 ± 0.059	-35.841 ± 0.060
ΔE	0.089 ± 0.065	22.412 ± 0.047	24.778 ± 0.050	28.735 ± 0.050	32.701 ± 0.048	36.319 ± 0.061
ΔH	0.028 ± 0.022	12.505 ± 0.026	11.957 ± 0.024	11.594 ± 0.026	10.032 ± 0.021	4.538 ± 0.028

	FJ25					
Month / **Parameter**	0	1	2	3	4	5
L	55.633 ± 0.002	48.296 ± 0.005	39.978 ± 0.032	49.467 ± 0.002	30.591 ± 0.052	1.615 ± 0.030
a	32.195 ± 0.005	16.387 ± 0.004	16.259 ± 0.011	17.514 ± 0.003	17.361 ± 0.017	2.471 ± 0.027
b	8.725 ± 0.001	38.821 ± 0.007	41.592 ± 0.046	50.003 ± 0.019	41.819 ± 0.082	2.566 ± 0.022
ΔC	-42.818 ± 0.060	-34.036 ± 0.059	-31.517 ± 0.072	-23.193 ± 0.062	-30.895 ± 0.096	-72.612 ± 0.061
ΔE	44.487 ± 0.059	51.780 ± 0.039	53.027 ± 0.041	52.813 ± 0.029	54.452 ± 0.045	87.027 ± 0.061
ΔH	10.256 ± 0.018	39.009 ± 0.005	41.620 ± 0.027	47.447 ± 0.011	40.764 ± 0.053	5.508 ± 0.128

	J100					
Month / **Parameter**	0	1	2	3	4	5
L	27.164 ± 0.004	23.024 ± 0.011	21.243 ± 0.013	22.658 ± 0.016	24.410 ± 0.028	20.571 ± 0.009
a	60.276 ± 0.005	56.359 ± 0.006	54.559 ± 0.018	56.015 ± 0.010	57.664 ± 0.021	51.326 ± 0.015
b	45.778 ± 0.078	39.068 ± 0.026	36.012 ± 0.015	38.417 ± 0.021	41.468 ± 0.022	35.066 ± 0.053
ΔC	-0.489 ± 0.070	-7.599 ± 0.060	-10.802 ± 0.063	-8.252 ± 0.061	-5.149 ± 0.063	-14.013 ± 0.070
ΔE	26.028 ± 0.027	29.074 ± 0.028	31.110 ± 0.033	29.448 ± 0.029	27.824 ± 0.034	33.180 ± 0.037
ΔH	13.733 ± 0.056	9.942 ± 0.029	8.107 ± 0.019	9.538 ± 0.023	11.389 ± 0.023	9.001 ± 0.041

6.3 Discussion

Dried samples (powders)

As previously discussed, the colour of anthocyanin depends on their pH. Foam-mat freeze-dried blackcurrant juice (FJ25) showed higher pH values than both the blackcurrant juice (J25) and the blackcurrant juice mixed only with xanthan gum (Xanthan) (Table 6.1). The pH of the media containing anthocyanins affects the formation of the four species of anthocyanin: flavylium cation, quinoidal base, carbinol pseudo base and chalcone. These four species absorb and reflect different energy wavelengths and therefore they have different colours. The flavylium cation is dominant at pH 1 and reflects orange/red colours, the quinoidal base is dominant at pH 6-7 and reflects purple/blue colour, the carbinol pseudo base is dominant at pH 4-5 and is colourless and finally, the chalcone is dominant at pH 7-8 and reflects yellow (Wrolstad, 1993, Lee et al., 2005, Nielsen et al., 2003). In Figure 6.1, these phenomena can be seen. Samples with pH 1 (and also pH 2 and 3) had their maximum %T at the wavelengths (λ) corresponding to red (flavylium cation), and their minimum %T at λ corresponding to green. Lower %T in the violet/blue region were observed for samples with pH 1,2 and 3 than with pH 4,5 and 6. The dominant quinoidal base observed in samples with pH 6 is presumably responsible for the higher values of %T in the green and violet/blue regions. Thus, lower %T in the beforementioned region was observed in samples with pH 1, 2 and 3 where the quinoidal base was less dominant. The highest %T of all pH tested corresponded to samples with pH 5 where the dominant species was the carbinol pseudo base. This was because the carbinol pseudo base is colourless so

the colorimeter detected large amounts of light passing through the sample which corresponds to large % transmittance. All pHs produced similar values of %T in the red region with the exception of pH 6.

These four species of anthocyanins have the property of being able to coexist in equilibrium in acidic aqueous solutions at 25 °C. However, the dominant species confers a sample's characteristic colour. In the colorimeter, the dominant colour was observed as an increase in the % reflectance/transmittance at a certain wavelength. Figures 6.2 and 6.3 depict the % reflectance (%R, powders) of conventional freeze-dried blackcurrant juice (J25) and juice mixed with xanthan gum (Xanthan, 0.05 g xanthan gum per 100 ml blackcurrant juice) and also the %R of foam-mat freeze-dried blackcurrant juice (FJ25, 4 g egg albumin and 0.05 g xanthan gum per 100 ml blackcurrant juice) of samples stored with (Vac) and without (Air) vacuum, respectively.

Figures 6.2 and 6.3 show that the highest %R values of all the samples were at the λ corresponding to red (dominant flavylium cation). As expected, each sample had its minimum at λ corresponding to green. In the same Figures, all samples had a small increment in %R (between 10 and 50%) over λ corresponding to violet and blue (≈400 to 500 nm) which corresponded to the appearance of the quinoidal base. Both Figures (6.2 and 6.3) show the highest %R in λ corresponding to violet and blue in FJ25, suggesting that the foam-mat freeze-dried blackcurrant juice was bluer (See pictures of Figure 6.4) than the conventional freeze-dried samples.

Table 6.2 shows the colour profile of all powder samples. It can be observed that the *a* value (+*a* = red. -*a* = green) of FJ25 was lower than in the

conventional freeze-dried powders (J25 and Xanthan). Only a small difference was observed between J25 and Xanthan samples.

FJ25 was visibly bluer than the other samples (Figure 6.4). Contrary to Xanthan, FJ25 had lower *b* (+*b* = yellowness. -*b* = blueness) values than the standard colour (J25,to). Lower values of *b* are related to bluer samples.

ΔE, ΔH and ΔC relate the coordinate values *L*, *a* and *b* into positions with respect to the standard colour (J25,to). For ΔE, the statistical model suggests significant differences between all samples (Figure 6.5, upper left graph), and the largest pairwise difference was FJ25 versus J25 and Xanthan. This means that the consumer will notice differences between samples, especially with respect to FJ25. Storing any sample with vs. without vacuum was also significant for this response (ΔE). Change in ΔE of samples over time was significant for FJ25 (p-value <0.0005) and J25 (p-value 0.013) but not for Xanthan (p-value 0.083). Therefore, conventional freeze-drying of juice with xanthan gum will produce powders of which the colour changes will not be easily detected by the consumer over time.

The difference in hue (ΔH) between the standard colour (J25,to) and FJ25 was observed from the beginning of the experiment and also increased over time (Table 6.2). In other words, FJ25 did not have the pure spectrum of red as J25,to and it kept losing its redness over time. FJ25 was not as red as the standard colour. Results of the statistical model suggested that storing the samples with or without vacuum modified their hue (ΔH). When comparing samples with each other, FJ25 had again the largest pairwise difference versus J25 and Xanthan for ΔH. However, for the same response, J25 and Xanthan did not have significant

differences from each other (Figure 6.5, lower centre graph). It is also suggested that the change in ΔH over time was not significant for J25 (p-value 0.072) and Xanthan (p-value 0.057) but FJ25 (p-value <0.0005) had a significant augment by 3.53 ± 0.95 units of ΔH/month.

For ΔC, significant differences between all samples were obtained (Figure 6.5, up right graph), whereas storing the samples with or without vacuum was not significant. Also, changes in ΔC over time for FJ25 (p-value 0.183) and J25 (p-value 0.077) were not significant. However, Xanthan had increased by 0.31± 0.10 units of ΔC/month (p-value 0.002). This means that Xanthan had a greater red saturation over time when compared to the standard colour.

In all cases, FJ25 powders obtained larger differences in ΔE, ΔH and ΔC than did J25 and Xanthan over time. This was presumably mainly due to the presence of the egg albumin in FJ25, the pH, % moisture content (%mc) and also the aeration during foaming. On the one hand, egg albumin alone had a pale-yellow tone before being added to the juice, causing a change in colour of the powders. This was also the main reason why powders of FJ25, despite containing more void space, i.e. higher porosity, (reflected in low densities) had higher %R than J25 and Xanthan powders. This difference might have been enhanced if the powders had been compacted in the cuvette. Also, the egg albumin-anthocyanin interaction hampered the reflectance of light of the powders. These results were in accordance with published results where a decrease in colour intensity of wine was observed after mixing it with egg albumin (González-Neves et al., 2014). The pH around 4 in FJ25 (Table 6.1) promoted the stability of the colourless pseudo base of the anthocyanin, which faded the colour of part of the

anthocyanin in the sample. On the other hand, as seen in Chapter 3, oxidation of the anthocyanin took place during foaming due to increased contact of air with anthocyanin. This darkened the sample as observed in higher values of *L* in FJ25 samples (both Air and Vac). Also, Maillard reaction could have occurred since proteins and sugars were the major components of FJ25. This oxidation of the powders and the higher %mc of FJ25 (Table 6.1) produced darker hues.

ΔE, ΔH and ΔC between J25 and Xanthan were similar over time and also with varying pH, %mc and density (Table 6.1). Xanthan in blackcurrant juice increased the redness (+*a*) of the sample as observed in Table 6.2. Xanthan gum is a heteropolysaccharide (Garcia-Ochoa et al., 2000) able to react with the anthocyanin due to its hydrophilic nature, which aided polymerization reactions between xanthan gum and anthocyanin, stabilising the colour of the latter (Liu et al., 2015). Also, xanthan gum aided the dehydration of the anthocyanin which favoured the stabilisation of the flavylium cation by reducing the nucleophilic attack of water which leads to colourless forms (Brouillard and Dangles, 1994). A similar effect has been reported in mixtures of other polyphenols like betacyanin with the polysaccharide carrageenan showing good stabilization of the *a* value (Kunnika and Pranee, 2011).

In general, both kinds of storage (Air and Vac) produced no major differences between drying treatments. However, the *L* values of J25 (Air) and Xanthan (Air) showed an increment (whitening of the samples produced by exposure to permeated water) in unopened bags. Also, the ρ values of both Air and Vac of Xanthan increased, probably due to absorption of water while the

colour measurements were being performed. Unopened bags of FJ25 showed similar values to those observed at M5 (Table 6.2).

Liquid samples

This section presents results of change in colour of non-freeze-dried (liquid) samples stored under the same conditions that the freeze-dried (powder) samples. The presence of the egg albumin in the blackcurrant juice produced differences in ΔE, ΔH and ΔC (Tables 6.3) when compared to the original juice, J25,to(liq). The largest difference was observed from month 4 to month 5 when a sudden change in colour occurred in FJ25. A decrease of ΔC in FJ25 in month 5 suggested loss of (red) colour saturation, and the corresponding decrease in *L*, *a* and *b* suggested an almost complete destruction of anthocyanin. A light brown colour was perceived in the samples during the measurements accompanied with a bad smell when FJ25 containers were opened. Since samples were not pasteurized, microorganisms may have had an effect on colour and smell. J100 and J25 also showed changes in colour at month 5 but colour and smell changes were imperceptible. %T of FJ25 (pH 4) at month 0 (Figure 6.6, bottom centre) was similar to that of J25 and of the sample with pH 4 shown in Figure 6.1 (which did not contain foaming agents). However, %T of FJ25 after month 1 began to follow a linear curve and %T of FJ25 at month 5 was almost 0 (characteristic of turbid samples). This suggests an important interference of the foaming agents over colour.

As previously seen, change in colour of samples was also probably due to anthocyanin oxidation. Anthocyanins are oxidised by the O_2 dissolved in water or in air. This generates quinones via polyphenol oxidase present in berries

(Chen et al., 2013, Zdzislaw and Haard, 2006), which confer a brownish colour to the samples.

It was important to compare the stability of colour in juice (J25) and foam (FJ25) to that of concentrated blackcurrant juice (J100) because the latter contained higher anthocyanin content. The concentrated blackcurrant juice (J100) was found to be much more stable over time, keeping similar differences in ΔE, ΔH and ΔC during the months analysed. Furthermore, the parameters *L, a* and *b* for J100 were also found stable during the time of the experiment, and no visual changes were perceived in J100. This was in accordance with other studies where high anthocyanin contents in juices were more stable than lower concentrations (Rein, 2005). The most interesting feature of J100 (pH 3) was observed in the colorimeter where the %T of all λ were closer to zero until reaching λ corresponding to orange/red (around 600 nm) (Figure 6.6 up right). This finding suggests that screen filters with extracted anthocyanins with similar concentrations (330.05 ± 12.56) to J100 could be used in industrial applications to absorb the beforementioned wavelengths .

The co-pigmentation property of anthocyanin, conferring interesting characteristics like the one mentioned above, also kept the colour of J100 more stable than the other samples where the anthocyanin was more prevalent in the free form. Co-pigmentation happens when high contents of certain molecules stack over themselves or over different species (Cacelli et al., 2016). This causes a protective effect, preventing oxidation of the molecules underneath and thus stabilising their colour. This effect can be seen in Tables 6.3 where from M0 to

M5, the *a* and *b* values of J25 decreased by 45 and 56% while in J100, the *a* and *b* values decreased by only 15 and 23%, respectively.

Figure 6.6 (up left) shows how the hydration of the anthocyanin in J25 faded the colour. A shift in wavelength absorption towards a longer wavelength (red) is termed a bathochromic shift and to a shorter wavelength (purple) a hypsochromic shift (Moss, 2002). Anthocyanins in J25 underwent a hypsochromic shift while concentrated anthocyanins in J100 underwent a bathochromic shift. A bathochromic shift of the colour might be obtained by increasing the electron-withdrawing power of the chromophore (chromophores are the group of atoms within the molecule responsible for the colour (Moss, 2002)), whereas it has also been suggested that this could be correlated with a higher antioxidant power of the anthocyanin (Christie, 2015). Future work to analyse the antioxidant power of anthocyanin after it has been stored in liquid form should be done using the ORAC method (oxygen radical absorbance capacity).

In the case of J25, a constant decrease in redness (ΔH) occurred from month 1 to month 4, and then a bigger decrease occurred at month 5 of storage. ΔE of J25 kept increasing its difference with respect to the standard colour till the end of the experiment. J25 experienced a steady loss of strength of colour reflected in ΔC. The %T of J25 was similar to its powder versions.

All of this is consistent with the findings of Boulton (2001). He summarised that any treatments (dilution or foaming) can cause anthocyanin dissociation of the co-pigmentation stack, oxidation or reactions with other

molecules like proteins, carbohydrates and water, and this can have a significant effect on colour.

6.4 Conclusions

Significant differences in hue between powders dried by foam-mat freeze-drying (FJ25) and conventional freeze-drying (J25 and Xanthan) were observed. FJ25 yielded less red and more blue hues than conventional freeze-dried samples. Also, colour differences over time of FJ25 versus the standard colour increased while J25 and Xanthan were more stable.

Samples with xanthan gum appeared to have the highest red intensity (ΔC) among all the samples. The use of small quantities of xanthan gum could be adopted to preserve the anthocyanin colour in blackcurrant juice.

Storage without vacuum of J25 and Xanthan promoted darkening of the samples due to oxidation.

The anthocyanin colour was found to be better stabilised in dehydrated samples than in their liquid forms. Concentrated blackcurrant juice presented smaller colour changes over time due to anthocyanin polymerization. The abrupt browning of the stored liquid foam after 5 months indicated anthocyanin destruction, possibly due to microorganisms. However, this effect was not observed in the freeze-dried foam.

Chapter 7 General conclusion

This research has contributed to our understanding of the benefits and drawbacks of foam-mat freeze-drying juices with high anthocyanin content and also offers some ideas for the development of food products based on dried juices. A new food analysis technique to separate protein from anthocyanin was developed in the process (Chapter 2).

In Chapter 3, it was observed that in blackcurrant juice, the anthocyanin retention after foam-mat freeze-drying was higher in high anthocyanin-sugar concentrations than in low ones. However, after pepsin pre-treatment, proportionally less anthocyanin was retrieved and measured in foams with higher anthocyanin-sugar concentrations. This suggested that 1) anthocyanin had high (or increased its) affinity to egg albumin, 2) high anthocyanin content may have inhibited the pepsin action and, 3) more co-pigmented anthocyanin may have sedimented during centrifugation.

In the same chapter, the presence of anthocyanin was also detected after foam-mat freeze-drying and pepsin pre-treatment using fluorescence. High anthocyanin contents decreased the RFU of egg albumin more than did low anthocyanin contents. RFU were particularly lower after freeze-drying, including after pepsin pre-treatment. Interestingly, RFU of egg albumin increased with increments of anthocyanin concentration if the egg albumin was foamed and digested previous to mixing with anthocyanin. It was proposed that the unfolding of the egg albumin in the presence of anthocyanin during whipping

and the dehydration of the sample promoted the formation of an anthocyanin-egg albumin complex.

In Chapter 4, foams with anthocyanin showed higher viscosities and air volume fractions and also lower densities and drainages than their counterparts without anthocyanin. Foams with high anthocyanin and high sugar content could therefore be used as an alternative for toppings in bakery products free from lactose, casein and soya. Foams with low sugars contents with and without anthocyanin produced similar mean bubble sizes, which were larger than the foams with high sugar contents with and without anthocyanin. In high sugar content foams, the presence of anthocyanin reduced the mean bubble size to less than half while their viscosity value increased almost twofold when compared to foams with zero anthocyanin content. Also, high viscosity values indicated more water content in the structures and thus slower drying rates.

From Chapter 5 it can be concluded that large mean bubble sizes correlate well with large diffusivity values and vice versa. Drying rate in foams are higher in foams with large mean bubble size and low viscosities; therefore, higher % water loss will be observed. The presence of anthocyanin reduces drying rates of foams for a given sugar content.

Also in Chapter 5, it was suggested that non-foamed blackcurrant juice will have a higher drying rate than egg albumin foams. Unfortunately, time to constant weight for non-foamed blackcurrant juice was considerably longer than in foams, for equal volumes. This was because the water content of non-foamed blackcurrant juice was larger than in foams and dried layers hinder mass transfer. Therefore, formulations for foam-mat freeze-drying juices should have

an appropriate ratio of solid to water contents for a desired balance of drying speed and final water content.

The mathematical model here developed (in Chapter 2) aided elucidation of the differences in drying rate between samples. The reported error between experimental and predicted values was < 5 % in all samples (See Chapter 5). The model made it possible to predict the change in mass of the samples during the first stage of freeze-drying.

Chapter 6 depicted how changes in the colour of anthocyanin in foam-mat freeze-dried blackcurrant juice were smaller over time than in the conventional freeze-dried juice. However, the red intensity was considerably lower in foam-mat freeze-dried blackcurrant juice than in the conventional freeze-dried juice powders. The use of small quantities of xanthan gum in blackcurrant juice before freeze-drying was proposed to increase the red intensity of the samples.

Interestingly, Chapter 6 shows that concentrated blackcurrant juice (liquid) absorbs at all wavelengths from 400 to 600 nm. This could be useful as a screen filter of all those wavelengths if required in industry. During cold storage, the liquid foam (non-freeze-dried) increased the colour differences compared to the standard colour (juice at time 0) over time, where bigger differences occurred from month 4 to month 5 of storage. Thus, the anthocyanin-egg albumin interaction continued over time at 6 °C but the interaction was slower in dried samples.

The powders obtained by both foam-mat freeze-drying and conventional freeze-drying could be used in bakery, confectionary or as food supplements.

Dried egg albumin with blackcurrant as a food supplement is currently not on the market and it could be a good idea for people who exercise or who enjoy high protein diets.

Finally, if pure juice is needed in a process, foam-mat freeze-drying will not be recommended since it adds steps for processing and purification of the sample (that decrease the anthocyanin content of blackcurrant juices). However, the use of egg albumin as foaming agent in high anthocyanin/high sugar liquids shortens the drying process time (not the drying rate) which could be useful if small quantities of this kind of product are needed.

References

ABBASI, E. & AZIZPOUR, M. 2016. Evaluation of physicochemical properties of foam mat dried sour cherry powder. *LWT - Food Science and Technology,* 68**,** 105-110.

AGUILERA, Y., MOJICA, L., REBOLLO-HERNANZ, M., BERHOW, M., GONZALEZ DE MEJIA, E. & MARTIN-CABREJAS, M. A. 2016. Black bean coats: New source of anthocyanins stabilized by b-cyclodextrin copigmentation in a sport beverage. *Food Chemistry,* 212**,** 561-570.

AHMED, J., SHIVHARE, U. S. & RAGHAVAN, G. S. V. 2004. Thermal degradation kinetics of anthocyanin and visual colour of plum puree. *Eur Food Res Technol,* 218**,** 525-528.

ANTTONEN, M. J. & KARJALAINEN, R. O. 2006. High-Performance Liquid Chromatography Analysis of Black Currant (Ribes nigrum L.) Fruit Phenolics Grown either Conventionally or Organically. *Journal of Agricultural and Food Chemistry,* 54**,** 7530-7538.

ASAMI, D., HONG, Y.-J., BARRET, D. & MITCHELL, A. 2003. Comparison of the Total Phenolic and Ascorbic Acid Content of Freeze-Dried and Air-Dried Marionberry, Strawberry, and Corn Grown Using Conventional, Organic, and Sustainable Agricultural Practices. *Journal of Agricultural and Food Chemistry,* 51**,** 1237-1241.

ASANO, K., SHINAGAWA, K. & HASHIMOTO, N. 1982. Characterization of Haze-Forming Proteins of Beer and Their Roles in Chill Haze Formation. *American Society of Brewing Chemists, Inc. Presented at the 48th Annual Meeting. Kansas City. MO.,* 40**,** 147-154.

ASEN, S., NORRIS, K. H. & STEWART, R. N. 1969. Absorption Spectra and Color of aluminium-cyanidin 3-glucoside complexes as influenced by pH. *Phytochemistry,* 8**,** 653-659.

AWIKA, J. M., ROONEY, L. W. & WANISKA, R. D. 2004. Anthocyanins from black sorghum and their antioxidant properties. *Food Chemistry,* 90**,** 293-301.

AZIMA, S., NORIHAM, A. & MANSHOOR, N. 2014. Anthocyanin content in relation to the antioxidant activity and colour properties of Garcinia mangostana peel, Syzigium cumini and Clitoria ternatea extracts. *International Food Research Journal,* 21(6)**,** 2369-2375.

AZIZPOUR, M., MOHEBBI, M., KHODAPARAST, M. H. H. & VARIDI, M. 2014. Optimization of Foaming Parameters and Investigating the Effects of Drying Temperature on the Foam-Mat Drying of Shrimp (Penaeus indicus). *Drying Technology,* 32**,** 374-384.

BAMFIELD, P. & HUTCHINGS, M. G. 2010. Chromic Phenomena - Technological Applications of Colour Chemistry (2nd Edition). Royal Society of Chemistry.

BANTLE, M. 2011. *Study of high intensity, airborne ultrasound in atmospheric freeze-drying.* PhD, Norwegian University of Science and Technology.

BARBOSA-CANOVAS, G. V. & VEGA-MERCADO, H. 1996. Freeze dehydration. *Dehydration of foods.* New York, U.S. A.: Chapman & Hall.

BELITZ, H., GROSCH, W. & SCHIEBERLE, P. 2004. *Food Chemistry,* Berlin, Germany, Springer
BERNS, R. S. 2000. *Billmeyer and Saltzman's Principles of Color Technology,* USA, John Wiley & Sons, Inc.
BMGLABTECH 2016. PHERAstar FSX. The new gold standard for high-throughput screening. Ortenberg, Germany.
BOBBIO, F. O., DO NASCIMIENTO VARELLA, M. T. & BOBBIO, P. A. 1994. Effect of light and tannic acid on the stability of anthocyanin in DMSO and in water. *Food Chemistry,* 51**,** 183-185.
BOBERT, M., PERSSON, H. & PERSSON, B. 1997. Foam concentrates: viscosity and flow characteristics. *Fire technology,* 33**,** 336-355.
BOCCORH, R. K., PATERSON, A. & PIGGOTT, J. 1998. Factors influencing quantities of sugars and organic acids in blackcurrant concentrates. *Z Lebensm Unters Forsch A,* 206**,** 273-278.
BOSS, E. A., FILHO, R. M. & COSELLI VASCO DE TOLEDO, E. 2004. Freeze drying process: real time model and optimization. *Chemical Engineering and Processing,* 43**,** 1475-1485.
BOULTON, R. 2001. The Copigmentation of Anthocyanins and Its Role in the Color of Red Wine: A Critical Review. *Am. J. Enol. Vitic.,* 52:2**,** 67-87.
BOURNE, M. C. 2002. Texture, viscosity and food. *Food Texture and viscosity - Concept and Measurement.* 2nd ed. Geneva, New York: Academic Press.
BRIDLE, P. & TIMBERLAKE, C. F. 1997. Anthocyanins as natural food colours-selected aspects. *Food Chemistry,* 58**,** 103-109.
BROUILLARD, R. & DANGLES, O. 1994. Anthocyanin molecular interactions: the first step in the formation of new pigments during wine aging? *Food Chemistry,* 51**,** 365-371.
BRUHN, C. M. 2007. Enhancing consumer acceptance of new processing technologies. *Innovative Food Science and Emerging Technologies* 8**,** 555-558.
BRYGIDYR, A. M., RZEPECKA, M. A. & MCCONNELL, M. B. 1977. Characterization and Drying of Tomato Paste Foam by Hot Air and MIcrowave Energy. *J. Inst. Can. Sci. Technol. Aliment.,* 10**,** 313-319.
CACELLI, I., FERRETTI, A. & PRAMPOLINI, G. 2016. Predicting light absorption properties of anthocyanidins in solution: a multi‑level computational approach. *Theor Chem Acc. Published as part of the special collection of articles "Health & Energy from the Sun".* 135-156.
CAETANO DA SILVA-LANNES, S. & MIQUELIM, J. N. 2013. Interfacial Behavior of Food Proteins. *Current Nutrition & Food Science,* 9**,** 10-14.
CALOGERO, G., YUM, J.-H., SINOPOLI, A., DI MARCO, G. & GRATZEL, M. 2012. Anthocyanins and betalains as light-harvesting pigments for dye-sensitized solar cells. *Solar Energy,* 86**,** 1563-1575.
CAMPBELL, G. M. & MOUGEOT, E. 1999. Creation and characterisation of aerated food products. *Trends in Food Science & Technology,* 10**,** 283-296.
CARRARO-ALLEONI, A. C. 2006. Albumen protein and functional properties of gelation and foaming. *Sci. Agric. (Piracicaba, Braz.),* 63**,** 291-298.

CHAKRABORTY, R., SAHA, A. R. & BHATTACHARYA, P. 2006. Modeling and simulation of parametric sensitivity in primary freeze-drying of foodstuffs. *Separation and Purification Technology,* 49**,** 258–263.
CHEN, J., TAO, X., ZHANG, M., SUNA, A. & ZHAO, L. 2013. Properties and stability of blueberry anthocyanin–bovine serum albumin nanoparticles. *Wiley Online Library,* 94**,** 1781-1786.
CHENG, H. C. & LEMLICH, R. 1983. Errors in the measurement of bubble size distribution in foam. *Ind. Eng. Chem. Fundam.,* 22**,** 105-109.
CHOI, I., LEE, J. Y., LACROIX, M. & HAN, J. 2017. Intelligent pH indicator film composed of agar/potato starch and anthocyanin extracts from purple sweet potato. *Food Chemistry,* 218**,** 122-128.
CHRISTIE, R. M. 2015. The Physical and Chemical basis of Colour. *In:* ROBERT M CHRISTIE (ed.) *Colour Chemistry (2nd Edition).* Cambridge, UK: Royal Society of Chemistry.
CHUNG, C., ROJANASASITHARA, T., MUTILANGI, W. & MCCLEMENTS, D. J. 2016. Stabilization of natural colors and nutraceuticals: Inhibition of anthocyanin degradation in model beverages using polyphenols. *Food Chemistry,* 212**,** 596-603.
CLAUSSEN, I. C., USTAD, T. S., STROMMEN, I. & WALDE, P. M. 2007. Atmospheric Freeze Drying—A Review. *Drying Technology,* 25**,** 957-967.
COIMBRA, J. S. R., GABAS, A. L., MINIM, L. A., GARCIA ROJAS, E. E., TELIS, V. R. N. & TELIS-ROMERO, J. 2006. Density, heat capacity and thermal conductivity of liquid egg products. *Journal of Food Engineering,* 74**,** 186-190.
CONSIDINE, D. M. & CONSIDINE, G. D. 1982. Foods and Food Production Encyclopedia. *In:* CONSIDINE, D. M. (ed.). New York, U.S.A.: Van Nostrand Reinhold Company.
CORTEZ, R., LUNA-VIDAL, D. A., MARGULIS, D. & GONZALEZ DE MEJIA, E. 2017. Natural Pigments: Stabilization Methods of Anthocyanins for Food Applications. *Comprehensive Reviews in Food Science and Food Safety,* 16**,** 180-198.
DE ROSSO, V. & MERCADANTE, A. 2007. The high ascorbic acid content is the main cause of the low stability of anthocyanin extracts from acerola. *Food Chemistry,* 103**,** 935-943.
DELGADO-SÁNCHEZ, C., FIERRO, V., LI, S., PASC, A., PIZZI, A. & CELZARD, A. 2017. Stability analysis of tannin-based foams using multiple light-scattering measurements. *European Polymer Journal,* 87**,** 318-330.
DICKINSON, E. 2010. Food emulsions and foams: Stabilization by particles. *Current Opinion in Colloid & Interface Science***,** 40-49.
DIONEX 1995. ED40 Electrochemical Detector Operator´s Manual. *In:* CORPORATION, D. (ed.). Sunnyvale, CA., USA.
DIONEX 2011. Product Manual CarboPac PA20. *In:* SCIENTIFIC, T. (ed.). Sunnyvale, CA, USA.
DOLLET, B. & RAUFASTE, C. 2014. Rheology of aqueous foams. *Comptes rendus de l´Académie des sciences. Série IV, Physique, astrophysique, Elsevier,* 15**,** 731-747.

ESPOSITO, D., DAMSUD, T., WILSON, M., GRACE, M., STRAUCH, R., LI, X., LILA, M. A. & KOMARNYTSKY, S. 2015. Black Currant Anthocyanins Attenuate Weight Gain and Improve Glucose Metabolism in Diet-Induced Obese Mice with Intact, but Not Disrupted, Gut Microbiome. *Journal of Agricultural and Food Chemistry,* 63**,** 6172-6180.

ETTELAIE, R. & MURRAY, B. S. 2015. Evolution of bubble size distribution in particle stabilised bubble dispersions: Competition between particle adsorptionand dissolution kinetics. *Colloids and Surfaces A: Physicochem. Engineering Aspects,* 475**,** 27-36.

EUROPEAN COMMISSION 2011. Commission Regulation (EU) No 1129/2011 amending Annex II to Regulation (EC) No 1333/2008 of the European Parliament and of the Councl by establishing a Union list of food additives. *In:* EUROPEAN PARLIAMENT (ed.) Brussels: Official Journal of the European Union.

FALADE, K. O., ADEYANJU, K. I. & UZO-PETERS, P. I. 2003. Foam-mat drying of cowpea (Vigna unguiculata) using glyceryl monostearate and egg albumin as foaming agents. *Eur Food Res Technol,* 217**,** 486-491.

FALADE, K. O. & OKOCHA, J. O. 2012. Foam-mat Drying of plantain and cooking banana (musa spp.). *Food Bioprocess Technol,* 5**,** 1173:1180.

FERREL, S. K. 2015. *Effects of metal and semiconducting nanoparticles on the fluorescence and optical band gap of Dy3+ doped lead borate and bismuth borate glasses.* Master of Science, Western Illinois University.

FIGUEIREDO-BORGOGNONI, C., DA SILVA-BEVILACQUA, J. & NOGUEIRA DE MORAES PITOMBO, R. 2012. Freeze-drying microscopy in mathematical modeling of a biomaterial freeze-drying. *Brazilian Journal of Pharmaceutical Sciences* 48**,** 203-208.

FIGURA, L. & TEIXEIRA, A. 2007. *Food Physics. Physical properties - measurement and applications,* Berlin Heidelberg, Springer-Verlag.

FILIPPA, L., TRENTO, A. & ALVAREZ, A. M. 2012. Sauter mean diameter determination for the fine fraction of suspended sediments using a LISST-25X diffractometer. *Measurement* 45**,** 364-368.

FOEGEDING, E. A., LUCK, P. J. & DAVIS, J. P. 2006. Factors determining the physical properties of protein foams. *Food Hydrocolloids,* 20**,** 284-292.

GARCIA-OCHOA, F., SANTOS, V. E., CASAS, J. A. & GOMEZ, E. 2000. Xanthan gum: production, recovery, and properties. *Biotechnology Advances,* 18**,** 549-579.

GONZÁLEZ-NEVES, G., FAVRE, G. & GIL, G. 2014. Effect of fining on the colour and pigment composition of young red wines. *Food Chemistry,* 157**,** 385-392.

GOSSETT, P. W., RIZVI, S. S. H. & BAKER, R. C. 1984. Quantitative Analysis of Gelation in Egg Protein Systems. Symposium: Gelation in Food Protein Systems. . *Food Technology,* 38**,** 67-96.

HAN, K.-H., SEKIKAWA, M., SHIMADA, K.-I., HASHIMOTO, M., HASHIMOTO, N., NODA, T., TANAKA, H. & FUKUSHIMA, M. 2006.

Anthocyanin-rich purple potato flake extract has antioxidant capacity and improves antioxidant potential in rats. *British Journal of Nutrition,* 96**,** 1125–1133.

HAN, Y.-P., LI, Z.-Y., LI, B.-C., SUN, X., ZHU, C.-C., LING, X.-T., ZHENG, H.-Q., WU, Z.-D. & LV, Z.-Y. 2011. Molecular cloning and characterization of a cathepsin B from Angiostrongylus cantonensis. *Parasitol Res,* 109**,** 369-378.

HAO, S., WU, J., HUANG, Y. & LIN, J. 2006. Natural dyes as photosensitizers for dye-sensitized solar cell. *Solar Energy,* 80**,** 209-214.

HASSAN, M. S. A. 2012. *Egg protein interactions with phenolic compounds: Effect on protein properties.* Master of Science, McGill University.

HELLSTROM, J., MATTILA, P. & KARJALAINEN, R. 2013. Stability of anthocyanins in berry juices stored at different temperatures. *Journal of Food Composition and Analysis,* 31**,** 12-19.

HERMANSSON, A.-M. 1979. Aggregation and denaturation involved in gel formation. In "Functionality and Protein Structure,". *A. Pour-El, ed., ACS Symp. Am. Chem. Soc., Washington, DC,* 92**,** 83.

HETTIARACHCHI, C. A., CORZO-MARTÍNEZ, M., MOHAN, M. S. & HARTE, F. M. 2018. Enhanced foaming and emulsifying properties of high-pressure-jet-processed skim milk. *International Dairy Journal,* 87**,** 60-66.

HOLLANDS, W., BRETT, G. M., RADREAU, P., SAHA, S., TEUCHER, B., BENNETT, R. N. & KROON, P. A. 2008. Processing blackcurrants dramatically reduces the content and does not enhance the urinary yield of anthocyanins in human subjects. *Food Chemistry,* 108**,** 869-878.

HUA, T.-C., LIU, B.-L. & ZHANG, H. 2010. Freeze-drying of pharmaceutical and food products. *Woodhead Publishing Series in food Science, Technology and Nutrition: Number 198,* Science Press.

HUANG, Y., YANG, J., CHEN, L. & ZHANG, L. 2018. Chitin Nanofibrils to Stabilize Long-Life Pickering Foams and Their Application for Lightweight Porous Materials. *ACS Sustainable Chemistry & Engineering,* 6**,** 10552-10561.

HUBBERMANN, E. M., HEINS, A., STOCKMANN, H. & SCHWARZ, K. 2006. Influence of acids, salt, sugars and hydrocolloids on the colour stability of anthocyanin rich black currant and elderberry concentrates. *Eur Food Res Technol,* 223**,** 83-90.

HUNTINGTON, J. A. & STEIN, P. E. 2001. Structure and properties of ovalbumin. *Journal of Chromatography,* 756**,** 189-198.

JADWIGA, W.-J. 2006. Food Colorants. *In:* SIKORSKI, Z. E. (ed.) *Chemical and Functional Properties of Food Components.* Third Edition ed.: CRC Press.

JAKOBEK, L., SERUGA, M., MEDVIDOVIC-KOSANOVIC, M. & NOVAK, L. 2007. Anthocyanin content and antioxidant activity of various red fruit juices. *Deutsche Lebensmittel-Rundschau,* 103**,** 58-64.

JAWORSKA, G., SADY, M., GREGA, T., BERNAS, E. & POGON, K. 2011. Qualitative comparison of blackcurrant and blackcurrant--whey beverages. *Food Science and Technology International*.

JINGYU, Y. 2016. *Quantification of anthocyanins after submitting a dried anthocyanin-protein based additive to different food process conditions using an enzymatic digestion, and HPLC.* Master of Science, University of Leeds.
KADAM, D., WILSON, R. A. & KAUR, S. 2012. Influence of foam-mat drying on quality of tomato powder *International Journal of Food Properties,* 15**,** 211-220.
KANDASAMY, P., VARADHARAJU, N., KALEMULLAH, S. & MALADHI, D. 2014. Optimization of process parameters for foam-mat drying of papaya pulp. *J Food Sci Technol,* 51**,** 2526-2534.
KAREL, M. & LUND, D. B. 2003. Physical Principles of Food Preservation. New York, USA: Marcel Dekker, Inc.
KARIM, A. A. & WAI, C. C. 1999. Foam-mat drying of starfruit (Averrhoa carambola L.) pure. Stability and air drying characteristics. *Food Chemistry,* 64**,** 337-343.
KARIM, Z., HOLMES, M. & ORFILA, C. 2017. Inhibitory effect of chlorogenic acid on digestion of potato starch. *Food Chemistry,* 217**,** 498-504.
KHOO, G. M., CLAUSSEN, M. R., PEDERSEN, H. L. & LARSEN, E. 2012. Bioactivity and chemical composition of blackcurrant (Ribes nigrum) cultivars with and without pesticide treatment. *Food Chemistry,* 132**,** 1214-1220.
KROEZEN, A. B. J., WASSINK, J. G. & SCHIPPER, C. A. C. 1988. The flow properties of foam. *JSDC,* 104**,** 393-400.
KROKIDA, M. & PHILIPPOPOULOS, C. 2006. Volatility of apples during air and freeze drying. *Journal of Food Engineering,* 73**,** 135-141.
KRÖNER, S. & DOMÉNECH CARBÓ, M. T. 2013. Determination of minimum pixel resolution for shape analysis: Proposal of a new data validation method for computerized images. *Power Technology,* 245**,** 297-313.
KUNNIKA, S. & PRANEE, A. 2011. Influence of enzyme treatment on bioactive compounds and colour stability of betacyanin in flesh and peel of red dragon fruit Hylocereus polyrhizus (Weber) Britton and Rose. *International Food Research Journal,* 18**,** 1437-1448.
LALEH, G. H., FRYDOONFAR, H., HEIDARY, R., JAMEEI, R. & ZARE, S. 2006. The Effect of Light, Temperature, pH and Species on Stability of Anthocyanin Pigments in Four Berberis Species. *Pakistan Journal of Nutrition,* 5(1)**,** 90-92.
LE BOURVELLEC, C. & RENARD, C. M. G. C. 2012. Interactions between Polyphenols and Macromolecules: Quantification Methods and Mechanisms. *Critical Reviews in Food Science and Nutrition,* 52**,** 213-248.
LEE, J.-P., LEE, K.-H. & SONG, H.-K. 1997. Manufacture of biodegradable packaging foams from agar by freeze-drying. *Journal of Materials Science,* 32**,** 5825-5832.
LEE, J., DURST, R. & WROLSTAD, R. 2002. Impact of Juice Processing on Blueberry Anthocyanins and Polyphenolics: Comparison of Two Pretreatments. *Journal of Food Science,* 67**,** 1660-1667.
LEE, J., DURST, R. & WROLSTAD, R. 2005. Determination of Total Monomeric Anthocyanin Pigment Content of Fruit Juices, Beverages,

Natural Colorants, and Wines by the pH Differential Method: Collaborative tudy. *Journal of AOAC International,* 88**,** 1269-1278.
LEE, J., RENNAKER, C. & WROLSTAD, R. 2008. Correlation of two anthocyanin quantification methods: HPLC and spectrophotometric methods. *Food Chemistry,* 110**,** 782-786.
LEFEVRE, I., ZIEBEL, J., GUIGNARD, C., SOROKIN, A., TIKHONOVA, O., DOLGANOVA, N., HOFFMANN, L., EYZAGUIRRE, P. & HAUSMAN, J.-F. 2011. Evaluation and comparison of nutritional quality and bioactive compounds of berry fruits from Lonicera caerulea, Ribes L. species and Rubus idaeus grown in Russia. *Journal of Berry Research***,** 159-167.
LIAPIS, A. I. & BRUTTINI, R. 1994. A theory for the primary and secondary drying stages of the freeze-drying of pharmaceutical crystalline and amorphous solutes: comparison between experimental data and theory. *Separations technology,* 4**,** 144-155.
LIN, T., SHU, L., HONGNA, B. & XIN, G. 2016. Interaction of cyanidin-3-O-glucoside with three proteins. *Food Chemistry,* 196**,** 550-559.
LIU, S.-X., YANG, H.-Y., LI, S.-Y., ZHANG, J.-Y., LI, T., ZHU, B.-Q. & ZHANG, B.-L. 2015. Polyphenolic compositions and chromatic characteristics of bog bilberry syrup wines. *Molecules,* 20**,** 19865-19877.
LU, Y., WANG, Y.-L., GAO, S.-H., WANG, G.-K., YAN, C.-L. & CHEN, D.-J. 2009. Interaction of quercetin with ovalbumin: Spectroscopic and molecular modeling studies. *Journal of Luminescence,* 129**,** 1048-1054.
LV, Q. & FENG, Q. 2006. Preparation of 3-D regenerated fibroin scaffolds with freeze drying method and freeze drying/foaming technique. *J Mater Sci:Mater Med,* 17**,** 1349-1356.
MA, Y. H. & PELTRE, P. R. 1975. Freeze dehydration by microwave energy: Part I. Theoretical investigation. *AIChE Journal,* 21**,** 335-344.
MARGALIT, Y. 2016. Concepts in wine chemistry. *In:* CRUM, J. (ed.) Third edition ed. USA: Board and Bench Publishing.
MARTELO-VIDAL, M. J. & VAZQUEZ, M. 2016. Advances in Ultraviolet and Visible Light Spectroscopy for Food Authenticity Testing. *In:* DOWNEY, G. (ed.) *Advances in Food Authenticity Testing.* Duxford, UK: Elsivier.
MASCARENHAS, W. J., AKAY, H. U. & PIKAL, M. J. 1997. A computational model for finite element analysis of the freeze-drying process. *Computer Methods in Applied Mechanics and Engineering,* 148**,** 105-124.
MATHLOUTHI, M. & GENOTELLE, J. 1998. Role of water in sucrose crystallization. *Carbohydrate polymers,* 37**,** 335-342.
MATTILA, P. H., HELLSTRÖM, J., MCDOUGALL, G., DOBSON, G., PIHLAVA, J.-M., TIIRIKKA, T., STEWART, D. & KARJALAINEN, R. 2011. Polyphenol and vitamin C contents in European commercial blackcurrant juice products. *Food Chemistry,* 127**,** 1216-1223.
MAZZA, G. & BROUILLARD, R. 1987. Recent Developments in the Stabilization of Anthocyanins in Food Products. *Food Chemistry,* 25**,** 207-225.

MERYMAN, H. T. 1959. Sublimation Freeze-drying without vacuum. *Science,* 130**,** 628-629.
MICHAELIS, L., SCHUBERT, M. & SMYTHE, C. V. 1936. Potentiometric study of the favins. *J. Biol. Chem.,* 116**,** 587-607.
MICHALCZYK, M., MACURA, R. & MATUSZAK, I. 2009. The effect of air-drying, freeze-drying and storage on the quality and antioxidant activity of some selected berries. *Journal of Food Processing and Preservation,* 33**,** 11-21.
MIETTINEN, L., KEKALAINEN, P., TURPEINEN, T., HYVALUOMA, J., MERIKOSKI, J. & TIMONEN, J. 2012. Dependance of thermal conductivity on structural parameters in porous samples. *AIP Advances,* 012101.
MINIHANE, A. M., VINOY, S., RUSSELL, W. R., BAKA, A., ROCHE, H. M., TUOHY, K. M., TEELING, J. L., BLAAK, E. E., FENECH, M., VAUZOUR, D., MCARDLE, H. J., KREMER, B. H. A., STERKMAN, L., VAFEIADOU, K., BENEDETTI, M. M., WILLIAMS, C. M. & CALDER, P. 2015. Low-grade inflammation, diet composition and health: current research evidence and its translation. *British Journal of Nutrition,* 114**,** 999-1012.
MIQUELIM, J. N. & CAETANO DA SILVA-LANNES, S. 2009. Egg albumin and guar gum influence on foam thixotropy. *Journal of Texture studies,* 40**,** 623-636.
MLEKO, S., KRISTINSSON, H. G., LIANG, Y. & GUSTAW, W. 2007. Rheological properties of foams generated from egg albumin after pH treatment. *LWT,* 40**,** 908-914.
MORE, G. R. & PRASAD, S. 1988. Thermal conductivity of concentrated whole milk. *Journal of Food Process Engineering,* 10**,** 105-112.
MOSS, B. W. 2002. The chemistry of food colour. *In:* MACDOUGALL, D. B. (ed.) *Colour in food. Improving quality.* Cambridge, England, UK: Woodhead Publishing Limited.
MPHAHLELE, R. R., FAWOLE, O. A., MAKUNGA, N. P. & OPARA, U. L. 2016. Effect of drying on the bioactive compounds, antioxidant, antibacterial and antityrosinase activities of pomegranate peel. *BMC Complementary and Alternative Medicine,* 16**,** 143.
MULAUDZI, R. B., NDHLALA, A. R., KULKARNI, M. G. & VANSTADEN, J. 2012. Pharmacological properties and protein binding capacity of phenolic extracts of some Venda medicinal plants used against cough and fever. *Journal of Ethnopharmacology,* 143**,** 185-193.
MURRAY, B. S. 2007. Stabilization of bubbles and foams. *Current Opinion in Colloid & Interface Science,* 12**,** 232-241.
MURRAY, B. S. & ETTELAIE, R. 2004. Foam stability: proteins and nanoparticles. *Current Opinion in Colloid & Interface Science,* 9**,** 314-320.
MURRAY, B. S., FAERGEMAND, M., TROTEREAU, M. & VENTURA, A. 1999. Comparison of the Dynamic Behaviour of Protein Films at Air-Water and Oil-Water Interfaces. *In:* DICKINSON, E. R. P., J. M. (ed.) *Emulsions and Foams. Interfaces, Interactions and Stability.* Cambridge, U.K.: The Royal Society of Chemistry.

MUTHUKUMARAN, A. 2007. *Foam-mat freeze-drying of egg white and mathematical modeling.* Master of Science., McGill University.
NARAYAN, R. M. 2012. Review: Dye sensitized solar cells based on natural photosensitizers. *Renewable and Sustainable Energy Reviews,* 16**,** 208-215.
NASTAJ, J. F. & WITKIEWICZ, K. 2009. Mathematical modeling of the primary and secondary vacuum freeze drying of random solids at microwave heating. *International Journal of Heat and Mass transfer,* 52**,** 4796-4806.
NIELSEN, I. L. F., HAREN, G. R., MAGNUSSEN, E. L., DRAGSTED, L. O. & RASMUSSEN, S. E. 2003. Quantification of Anthocyanins in Commercial Black Currant Juices by Simple High-Performance Liquid Chromatography. Investigation of Their pH Stability and Antioxidative Potency. *Journal of Agricultural and Food Chemistry,* 51**,** 5861-5866.
NILE, S. H. & PARK, S. W. 2014. Edible berries: Bioactive components and their effect on human health. *Nutrition,* 30**,** 134-144.
NUALKAEKUL, S., DEEPIKA, G. & CHARALAMPOPOULOS, D. 2012. Survival of freeze dried Lactobacillus plantarum in instant fruit powders and reconstituted fruit juices. *Food Research International,* 48**,** 627-633.
OCHI, A., KATSUTA, K., MARUYAMA, E., KUBO, M. & UEDA, T. 2000. Effects of sugars on stability of egg foam and their rheological properties. *In:* NISHINARI, K. (ed.) *Hydrocolloids - Part 2.* Elsevier.
ORAK, H., AKTAS, T., YAGAR, H., SELEN ISBILIR, S., EKINCI, N. & HASTURK SAHIN, F. 2012. Effects of hot air and freeze drying methods on antioxidant activity, colour and some nutritional characteristics of strawberry tree (Arbutus unedo L) fruit. *Food Science and Technology International,* 18(4)**,** 391-402.
OWEN, T. 1996. Fundamentals of UV-visible spectroscopy. Germany: Hewlett-Packard Company.
OZDAL, T., CAPANOGLU, E. & ALTAY, F. 2013. A review on protein–phenolic interactions and associated changes. *Food Research International,* 51**,** 954-970.
PACE, C., GIACOSA, S., TORCHIO, F., RÍO SEGADE, S., CAGNASSO, E. & ROLLE, L. 2014. Extraction kinetics of anthocyanins from skin to pulp during carbonic maceration of winegrape berries with different ripeness levels. *Food Chemistry,* 165**,** 77-84.
PADAYACHEE, A., NETZEL, G., NETZEL, M., DAY, L., MIKKELSENA, D. & GIDLEY, M. J. 2013. Lack of release of bound anthocyanins and phenolic acids from carrot plant cell walls and model composites during simulated gastric and small intestinal digestion. *Food Funct.,* 4**,** 906-916.
PAPADOPOULOU, A., GREEN, R. J. & FRAZIER, R. A. 2005. Interaction of Flavonoids with Bovine Serum Albumin: A Fluorescence Quenching Study. *Journal of Agricultural and Food Chemistry,* 53**,** 158-163.
PATRAS, A., BRUNTON, N. P., O'DONNELL, C. & TIWARI, B. K. 2010. Effect of thermal processing on anthocyanin stability in foods; mechanisms and kinetics of degradation. *Food Science and Technology,* 21**,** 3-11.

PERKIN-ELMER 2006. An Introduction to Fluorescence Spectroscopy. *In:* SCIENCES, P. E. A. A. (ed.). Shelton, USA.
PETRONI, K. & CHIARA, T. 2011. Recent advances on the regulation of anthocyanin synthesis in reproductive organs. *Plant Science,* 181**,** 219-229.
PRAKOTMAK, P., SOPONRONNARIT, S. & PRACHAYAWARAKORN, S. 2010. Modelling of moisture diffusion in pores of banana foam mat using a 2-D stochastic pore network: Determination of moisture diffusion coefficient during adsorption process. *Journal of Food Engineering,* 96**,** 119-126.
PRINS, A. 1988. Principles of Foam Stability. *In:* DICKINSON, E. S., G. (ed.) *Advances in Food Emulsions and Foams.* Essex, England: Elsevier Applied Science Publishers Ltd.
PTASZEK, P., ZMUDZINSKI, D. & KRUK, J. 2014. The Physical and Linear Viscoelastic Properties of Fresh Wet Foams Based on Egg White Proteins and Selected Hydrocolloids. *Food Biophysics,* 9**,** 76-87.
QUE, F., MAO, L., FANG, X. & WU, T. 2008. Comparison of hot air-drying and freeze-drying on the physicochemical properties and antioxidant activities of pumpkin (Cucurbita moschata Duch.) flours. *International Journal of Food Science and Technology,* 43**,** 1195-1201.
RAHARITSIFA, N., GENOVESE, D. & RATTI, C. 2006. Characterization of Apple Juice Foams for Foam-mat Drying Prepared with Egg White Protein and Methylcellulose. *Journal of Food Science,* 71**,** E142-E151.
RAHARITSIFA, N. & RATTI, C. 2010a. Foam-mat freeze-drying of apple juice part 1: experimental data and ann simulations. *Journal of Food Process Engineering,* 33**,** 268-283.
RAHARITSIFA, N. & RATTI, C. 2010b. Foam-mat freeze-drying of apple juice part 2: stability of dry products during storage. *Journal of Food Process Engineering,* 33**,** 341-364.
RAHMAN, M. S. 2008. Dehydration and Microstructure. *Advances in Food Dehydration.* CRC Press.
RAIKOS, V., CAMPBELL, L. & EUSTON, S. 2007. Effects of sucrose and sodium chloride on foaming properties of egg white proteins. *Food Research International,* 40**,** 347-355.
RATTI, C. 2001. Hot air and freeze-drying of high value foods: a review. *Journal of Food Engineering,* 49**,** 311-319.
RATTI, C. & KUDRA, T. 2006. Drying of Foamed Biological Materials: Opportunities and Challenges. *Drying Technology,* 24:9**,** 1101-1108.
REIN, M. 2005. *Copigmentation reactions and color stability of berry anthocyanins.* Academic dissertation, University of Helsinki.
REYES, L. F. & CISNEROS-ZEVALLOS, L. 2007. Degradation kinetics and colour of anthocyanins in aqueous extracts of purple- and red-flesh potatoes (Solanum tuberosum L.). *Food Chemistry,* 100**,** 885-894.
RODRIGUEZ, S. D., VON STASZEWSKI, M. & PILOSOF, A. M. R. 2015. Green tea polyphenols-whey proteins nanoparticles: Bulk, interfacial and foaming behaviour. *Food Hydrocolloids,* 50**,** 108-115.

ROHRER, J. 2013. nalysis of carbohydrates by high - performance anion exchange chromatography with pulsed amperometric detection (HPAE-PAD). *In:* SCIENTIFIC, T. F. (ed.). Sunnyvale, CA, USA.
ROSALES-SOTO, M. U., POWERS, J. R. & ALLDREDGE, R. 2012. Effect of mixing time, freeze-drying and baking on phenolics, anthocyanins and antioxidant capacity of raspberry juice during processing of muffins. *Wiley Online Library*.
ROY, I. & GUPTA, M. N. 2004. REVIEW Freeze-drying of proteins: some emerging concerns. *Biotechnol. Appl. Biochem.,* 39**,** 165-177.
ROYER, C. A. 1995. Fluorescence Spectroscopy. *In:* SHIRLEY, B. A. (ed.) *Methods in Molecular Biology.* Totowa, NJ: Humana Press Inc.
SADAHIRA, M. S., RODRIGUES, M. I., AKHTAR, M., MURRAY, B. S. & NETTO, F. M. 2016. Effect of egg white protein-pectin electrostatic interactions in a high sugar content system on foaming and foam rheological properties. *Food Hydrocolloids,* 58**,** 1-10.
SADIKOGLU, H. & LIAPIS, A. I. 1997. Mathematical modelling of the primary and secondary drying stages of bulk solution freeze-drying in trays: parameter estimation and model discrimination by comparison of theoretical results with experimental data. *Drying Technology,* 15**,** 791-810.
SANDELL, M., LAAKSONEN, O., JARVINEN, R., ROSTIALA, N., POHJANHEIMO, T., TIITINEN, K. & KALIO, H. 2009. Orosensory Profiles and Chemical Composition of Black Currant (Ribes nigrum) Juice and Fractions of Press Residue. *Journal of Agricultural and Food Chemistry,* 57**,** 3718-3728.
SANGAMITHRA, A., VENKATACHALAM, S., GABRIELA JOHN, S. & KUPPUSWAMY, K. 2015. Foam mat drying of food materials: a review. *Journal of Food Processing and Preservation,* 39**,** 3165-3174.
SARKER, D. K., WILDE, P. J. & CLARK, D. C. 1995. Control of Surfactant-Induced Destabilization of Foams through Polyphenol-Mediated Protein-Protein Interactions. *Journal of Agricultural and Food Chemistry,* 43**,** 295-300.
SCHNEIDER, M., ESPOSITO, D., LILA, M. A. & FOEGEDING, A. 2016. Formation of whey protein–polyphenol mesostructures as a natural means of creating functional particles. *Food Funct.,* 7**,** 1306-1318.
SCHOEN, M. P., BRAXTON, B. K., GATLIN, L. A. & JEFFERIS, R. P. I. 1995. A simulation model for the primary drying phase of the freeze-drying cycle. *International Journal of Pharmaceutics,* 114**,** 159-170.
SCIBISZ, I., ZIARNO, M., MITEK, M. & ZAREBA, D. 2012. Effect of probiotic cultures on the stability of anthocyanins in blueberry yoghurts. *LWT - Food Science and Technology,* 49**,** 208-212.
SHEEHAN, P. & LIAPIS, A. I. 1998. Modeling of the Primary and Secondary Drying Stages of the Freeze Drying of Pharmaceutical Products in Vials: Numerical Results Obtained from the Solution of a Dynamic and Spatially Multi-Dimensional Lyophilization Model for Different Operational Policies. *Biotechnology and Bioengineering,* 60**,** 712-728.
SHIMADA, K. & MATSUSHITA, S. 1980. Relationship between thermocoagulation of proteins and amino acid compositions. *J. Agric. Food Chem,* 28**,** 416.

SIEBERT, K. J. 1999. Effects of Protein-Polyphenol Interactions on Beverage Haze, Stabilization, and Analysis. *Journal of Agricultural and Food Chemistry,* 47**,** 353-362.
SIEBERT, K. J., TROUKHANOVA, N. V. & LYNN, P. Y. 1996. Nature of Polyphenol-Protein Interactions. *Journal of Agricultural and Food Chemistry,* 44**,** 80-85.
SOCHANSKI, J., GOYETTE, J., BOSE, T., AKYEL, C. & BOSISIO, R. 1990. Freeze dehydration of foamed milk by microwaves. *Drying Technology,* 8(5)**,** 1017-1037.
SVENSSON, D. 2010. *Effects of heat treatment and additives on the anthocyanin content in blackcurrants and its relation to colour and texture.* Master of Science, Chalmers University of Technology.
TAKEOKA, G. & DAO, L. 2002. Anthocyanins. *In:* HURST, J. (ed.) *Methods of Analysis for Functional Foods and Nutraceuticals.* Florida, United States of America: CRC Press.
TEIXEIRA-BARCIA, M., BECKER PERTUZATTI, P., GÓMEZ-ALONSO, S., TEIXEIRA GODOY, H. & HERMOSÍN-GUTIÉRREZ, I. 2014. Phenolic composition of grape and winemaking by-products of Brazilian hybrid cultivars BRS Violeta and BRS Lorena. *Food Chemistry,* 159**,** 95-105.
THUWAPANICHAYANAN, R., PRACHAYAWARAKORN, S. & SOPONRONNARIT, S. 2008. Drying characteristics and quality of banana foam mat. *Journal of Food Engineering,* 86**,** 573-583.
TIMBERLAKE, C. F. & BRIDLE, P. 1976. The effect of processing and other factors on the colour characteristics of some red wines. *Vitis,* 15**,** 37-49.
TSAO, R. 2010. Chemistry and Biochemistry of Dietary Polyphenols. *Nutrients,* 2**,** 1231-1246.
UZUNOVIC, A. & VRANIC, E. 2008. Stability of anthocyanins from commercial blackcurrant juice under simulated gastrointestinal digestion *Bosnian Journal of basic medical sciences,* 3**,** 254-258.
VACLAVIK, V. A. & CHRISTIAN, E. W. 2014. Water. *Essentials of Food Science.* New York, U.S.A.: Springer Science+Business Media
VAN BUREN, J. P. & ROBINSON, W. B. 1969. Formation of Complexes between Protein and Tannic Acid. *Journal of Agricultural and Food Chemistry,* 17 No. 4**,** 772-777.
VAUZOUR, D., TEJERA, N., ONEILL, C., BOOZ, V., JUDE, B., WOLF, I. M. A., RIGBY, N., SILVAN, J. M., CURTIS, P. J., CASSIDY, A., DE PASCUAL-TERESA, S., RIMBACH, G. & MINIHANE, A. M. 2015. Anthocyanins do not influence long-chain n-3 fatty acid status: studies in cells, rodents and humans. *Journal of Nutritional Biochemistry,* 26**,** 211-218.
VELASCO, S., ROMAN, F. & WHITE, J. 2009. On the Clausius–Clapeyron Vapor Pressure Equation. *Journal of Chemical Education,* 86**,** 106-111.
VERNON-CARTER, E. J., ESPINOSA-PAREDES, G., BERISTAIN, C. I. & ROMERO-TEHUITZIL, H. 2001. Effect of foaming agents on the stability, rheological properties, drying kinetics and flavour retention of tamarind foam-mats. *Food Research International,* 34**,** 587-598.

VILJANEN, K., KYLLI, P., HUBBERMANN, E.-M., SCHWARZ, K. & HEINONEN, M. 2005. Anthocyanin Antioxidant Activity and Partition Behavior in Whey Protein Emulsion. *Journal of Agricultural and Food Chemistry,* 53**,** 2022-2027.

WALTERS, R. H., BHATNAGAR, B., TCHESSALOV, S., IZUTSU, K.-I., TSUMOTO, K. & OHTAKE, S. 2014. Next-Generation Drying Technologies for Pharmaceutical Applications. *Wiley Online Library*.

WEAIRE, D. 2008. The rheology of foam. *Current Opinion in Colloid & Interface Science,* 13**,** 171-176.

WIERENGA, P. A. & GRUPPEN, H. 2010. New views on foams from protein solutions. *Current Opinion in Colloid & Interface Science,* 15**,** 365-373.

WILSON, R. A., KADAM, D. M., CHADHA, S., GREWAL, M. K. & SHARMA, M. 2013. Evaluation of physical and chemical properties of foam-mat dried mango (Mangifera indica) powder during storage. *Journal of Food Processing and Preservation***,** 1-9.

WROLSTAD, R. 1993. Color and Pigment Analyses in Fruit Products. Oregon, USA: Agricultural Experiment Station, Oregon State University.

WU, H., TAO, Z., CHEN, G., DENG, H., XU, G. & DING, S. 2004. Conjugate heat and mass transfer process within porous media with dielectric cores in microwave freeze-drying. *Chemical Engineering Science,* 59**,** 2921-2928.

WU, W., CLIFFORD, M. & HOWELL, N. K. 2007. The effect of instant green tea on the foaming and rheological properties of egg albumen proteins. *Journal of the Science of Food and Agriculture,* 87**,** 1810-1819.

WU, X., LIANG, L., ZOU, Y., ZHAO, T., ZHAO, J., LI, F. & YANG, L. 2011. Aqueous two-phase extraction, identification and antioxidant activity of anthocyanins from mulberry (Morus atropurpurea Roxb.). *Food Chemistry,* 129**,** 443-453.

YANG, M., KOO, S. I., SONG, W. O. & CHUN, O. K. 2011. Food Matrix Affecting Anthocyanin Bioavailability: Review. *Current Medicinal Chemistry,* 18**,** 291-300.

YANG, X. 2008. *Effects of Sucrose on the Foaming and Interfacial Properties of Egg White Protein and Whey Protein Isolate.* PhD, North Carolina State University.

YANG, X., BERRY, T. K. & FOEGEDING, E. A. 2009. Foams prepared from whey protein isolate and egg white protein: 1. Physical, microstructural, and interfacial properties. *Journal of Food Science,* 74**,** E259-E268.

YANG, X. & FOEGEDING, A. 2010. Effects of sucrose on egg white protein and whey protein isolate foams: Factors determining properties of wet and dry foams (cakes). *Food Hydrocolloids,* 24**,** 227-238.

ZAYAS, J. F. 1997. Foaming Properties of Proteins. *Functionality of Proteins in Food.* Berlin, Heidelberg: Springer Berlin Heidelberg.

ZDZISLAW, E. S. & HAARD, N. 2006. Interactions of Food Components. *In:* ZDZISLAW, E. S. (ed.) *Chemical and Functional Properties of Food Components, Third Edition.* CRC Press.

ZHENG, X.-Z., LIU, C.-H. & ZHOU, H. 2011. Optimization of Parameters for Microwave-Assisted Foam Mat Drying of Blackcurrant Pulp. *Drying Technology,* 29**,** 230-238.
ZHOU, R., DONG, X., SONG, L. & JING, H. 2014. Interaction mode and nanoparticle formation of bovine serum albumin and anthocyanin in three buffer solutions. *Journal of Luminescence,* 155**,** 244-250.
ZOECKLEIN, B., FUGELSANG, K. C., GUMP, B. H. & NURY, F. S. 1995. *Wine Analysis and Production,* United States of America, Chapman & Hall Enology Library.

Appendix A

Mathematical Model Program MATLAB

```
NOTE: the 4 values of p (porosity) and d (density) were used
successively in each run. They were not used like a single array.

clear
clc

%Foam ZA100sf
A=0.005153; % [m^2] area of the container
L=2835036.09; % [J/kg] latent heat
R=461.5; % [J/kg K] gas constant
D=0.0271; % [m^2/s] diffusivity
k=0.407; % [W/m K] thermal conductivity of egg albumin
p=0.681, 0.679, 0.686, 0.675; % air volume fraction
d=171, 172, 165, 179; % [kg/m3] density
M=0.018; % [kg/mol] %molecular weight of water

Po=[6.3 6.3 5.9 5.3 4.8]';
%-50C   3.9Pa
To=[221.15  222.15  222.15  221.15  220.15]';%K

Pa=611.657; % Pascals, pressure triple point of water
Ta=273.16; % [K], temperature triple point of water
t=[0    3600    7200    11484   14400]';
t2=[0   60  84.85281374 107.1634266 120]';

for ii=1:length (Po)
    syms Ts
Po(ii)
To(ii)
a= (k*R)/(L*D)
b=(L/R)
eqn=(a*(To(ii)-Ts)*Ts)+((Po(ii)/To(ii))*(Ts))==Pa*exp(b*((1/Ta)-
(1/Ts))) %this comes from equalizing Ps. Units are [Pascals]
solTs=solve(eqn,Ts);
Ts=solTs;
Ts1(ii)=Ts;
Ts2=Ts1'

Ps(ii)=Pa*exp(b*((1/Ta)-(1/Ts1(ii)))) %[Pa]

%distance of the interface
u=k/(L*p*d);
rq=(2*u*(Ts1(ii)-To(ii)))*t %r^2=rq [meters^2]
r=sqrt(rq) %[m]

%DM=r(t)*A*p*d=
sq1=sqrt(2);
sq2=((k*p*d)/L);
c=A*sq1*sqrt((sq2)*(Ts1(ii)-To(ii)))*t2 %kg
c2=(c*1000)-1.3 %g
slope= A*sq1*sqrt((sq2)*(Ts1(ii)-To(ii)))%kg
slopeg=slope*1000 %g
```

```
end


clear
clc

%Foam ZA25sf
A=0.005153; % [m^2] area of the container
L=2835036.09; % [J/kg] latent heat
R=461.5; % [J/kg K] gas constant
D=0.0688; % [m^2/s] diffusivity
k=0.407; % [W/m K] thermal conductivity of egg albumin
p=0.761, 0.777, 0.755, 0.779; % air volume fraction
d=159.7, 140.3, 157, 127.9; % [kg/m3] density
M=0.018; % [kg/mol] %molecular weight of water

Po=[6.3 6.3 5.9 5.3 4.8]';
%-50C   3.9Pa
To=[221.15  222.15  222.15  221.15  220.15]';%K

Pa=611.657; % Pascals, pressure triple point of water
Ta=273.16; % [K], temperature triple point of water
t=[0    3600    7200    11484   14400]';
t2=[0   60  84.85281374 107.1634266 120]';

for ii=1:length (Po)
    syms Ts
Po(ii)
To(ii)
a= (k*R)/(L*D)
b=(L/R)
eqn=(a*(To(ii)-Ts)*Ts)+((Po(ii)/To(ii))*(Ts))==Pa*exp(b*((1/Ta)-
(1/Ts))) %this comes from equalizing Ps. Units are [Pascals]
solTs=solve(eqn,Ts);
Ts=solTs;
Ts1(ii)=Ts;
Ts2=Ts1'

Ps(ii)=Pa*exp(b*((1/Ta)-(1/Ts1(ii)))) %[Pa]

%distance of the interface
u=k/(L*p*d);
rq=(2*u*(Ts1(ii)-To(ii)))*t %r^2=rq [meters^2]
r=sqrt(rq) %[m]

%DM=r(t)*A*p*d=
sq1=sqrt(2);
sq2=((k*p*d)/L);
c=A*sq1*sqrt((sq2)*(Ts1(ii)-To(ii)))*t2 %kg
c2=(c*1000)-1.3 %g
slope= A*sq1*sqrt((sq2)*(Ts1(ii)-To(ii)))%kg
slopeg=slope*1000 %g
end

clear
clc

%Foam FJ100
A=0.005153; % [m^2] area of the container
```

```
L=2835036.09; % [J/kg] latent heat
R=461.5; % [J/kg K] gas constant
D=0.0125; % [m^2/s] diffusivity
k=0.407; % [W/m K] thermal conductivity of egg albumin
p=0.708, 0.713, 0.724, 0.699; % air volume fraction
d=126.6, 124.1, 116.9, 145.3; % [kg/m3] density
M=0.018; % [kg/mol] %molecular weight of water

Po=[6.3 6.3 5.9 5.3 4.8]';
%-50C   3.9Pa
To=[221.15  222.15  222.15  221.15  220.15]';%K

Pa=611.657; % Pascals, pressure triple point of water
Ta=273.16; % [K], temperature triple point of water
t=[0    3600    7200    11484   14400]';
t2=[0   60  84.85281374 107.1634266 120]';

for ii=1:length (Po)
    syms Ts
Po(ii)
To(ii)
a= (k*R)/(L*D)
b=(L/R)
eqn=(a*(To(ii)-Ts)*Ts)+((Po(ii)/To(ii))*(Ts))==Pa*exp(b*((1/Ta)-
(1/Ts))) %this comes from equalizing Ps. Units are [Pascals]
solTs=solve(eqn,Ts);
Ts=solTs;
Ts1(ii)=Ts;
Ts2=Ts1'

Ps(ii)=Pa*exp(b*((1/Ta)-(1/Ts1(ii)))) %[Pa]

%distance of the interface
u=k/(L*p*d);
rq=(2*u*(Ts1(ii)-To(ii)))*t %r^2=rq [meters^2]
r=sqrt(rq) %[m]

%DM=r(t)*A*p*d=
sq1=sqrt(2);
sq2=((k*p*d)/L);
c=A*sq1*sqrt((sq2)*(Ts1(ii)-To(ii)))*t2 %kg
c2=(c*1000)-1.3 %g
slope= A*sq1*sqrt((sq2)*(Ts1(ii)-To(ii)))%kg
slopeg=slope*1000 %g
end

clear
clc

%Foam FJ25
A=0.005153; % [m^2] area of the container
L=2835036.09; % [J/kg] latent heat
R=461.5; % [J/kg K] gas constant
D=0.0688; % [m^2/s] diffusivity
k=0.407; % [W/m K] thermal conductivity of egg albumin
p=0.762, 0.784, 0.775, 0.762; % air volume fraction
d=139.3, 117.4, 123.3, 138.4; % [kg/m3] density
M=0.018; % [kg/mol] %molecular weight of water
```

```
Po=[6.3 6.3 5.9 5.3 4.8]';
%-50C   3.9Pa
To=[221.15  222.15  222.15  221.15  220.15]';%K

Pa=611.657; % Pascals, pressure triple point of water
Ta=273.16; % [K], temperature triple point of water
t=[0    3600    7200    11484   14400]';
t2=[0   60  84.85281374 107.1634266 120]';

for ii=1:length (Po)
    syms Ts
Po(ii)
To(ii)
a= (k*R)/(L*D)
b=(L/R)
eqn=(a*(To(ii)-Ts)*Ts)+((Po(ii)/To(ii))*(Ts))==Pa*exp(b*((1/Ta)-
(1/Ts))) %this comes from equalizing Ps. Units are [Pascals]
solTs=solve(eqn,Ts);
Ts=solTs;
Ts1(ii)=Ts;
Ts2=Ts1'

Ps(ii)=Pa*exp(b*((1/Ta)-(1/Ts1(ii)))) %[Pa]

%distance of the interface
u=k/(L*p*d);
rq=(2*u*(Ts1(ii)-To(ii)))*t %r^2=rq [meters^2]
r=sqrt(rq) %[m]

%DM=r(t)*A*p*d=
sq1=sqrt(2);
sq2=((k*p*d)/L);
c=A*sq1*sqrt((sq2)*(Ts1(ii)-To(ii)))*t2 %kg
c2=(c*1000)-1.3 %g
slope= A*sq1*sqrt((sq2)*(Ts1(ii)-To(ii)))%kg
slopeg=slope*1000 %g
end


clear
clc

%Juice J25
A=0.005153; % [m^2]
L=2835036.09; % [J/kg]
R=461.5; %[J/kg K]
D=0.0218; %[m^2/s]
k=1.92; %[W/m K]
p=0.98, 0.87, 0.99,0.88; in freeze-drying models, porosity is
considered as the void space left behind after removing water
(Sochanski, 1999. Thus, porosity is proportional to the water
content of the sample.
d=1130.1, 1131.6, 1130.4, 1126.4; %kg/m3
M=0.018; %kg/mol

Po=[6.3 6.3 5.9 5.3 4.8 4.8 4.8]';
%-50C   3.9Pa
To=[221.15  222.15  222.15  221.15  220.15  220.15  220.15]';%K
```

```
Pa=611.657; %Pascals, pressure triple point of water
Ta=273.16;%K, temperature triple point of water
t=[10800 14400 18000 21600 25200 28800 32400]';
t2=[103.923 120 134.1640786 146.9693846 158.7450787 169.7056275
180]';

for ii=1:length (Po)
    syms Ts
Po(ii)
To(ii)
a= (k*R)/(L*D)
b=(L/R)
eqn=(a*(To(ii)-Ts)*Ts)+((Po(ii)/To(ii))*(Ts))==Pa*exp(b*((1/Ta)-
(1/Ts))) %this comes from equalizing Ps and the units are [Pascals]
solTs=solve(eqn,Ts);
Ts=solTs;
Ts1(ii)=Ts;
Ts2=Ts1'

Ps(ii)=Pa*exp(b*((1/Ta)-(1/Ts1(ii)))) %[Pa]

%distance of the interface
u=k/(L*p*d);
rq=(2*u*(Ts1(ii)-To(ii)))*t %r^2=rq [meters^2]
r=sqrt(rq) %[m]

%DM=r(t)*A*p*d=
sq1=sqrt(2);
sq2=((k*p*d)/L);
c=A*sq1*sqrt((sq2)*(Ts1(ii)-To(ii)))*t2 %kg
c2=(c*1000)-9.08 %g
slope= A*sq1*sqrt((sq2)*(Ts1(ii)-To(ii)))%kg
slopeg=slope*1000 %g
end
```

MATLAB program to obtain charts of predicted drying rate vs AVF/porosity with three levels of density

```
clear
clc

%Foam ZA100sf density-avf-drying rate
A=0.005153; % [m^2] area of the container
L=2835036.09; % [J/kg] latent heat
R=461.5; % [J/kg K] gas constant
D=0.0271; % [m^2/s] diffusivity
k=0.407; % [W/m K] thermal conductivity of egg albumin
p=linspace(0.67,0.69);% air volume fraction
d=160,170,180;% [kg/m3] density
M=0.018; % [kg/mol] %molecular weight of water

Po=[6.3 6.3 5.9 5.3 4.8]';
%-50C   3.9Pa
```

```
To=[221.15  222.15  222.15  221.15  220.15]';%K

Pa=611.657; % Pascals, pressure triple point of water
Ta=273.16; % [K], temperature triple point of water
t=[0    3600    7200    11484   14400]';
t2=[0   60  84.85281374 107.1634266 120]';

for ii=1:length (Po)
    syms Ts
Po(ii);
To(ii);
a= (k*R)/(L*D);
b=(L/R);
eqn=(a*(To(ii)-Ts)*Ts)+((Po(ii)/To(ii))*(Ts))==Pa*exp(b*((1/Ta)-
(1/Ts))); %this comes from equalizing Ps. Units are [Pascals]
solTs=solve(eqn,Ts);
Ts=solTs;
Ts1(ii)=Ts;
Ts2=Ts1';

Ps(ii)=Pa*exp(b*((1/Ta)-(1/Ts1(ii)))); %[Pa]
end

 for i=1:length(p)
     p(i);
%distance of the interface
u=k/(L*p(i)*d);
rq=(2*u*(Ts1(ii)-To(ii)))*t; %r^2=rq [meters^2]
r=sqrt(rq); %[m]

%DM=r(t)*A*p*d=
sq1=sqrt(2);
sq2=((k*p(i)*d)/L);
c=A*sq1*sqrt((sq2)*(Ts1(ii)-To(ii)))*t2; %kg
c2=(c*1000)-1.3; %g
slope= A*sq1*sqrt((sq2)*(Ts1(ii)-To(ii)));%kg
slopeg=slope*1000 %g
end

clear
clc

%Foam ZA25sf density-avf-drying rate
A=0.005153; % [m^2] area of the container
L=2835036.09; % [J/kg] latent heat
R=461.5; % [J/kg K] gas constant
D=0.0271; % [m^2/s] diffusivity
k=0.407; % [W/m K] thermal conductivity of egg albumin
p=linspace(0.75,0.78);% air volume fraction
d=120,140,160;% [kg/m3] density
M=0.018; % [kg/mol] %molecular weight of water

Po=[6.3 6.3 5.9 5.3 4.8]';
%-50C   3.9Pa
To=[221.15  222.15  222.15  221.15  220.15]';%K

Pa=611.657; % Pascals, pressure triple point of water
Ta=273.16; % [K], temperature triple point of water
```

```
t=[0    3600    7200    11484   14400]';
t2=[0   60  84.85281374 107.1634266 120]';

for ii=1:length (Po)
    syms Ts
Po(ii);
To(ii);
a= (k*R)/(L*D);
b=(L/R);
eqn=(a*(To(ii)-Ts)*Ts)+((Po(ii)/To(ii))*(Ts))==Pa*exp(b*((1/Ta)-
(1/Ts))); %this comes from equalizing Ps. Units are [Pascals]
solTs=solve(eqn,Ts);
Ts=solTs;
Ts1(ii)=Ts;
Ts2=Ts1';

Ps(ii)=Pa*exp(b*((1/Ta)-(1/Ts1(ii)))); %[Pa]
end

 for i=1:length(p)
     p(i);
%distance of the interface
u=k/(L*p(i)*d);
rq=(2*u*(Ts1(ii)-To(ii)))*t; %r^2=rq [meters^2]
r=sqrt(rq); %[m]

%DM=r(t)*A*p*d=
sq1=sqrt(2);
sq2=((k*p(i)*d)/L);
c=A*sq1*sqrt((sq2)*(Ts1(ii)-To(ii)))*t2; %kg
c2=(c*1000)-1.3; %g
slope= A*sq1*sqrt((sq2)*(Ts1(ii)-To(ii)));%kg
slopeg=slope*1000 %g
end

clear
clc

%Foam FJ100sf density-avf-drying rate
A=0.005153; % [m^2] area of the container
L=2835036.09; % [J/kg] latent heat
R=461.5; % [J/kg K] gas constant
D=0.0271; % [m^2/s] diffusivity
k=0.407; % [W/m K] thermal conductivity of egg albumin
p=linspace(0.69,0.73);% air volume fraction
d=115,132.5,150;% [kg/m3] density
M=0.018; % [kg/mol] %molecular weight of water

Po=[6.3 6.3 5.9 5.3 4.8]';
%-50C   3.9Pa
To=[221.15  222.15  222.15  221.15  220.15]';%K

Pa=611.657; % Pascals, pressure triple point of water
Ta=273.16; % [K], temperature triple point of water
t=[0    3600    7200    11484   14400]';
t2=[0   60  84.85281374 107.1634266 120]';

for ii=1:length (Po)
```

```
    syms Ts
Po(ii);
To(ii);
a= (k*R)/(L*D);
b=(L/R);
eqn=(a*(To(ii)-Ts)*Ts)+((Po(ii)/To(ii))*(Ts))==Pa*exp(b*((1/Ta)-
(1/Ts))); %this comes from equalizing Ps. Units are [Pascals]
solTs=solve(eqn,Ts);
Ts=solTs;
Ts1(ii)=Ts;
Ts2=Ts1';

Ps(ii)=Pa*exp(b*((1/Ta)-(1/Ts1(ii)))); %[Pa]
end

 for i=1:length(p)
     p(i);
%distance of the interface
u=k/(L*p(i)*d);
rq=(2*u*(Ts1(ii)-To(ii)))*t; %r^2=rq [meters^2]
r=sqrt(rq); %[m]

%DM=r(t)*A*p*d=
sq1=sqrt(2);
sq2=((k*p(i)*d)/L);
c=A*sq1*sqrt((sq2)*(Ts1(ii)-To(ii)))*t2; %kg
c2=(c*1000)-1.3; %g
slope= A*sq1*sqrt((sq2)*(Ts1(ii)-To(ii)));%kg
slopeg=slope*1000 %g
end

clear
clc

%Foam FJ25 density-avf-drying rate
A=0.005153; % [m^2] area of the container
L=2835036.09; % [J/kg] latent heat
R=461.5; % [J/kg K] gas constant
D=0.0271; % [m^2/s] diffusivity
k=0.407; % [W/m K] thermal conductivity of egg albumin
p=linspace(0.76,0.79);% air volume fraction
d=120,130,140;% [kg/m3] density
M=0.018; % [kg/mol] %molecular weight of water

Po=[6.3 6.3 5.9 5.3 4.8]';
%-50C   3.9Pa
To=[221.15  222.15  222.15  221.15  220.15]';%K

Pa=611.657; % Pascals, pressure triple point of water
Ta=273.16; % [K], temperature triple point of water
t=[0    3600    7200    11484   14400]';
t2=[0   60  84.85281374 107.1634266 120]';

for ii=1:length (Po)
    syms Ts
Po(ii);
To(ii);
a= (k*R)/(L*D);
```

```
b=(L/R);
eqn=(a*(To(ii)-Ts)*Ts)+((Po(ii)/To(ii))*(Ts))==Pa*exp(b*((1/Ta)-
(1/Ts))); %this comes from equalizing Ps. Units are [Pascals]
solTs=solve(eqn,Ts);
Ts=solTs;
Ts1(ii)=Ts;
Ts2=Ts1';

Ps(ii)=Pa*exp(b*((1/Ta)-(1/Ts1(ii)))); %[Pa]
end

 for i=1:length(p)
     p(i);
%distance of the interface
u=k/(L*p(i)*d);
rq=(2*u*(Ts1(ii)-To(ii)))*t; %r^2=rq [meters^2]
r=sqrt(rq); %[m]

%DM=r(t)*A*p*d=
sq1=sqrt(2);
sq2=((k*p(i)*d)/L);
c=A*sq1*sqrt((sq2)*(Ts1(ii)-To(ii)))*t2; %kg
c2=(c*1000)-1.3; %g
slope= A*sq1*sqrt((sq2)*(Ts1(ii)-To(ii)));%kg
slopeg=slope*1000 %g
end

clear
clc

%Juice J25 density-porosity-drying rate
A=0.005153; % [m^2]
L=2835036.09; % [J/kg]
R=461.5; %[J/kg K]
D=0.0218; %[m^2/s]
k=1.92; %[W/m K]
p=linspace(0.8,0.999);% in freeze-drying models, porosity is
considered as the void space left behind after removing water
(Sochanski, 1999. Thus, porosity is proportional to the water
content of the sample.
d=1120,1127.5,1135; %kg/m3
M=0.018; %kg/mol

Po=[6.3 6.3 5.9 5.3 4.8 4.8 4.8]';
%-50C   3.9Pa
To=[221.15  222.15  222.15  221.15  220.15  220.15  220.15]';%K

Pa=611.657; %Pascals, pressure triple point of water
Ta=273.16;%K, temperature triple point of water
t=[10800 14400 18000 21600 25200 28800 32400]';
t2=[103.923 120 134.1640786 146.9693846 158.7450787 169.7056275
180]';

for ii=1:length (Po)
    syms Ts
Po(ii);
To(ii);
a= (k*R)/(L*D);
```

```
b=(L/R);
eqn=(a*(To(ii)-Ts)*Ts)+((Po(ii)/To(ii))*(Ts))==Pa*exp(b*((1/Ta)-
(1/Ts))); %this comes from equalizing Ps and the units are [Pascals]
solTs=solve(eqn,Ts);
Ts=solTs;
Ts1(ii)=Ts;
Ts2=Ts1';

Ps(ii)=Pa*exp(b*((1/Ta)-(1/Ts1(ii)))); %[Pa]
end
for i=1:length(p)
     p(i);
%distance of the interface
u=k/(L*p(i)*d);
rq=(2*u*(Ts1(ii)-To(ii)))*t; %r^2=rq [meters^2]
r=sqrt(rq); %[m]

%DM=r(t)*A*p*d=
sq1=sqrt(2);
sq2=((k*p(i)*d)/L);
c=A*sq1*sqrt((sq2)*(Ts1(ii)-To(ii)))*t2; %kg
c2=(c*1000)-9.08; %g
slope= A*sq1*sqrt((sq2)*(Ts1(ii)-To(ii)));%kg
slopeg=slope*1000 %g
end
```

Conditions reported for freeze-drying in skimmed milk from Liapis (1997) and used to test the mathematical model of this study.

```
A=0.05;% [m^2] area of the container
L=2840000; % [J/kg] latent heat
R=461.5; % [J/kg K] gas constant
D=0.003;% [m^2/s] diffusivity
k=0.491;%[W/m K] thermal conductivity
p=0.87; % water content (Hurley,
2009)http://ansci.illinois.edu/static/ansc438/Milkcompsynth/milkcomp
synthresources.html
d=1030;% [kg/m3] density
M=0.018; % [kg/mol] %molecular weight of water

Po=50;% Pa
To=218.15;% -55 C

Pa=611.657; % Pascals, pressure triple point of water
Ta=273.16; % [K], temperature triple point of water
t=[0 720 1440 2160 2880 3600 7200 10800 14400 18000 21600 25200
28800 32400 36000 39600 43200]';%s
t2=[0 26.83281573 37.94733192 46.47580015 53.66563146 60 84.85281374
103.9230485 120 134.1640786 146.9693846 158.7450787 169.7056275 180
189.7366596 198.9974874 207.8460969]';%sqrt(s)
wer=[0 0.2 0.4 0.6 0.8 1 2 3 4 5 6 7 8 9 10 11 12]';%h
```

```
for ii=1:length (Po)
    syms Ts
Po(ii)
To(ii)
a= (k*R)/(L*D)
b=(L/R)
eqn=(a*(To(ii)-Ts)*Ts)+((Po(ii)/To(ii))*(Ts))==Pa*exp(b*((1/Ta)-
(1/Ts))) %this comes from equalizing Ps. Units are [Pascals]
solTs=solve(eqn,Ts);
Ts=solTs;
Ts1(ii)=Ts;
Ts2=Ts1'

Ps(ii)=Pa*exp(b*((1/Ta)-(1/Ts1(ii)))) %[Pa]

%distance of the interface
u=k/(L*p*d);
rq=(2*u*(Ts1(ii)-To(ii)))*t %r^2=rq [meters^2]
r=sqrt(rq) %[m]

%DM=r(t)*A*p*d=
sq1=sqrt(2);
sq2=((k*p*d)/L);
c=A*sq1*sqrt((sq2)*(Ts1(ii)-To(ii)))*t2; %kg
c2=(c*1000)-9.08; %g
slope= A*sq1*sqrt((sq2)*(Ts1(ii)-To(ii)));%kg
slopeg=slope*1000 %g

plot(wer,c)
xlabel('time (h)')
ylabel('water removed [kg]')
end
```

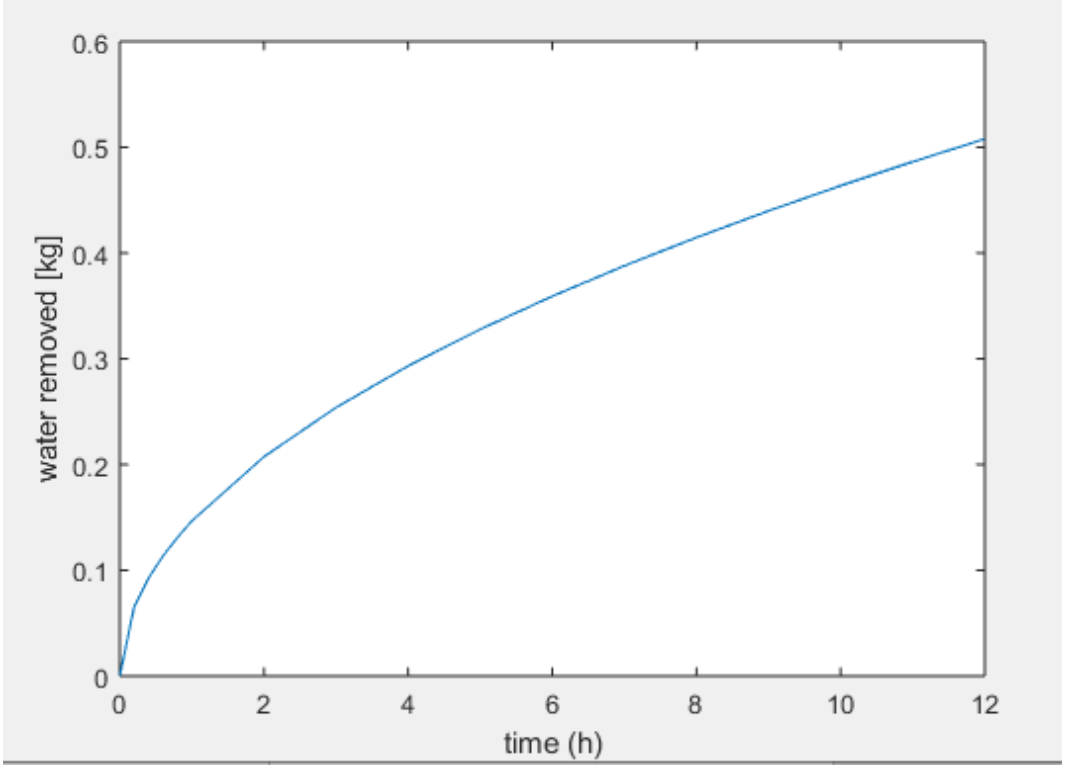

Appendix B

Statistical analysis of foam characteristics

General Linear Model: SM versus Anthocyanin concentration [mg l^{-1}], Sugars [high/low]. Error variance = 0.003. n=8.

Coefficients for Sauter Mean (SM in mm)

Term	Coef	SE Coef	95% CI	T-Value	P-Value	Variance Inflation Factor (VIF)
Constant	0.2220	0.0232	(0.1625, 0.2816)	9.58	0.000	
Anthocyanin	-0.000262	0.000155	(-0.000661, 0.000137)	-1.69	0.152	1.40
Sugars* (+/-)	-0.0564	0.0217	(-0.1121, -0.0007)	-2.60	0.048	1.40

Regression Equation

Sugars			
0	SM	=	0.1656 - 0.000262 Anthocyanin
1	SM	=	0.2784 - 0.000262 Anthocyanin

*Add the coefficient for Sugars 0 (concentrated). Subtract for Sugars 1 (diluted).

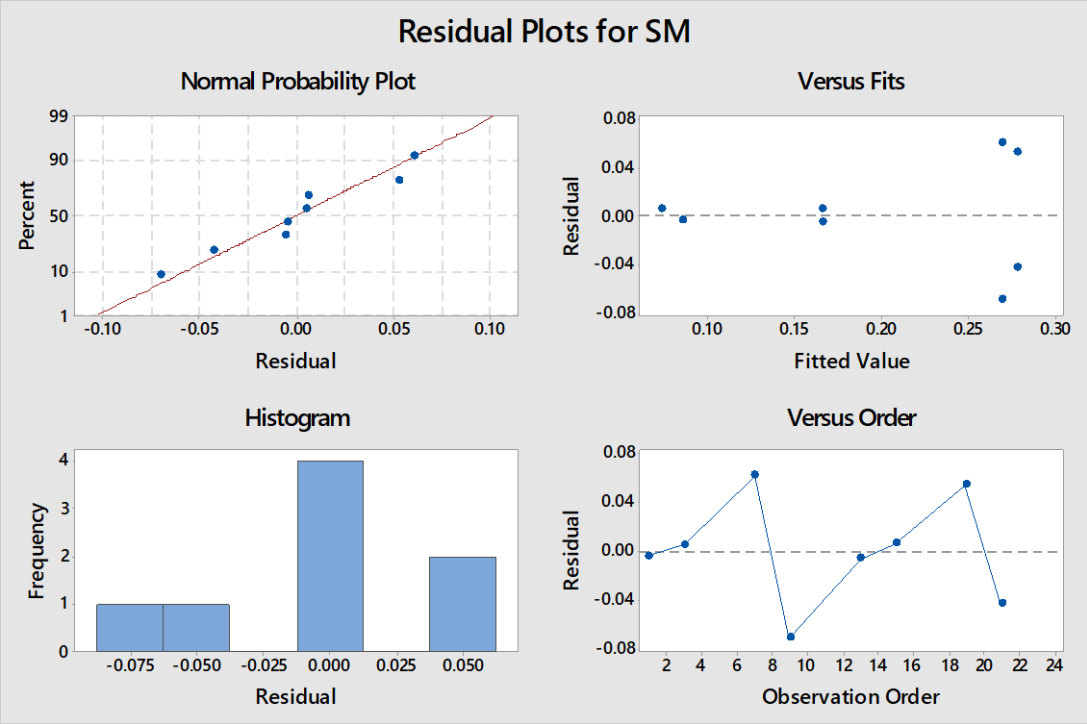
Residual Plots for SM
Normal Probability Plot
Percent
99
90
50
10
1
-0.10
-0.05
0.00
0.05
0.10
Residual
Versus Fits
Residual
0.08
0.04
0.00
-0.04
-0.08
0.10
0.15
0.20
0.25
0.30
Fitted Value
Histogram
Frequency
4
3
2
1
0
-0.075
-0.050
-0.025
0.000
0.025
0.050
Residual
Versus Order
Residual
0.08
0.04
0.00
-0.04
-0.08
2
4
6
8
10
12
14
16
18
20
22
24
Observation Order

Mixed Effects Model: drainage versus Anthocyanin concentration [mg l^{-1}], Sugars [high/low]. Batch was a random grouping factor with variance = 0.285. Error variance = 0.018. n=24.

Coefficients

Term	Coef	SE Coef	DF	95% CI	T-Value	P-Value
Constant	1.188212	0.196969	9.00	(0.742637, 1.63379)	6.032486	0.000
Anthocyanin	-0.003884	0.001306	9.00	(-0.006840, -0.00093)	-2.973438	0.016
Sugars* (+/-)	0.069474	0.180568	9.00	(-0.338998, 0.47795)	0.384754	0.709

*Add the coefficient for Sugars 0 (concentrated). Subtract for Sugars 1 (diluted).

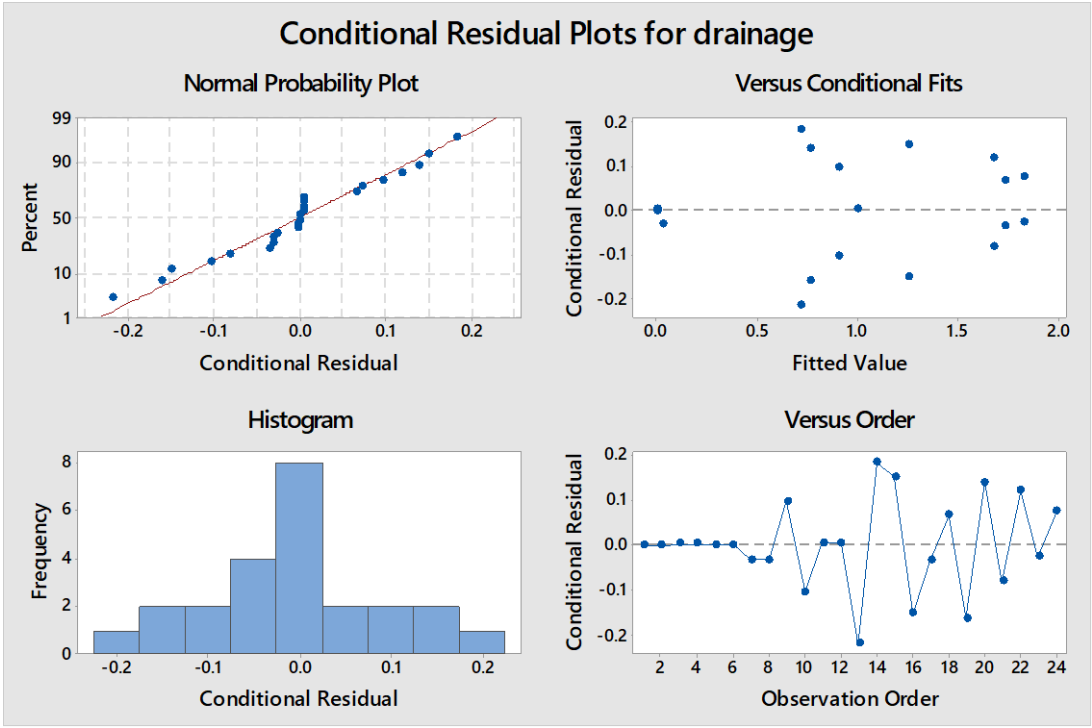
Conditional Residual Plots for drainage
Normal Probability Plot
Percent
99
90
50
10
1
-0.2
-0.1
0.0
0.1
0.2
Conditional Residual
Versus Conditional Fits
Conditional Residual
0.2
0.1
0.0
-0.1
-0.2
0.0
0.5
1.0
1.5
2.0
Fitted Value
Histogram
Frequency
8
6
4
2
0
-0.2
-0.1
0.0
0.1
0.2
Conditional Residual
Versus Order
Conditional Residual
0.2
0.1
0.0
-0.1
-0.2
2
4
6
8
10
12
14
16
18
20
22
24
Observation Order

Mixed Effects Model: AVF versus Anthocyanin concentration [mg l^{-1}], Sugars [high/low]. Batch was a random grouping factor with variance < 0.0005. Error variance = 0.0001.n=24.

Coefficients

Term	Coef	SE Coef	DF	95% CI	T-Value	P-Value
Constant	0.724550	0.003338	9.00	(0.716999, 0.732100)	217.087438	0.000
Anthocyanin	0.000077	0.000022	9.00	(0.000027, 0.000127)	3.484580	0.007
Sugars* (+/-)	-0.043730	0.003060	9.00	(-0.050652, -0.036809)	-14.292505	0.000

*Add the coefficient for Sugars 0 (concentrated). Subtract for Sugars 1 (diluted).

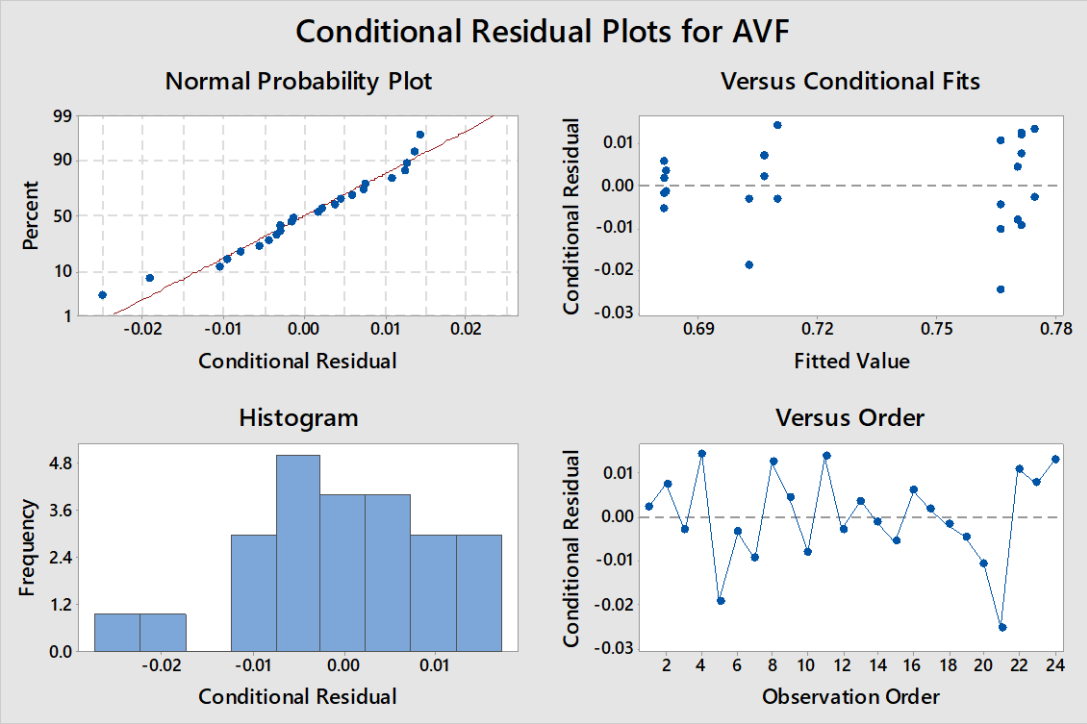
Conditional Residual Plots for AVF
Normal Probability Plot
Percent
99
90
50
10
1
-0.02
-0.01
0.00
0.01
0.02
Conditional Residual
Versus Conditional Fits
Conditional Residual
0.01
0.00
-0.01
-0.02
-0.03
0.69
0.72
0.75
0.78
Fitted Value
Histogram
Frequency
4.8
3.6
2.4
1.2
0.0
-0.02
-0.01
0.00
0.01
Conditional Residual
Versus Order
Conditional Residual
0.01
0.00
-0.01
-0.02
-0.03
2
4
6
8
10
12
14
16
18
20
22
24
Observation Order

Mixed Effects Model: density versus Anthocyanin concentration [mg l^{-1}], Sugars [high/low]. Batch was a random grouping factor with variance = 0.0001. Error variance = 0.0001.n=24.

Coefficients

Term	Coef	SE Coef	DF	95% CI	T-Value	P-Value
Constant	0.155278	0.004242	9.00	(0.145683, 0.164873)	36.607565	0.000
Anthocyanin	-0.000125	0.000028	9.00	(-0.000189, -0.000062)	-4.452977	0.002
Sugars* (+/-)	0.016725	0.003888	9.00	(0.007928, 0.025521)	4.301118	0.002

*Add the coefficient for Sugars 0 (concentrated). Subtract for Sugars 1 (diluted).

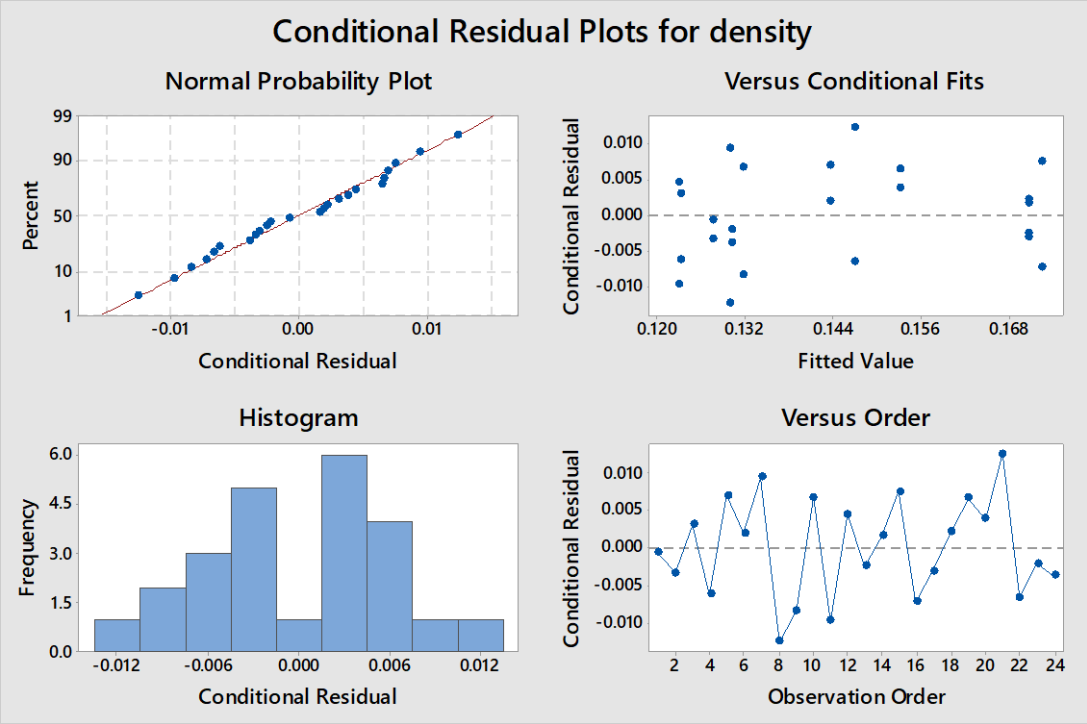
Conditional Residual Plots for density
Normal Probability Plot
Percent
99
90
50
10
1
-0.01
0.00
0.01
Conditional Residual
Versus Conditional Fits
Conditional Residual
0.010
0.005
0.000
-0.005
-0.010
0.120
0.132
0.144
0.156
0.168
Fitted Value
Histogram
Frequency
6.0
4.5
3.0
1.5
0.0
-0.012
-0.006
0.000
0.006
0.012
Conditional Residual
Versus Order
Conditional Residual
0.010
0.005
0.000
-0.005
-0.010
2
4
6
8
10
12
14
16
18
20
22
24
Observation Order

Statistical analysis of drying rate

Mixed Effects Model: DRexp [g/√s] versus Anthocyanin concentration [mg l^{-1}], Sugars [high = 0/low = 1] and Foam [foamed = 1/non-foamed = 2]. Batch was a random grouping factor with variance < 0.0005. Error variance < 0.0005.n=20.

Term	Coefficients	SE Coef	DF	95% CI	T-Value	P-Value
Constant	0.091639	0.003687	15.00	(0.0837807, 0.0994971)	24.855988	0.000
Anthocyanin	0.000120	0.000069	15.00	(-0.0000266, 0.0002663)	1.744463	0.102
Sugars						
0	-0.004594	0.001248	15.00	(-0.0072529, -0.0019343)	-3.681789	0.002
1	0.004594	0.001248	15.00	(0.0019343, 0.0072529)	3.681789	0.002
Foam						
1	-0.041276	0.003613	15.00	(-0.0489759, -0.0335757)	-11.425489	0.000
2	0.041276	0.003613	15.00	(0.0335757, 0.0489759)	11.425489	0.000
Anthocyanin*Foam						
1	-0.000163	0.000069	15.00	(-0.0003091, -0.0000161)	-2.366154	0.032
2	0.000163	0.000069	15.00	(0.0000161, 0.0003091)	2.366154	0.032

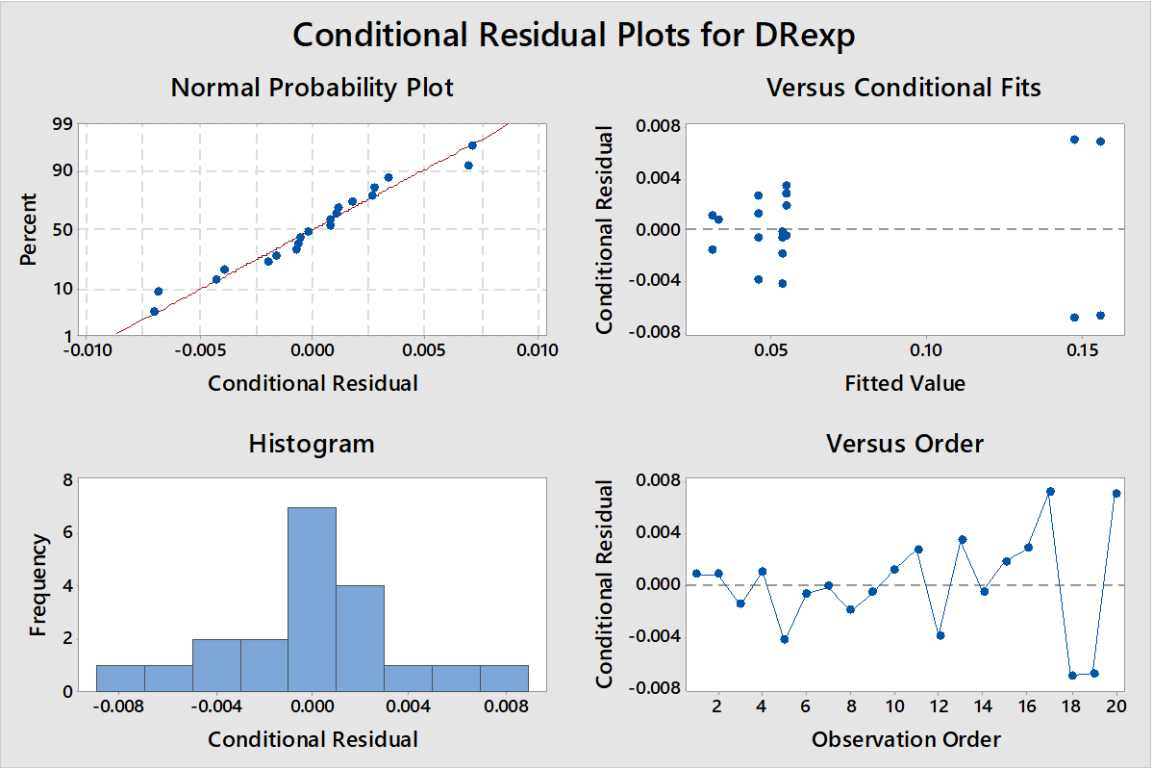
Conditional Residual Plots for DRexp
Normal Probability Plot
Percent
99
90
50
10
1
-0.010
-0.005
0.000
0.005
0.010
Conditional Residual
Versus Conditional Fits
Conditional Residual
0.008
0.004
0.000
-0.004
-0.008
0.05
0.10
0.15
Fitted Value
Histogram
Frequency
8
6
4
2
0
-0.008
-0.004
0.000
0.004
0.008
Conditional Residual
Versus Order
Conditional Residual
0.008
0.004
0.000
-0.004
-0.008
2
4
6
8
10
12
14
16
18
20
Observation Order

Mixed Effects Model: DRexp [g/√s] versus Anthocyanin concentration [mg l^{-1}] and Sugars [high/low] [between foams]. Batch was a random grouping factor with variance < 0.0005. Error variance < 0.0005.n=16.

Coefficients

Term	Coef	SE Coef	DF	95% CI	T-Value	P-Value
Constant	0.051182	0.000703	12.00	(0.0496491, 0.0527140)	72.768952	0.000
Anthocyanin	-0.000096	0.000021	12.00	(-0.0001420, -0.0000504)	-4.578618	0.001
Sugars‡ (+/-)	-0.005596	0.000703	12.00	(-0.0071281, -0.0040632)	-7.955839	0.000
Anthocyanin*Sugars (+/-)	0.000055	0.000021	12.00	(0.0000088, 0.0001004)	2.598892	0.023

‡Add the coefficient for Sugars 0 (concentrated). Subtract for Sugars 1 (diluted).

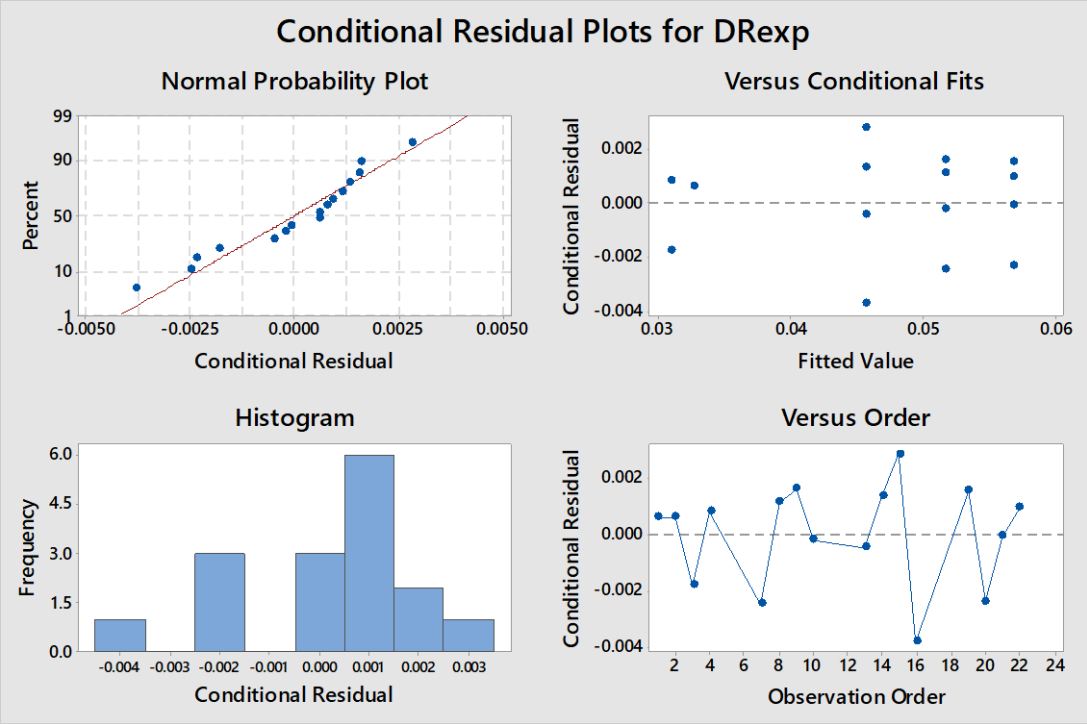
Conditional Residual Plots for DRexp
Normal Probability Plot
Percent
99
90
50
10
1
-0.0050
-0.0025
0.0000
0.0025
0.0050
Conditional Residual
Versus Conditional Fits
Conditional Residual
0.002
0.000
-0.002
-0.004
0.03
0.04
0.05
0.06
Fitted Value
Histogram
Frequency
6.0
4.5
3.0
1.5
0.0
-0.004
-0.003
-0.002
-0.001
0.000
0.001
0.002
0.003
Conditional Residual
Versus Order
Conditional Residual
0.002
0.000
-0.002
-0.004
2
4
6
8
10
12
14
16
18
20
22
24
Observation Order

Statistical analysis of colour over time of foam-mat freeze-dried vs conventional freeze-dried blackcurrant juice (powders)

Mixed Effects Model: ΔE versus time [month], Sample and Vacuum [vacuum = 1. Air = 2]. Batch was a random grouping factor with variance < 0.0005. Error variance = 5.62. n=204.

Term	Coefficients	SE Coef	DF	95% CI	T-Value	P-Value
Constant	10.777363	0.292241	197.00	(10.2010, 11.3537)	36.878277	0.000
time	0.256157	0.094740	197.00	(0.0693, 0.4430)	2.703777	0.007
Sample						
FJ25	14.656921	0.408910	197.00	(13.8505, 15.4633)	35.843901	0.000
J25	-8.615003	0.408910	197.00	(-9.4214, -7.8086)	-21.068226	0.000
Xanthan	-6.041918	0.421920	197.00	(-6.8740, -5.2099)	-14.320069	0.000
Vacuum						
1	-0.803737	0.166009	197.00	(-1.1311, -0.4764)	-4.841523	0.000
2	0.803737	0.166009	197.00	(0.4764, 1.1311)	4.841523	0.000
time*Sample						
FJ25	-0.569292	0.133789	197.00	(-0.8331, -0.3054)	-4.255133	0.000
J25	0.334926	0.133789	197.00	(0.0711, 0.5988)	2.503380	0.013
Xanthan	0.234366	0.134370	197.00	(-0.0306, 0.4994)	1.744187	0.083

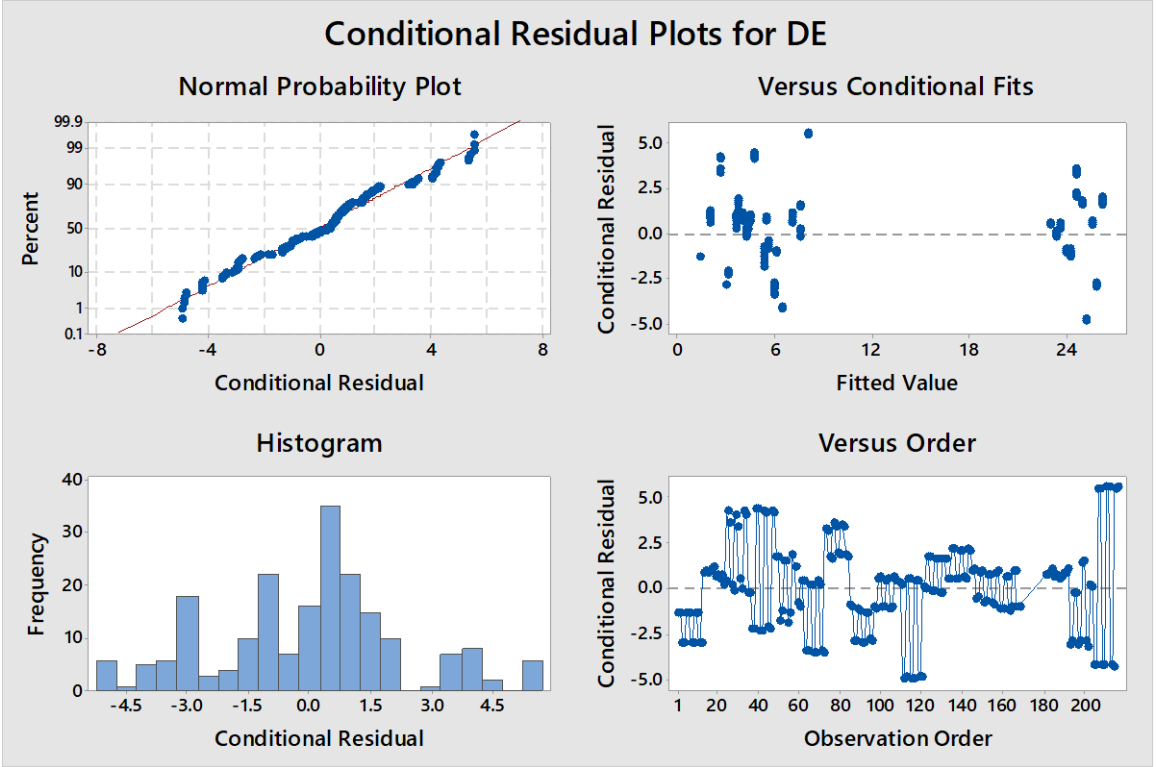
Conditional Residual Plots for DE
Normal Probability Plot
Percent
99.9
99
90
50
10
1
0.1
-8
-4
0
4
8
Conditional Residual
Versus Conditional Fits
Conditional Residual
5.0
2.5
0.0
-2.5
-5.0
0
6
12
18
24
Fitted Value
Histogram
Frequency
40
30
20
10
0
-4.5
-3.0
-1.5
0.0
1.5
3.0
4.5
Conditional Residual
Versus Order
Conditional Residual
5.0
2.5
0.0
-2.5
-5.0
1
20
40
60
80
100
120
140
160
180
200
Observation Order

Comparisons for ΔE

Fisher Pairwise Comparisons: Sample

Grouping Information Using the Fisher LSD Method and 95% Confidence

Sample	N	Mean	Grouping		
FJ25	72	24.6422	A		
Xanthan	60	5.9762		B	
J25	72	3.6575			C

Means that do not share a letter are significantly different.

Fisher Individual Tests for Differences of Means

Difference of Sample Levels	Difference of Means	SE of Difference	DF	Individual 95% CI	T-Value	P-Value
J25 - FJ25	-20.985	0.395	197	(-21.764, -20.205)	-53.09	0.000
Xanthan - FJ25	-18.666	0.415	197	(-19.484, -17.848)	-45.02	0.000
Xanthan - J25	2.319	0.415	197	(1.501, 3.136)	5.59	0.000

Simultaneous confidence level = 87.81%

Fisher Pairwise Comparisons: Vacuum

Grouping Information Using the Fisher LSD Method and 95% Confidence

Vacuum	N	Mean	Grouping	
2	102	12.2290	A	
1	102	10.6216		B

Means that do not share a letter are significantly different.

Fisher Individual Tests for Differences of Means

Difference of Vacuum Levels	Difference of Means	SE of Difference	DF	Individual 95% CI	T-Value	P-Value
2 - 1	1.607	0.332	197	(0.953, 2.262)	4.84	0.000

Simultaneous confidence level = 95.00%

Mixed Effects Model: $(\Delta H)^2$ versus time [month], Sample and Vacuum [vacuum = 1. Air = 2]. Batch was a random grouping factor with variance < 0.0005. Error variance = 282.65. n=204.

Term	Coefficients	SE Coef	DF	95% CI	T-Value	P-Value
Constant	52.517310	2.072173	197.00	(48.4308, 56.604)	25.344078	0.000
time	1.869236	0.671768	197.00	(0.5445, 3.194)	2.782561	0.006
Sample						
FJ25	104.058377	2.899423	197.00	(98.3405, 109.776)	35.889340	0.000
J25	-52.237801	2.899423	197.00	(-57.9557, -46.520)	-18.016620	0.000
Xanthan	-51.820575	2.991671	197.00	(-57.7204, -45.921)	-17.321617	0.000
Vacuum						
1	3.953272	1.177107	197.00	(1.6319, 6.275)	3.358466	0.001
2	-3.953272	1.177107	197.00	(-6.2746, -1.632)	-3.358466	0.001
time*Sample						
FJ25	3.533925	0.948650	197.00	(1.6631, 5.405)	3.725216	0.000
J25	-1.713428	0.948650	197.00	(-3.5842, 0.157)	-1.806175	0.072
Xanthan	-1.820498	0.952765	197.00	(-3.6994, 0.058)	-1.910751	0.057

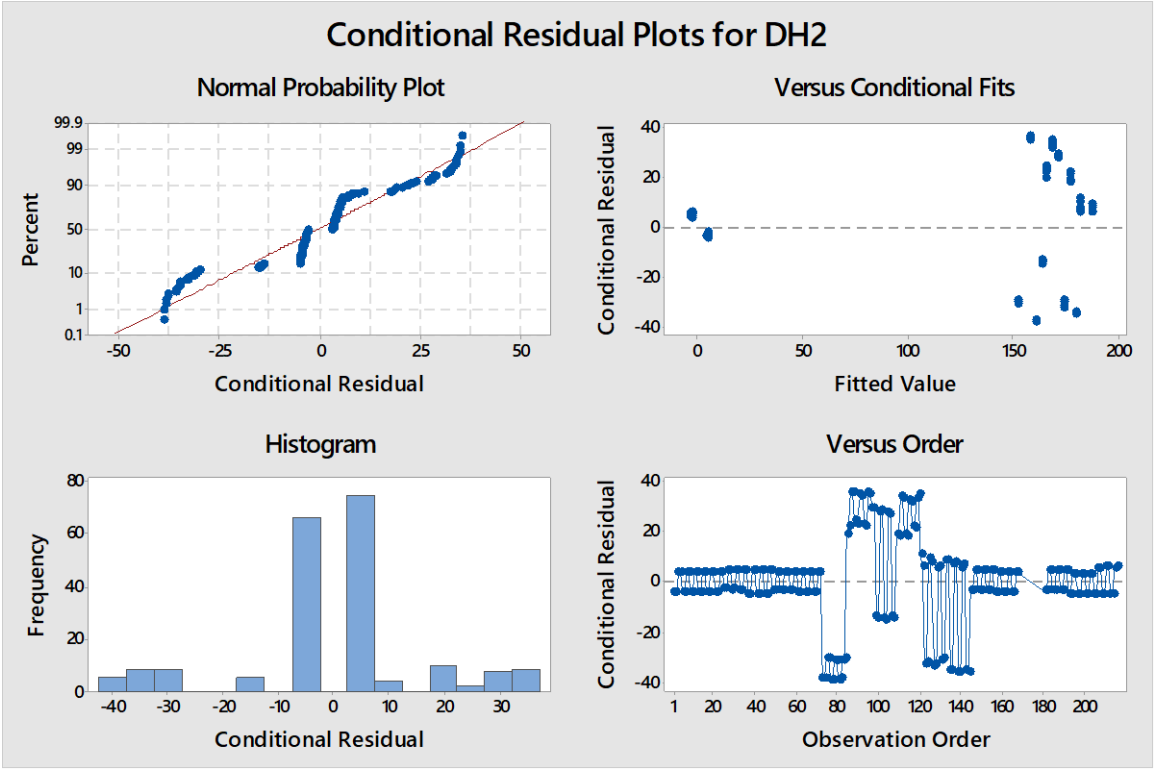
Conditional Residual Plots for DH2
Normal Probability Plot
Percent
99.9
99
90
50
10
1
0.1
-50
-25
0
25
50
Conditional Residual
Versus Conditional Fits
Conditional Residual
40
20
0
-20
-40
0
50
100
150
200
Fitted Value
Histogram
Frequency
80
60
40
20
0
-40
-30
-20
-10
0
10
20
30
Conditional Residual
Versus Order
Conditional Residual
40
20
0
-20
-40
1
20
40
60
80
100
120
140
160
180
200
Observation Order

Comparisons for $(\Delta H)^2$

Fisher Pairwise Comparisons: Sample

Grouping Information Using the Fisher LSD Method and 95% Confidence

Sample	N	Mean	Grouping	
FJ25	72	170.243	A	
Xanthan	60	0.820		B
J25	72	0.674		B

Means that do not share a letter are significantly different.

Fisher Individual Tests for Differences of Means

Difference of Sample Levels	Difference of Means	SE of Difference	DF	Individual 95% CI	T-Value	P-Value
J25 - FJ25	-169.57	2.80	197	(-175.10, -164.04)	-60.51	0.000
Xanthan - FJ25	-169.42	2.94	197	(-175.22, -163.62)	-57.62	0.000
Xanthan - J25	0.15	2.94	197	(-5.65, 5.94)	0.05	0.960

Simultaneous confidence level = 87.81%

Fisher Pairwise Comparisons: Vacuum

Grouping Information Using the Fisher LSD Method and 95% Confidence

Vacuum	N	Mean	Grouping	
1	102	61.1986	A	
2	102	53.2921		B

Means that do not share a letter are significantly different.

Fisher Individual Tests for Differences of Means

Difference of Vacuum Levels	Difference of Means	SE of Difference	DF	Individual 95% CI	T-Value	P-Value
2 - 1	-7.91	2.35	197	(-12.55, -3.26)	-3.36	0.001

Simultaneous confidence level = 95.00%

Mixed Effects Model: ΔC versus time [month], Sample and Vacuum [vacuum = 1. Air = 2]. Batch was a random grouping factor with variance < 0.0005. Error variance = 3.16. n=204.

Term	Coefficients	SE Coef	DF	95% CI	T-Value	P-Value
Constant	-6.230790	0.219312	197.00	(-6.6633, -5.7983)	-28.410676	0.000
time	0.362224	0.071098	197.00	(0.2220, 0.5024)	5.094741	0.000
Sample						
FJ25	-11.405872	0.306865	197.00	(-12.0110, -10.8007)	-37.169043	0.000
J25	5.787529	0.306865	197.00	(5.1824, 6.3927)	18.860188	0.000
Xanthan	5.618344	0.316628	197.00	(4.9939, 6.2428)	17.744304	0.000
Vacuum						
1	-0.002362	0.124581	197.00	(-0.2480, 0.2433)	-0.018962	0.985
2	0.002362	0.124581	197.00	(-0.2433, 0.2480)	0.018962	0.985
time*Sample						
FJ25	-0.134057	0.100402	197.00	(-0.3321, 0.0639)	-1.335209	0.183
J25	-0.178301	0.100402	197.00	(-0.3763, 0.0197)	-1.775873	0.077
Xanthan	0.312358	0.100837	197.00	(0.1135, 0.5112)	3.097644	0.002

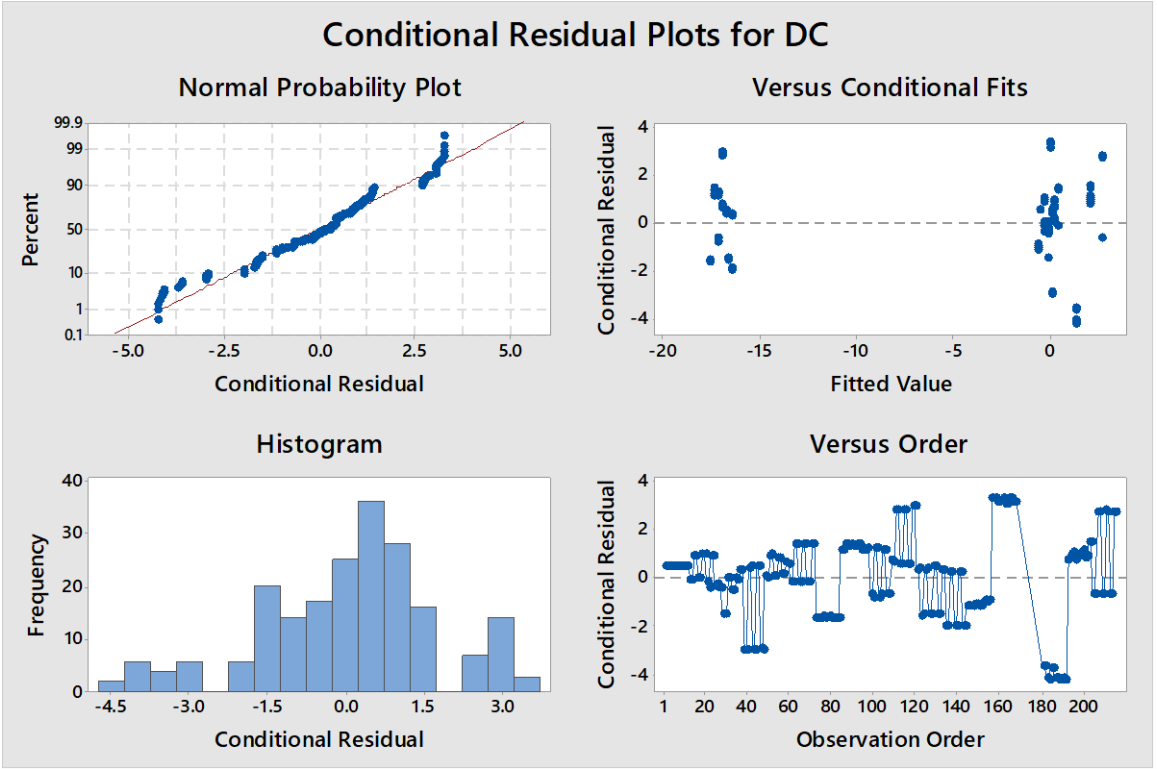
Conditional Residual Plots for DC
Normal Probability Plot
Percent
99.9
99
90
50
10
1
0.1
-5.0
-2.5
0.0
2.5
5.0
Conditional Residual
Versus Conditional Fits
Conditional Residual
4
2
0
-2
-4
-20
-15
-10
-5
0
Fitted Value
Histogram
Frequency
40
30
20
10
0
-4.5
-3.0
-1.5
0.0
1.5
3.0
Conditional Residual
Versus Order
Conditional Residual
4
2
0
-2
-4
1
20
40
60
80
100
120
140
160
180
200
Observation Order

Comparisons for ΔC

Fisher Pairwise Comparisons: Sample

Grouping Information Using the Fisher LSD Method and 95% Confidence

Sample	N	Mean	Grouping		
Xanthan	60	1.0939	A		
J25	72	0.0220		B	
FJ25	72	-17.0595			C

Means that do not share a letter are significantly different.

Fisher Individual Tests for Differences of Means

Difference of Sample Levels	Difference of Means	SE of Difference	DF	Individual 95% CI	T-Value	P-Value
J25 - FJ25	17.081	0.297	197	(16.497, 17.666)	57.59	0.000
Xanthan - FJ25	18.153	0.311	197	(17.540, 18.767)	58.34	0.000
Xanthan - J25	1.072	0.311	197	(0.458, 1.686)	3.44	0.001

Simultaneous confidence level = 87.81%

Fisher Pairwise Comparisons: Vacuum

Grouping Information Using the Fisher LSD Method and 95% Confidence

Vacuum	N	Mean	Grouping
2	102	-5.31221	A
1	102	-5.31694	A

Means that do not share a letter are significantly different.

Fisher Individual Tests for Differences of Means

Difference of Vacuum Levels	Difference of Means	SE of Difference	DF	Individual 95% CI	T-Value	P-Value
2 - 1	0.005	0.249	197	(-0.487, 0.496)	0.02	0.985

Simultaneous confidence level = 95.00%